INFORMATION TO USERS

This manuscript has been reproduced from the microfilm master. UMI films the text directly from the original or copy submitted. Thus, some thesis and dissertation copies are in typewriter face, while others may be from any type of computer printer.

The quality of this reproduction is dependent upon the quality of the copy submitted. Broken or indistinct print, colored or poor quality illustrations and photographs, print bleedthrough, substandard margins, and improper alignment can adversely affect reproduction.

In the unlikely event that the author did not send UMI a complete manuscript and there are missing pages, these will be noted. Also, if unauthorized copyright material had to be removed, a note will indicate the deletion.

Oversize materials (e.g., maps, drawings, charts) are reproduced by sectioning the original, beginning at the upper left-hand corner and continuing from left to right in equal sections with small overlaps.

Photographs included in the original manuscript have been reproduced xerographically in this copy. Higher quality 6" x 9" black and white photographic prints are available for any photographs or illustrations appearing in this copy for an additional charge. Contact UMI directly to order.

ProQuest Information and Learning
300 North Zeeb Road, Ann Arbor, MI 48106-1346 USA
800-521-0600

Oxidative Stress Induces Up-Regulation Of Elongation Factor-1 Alpha (EF-1α) En Route To Apoptosis

by

Edwin Chen

A Thesis
submitted to the Faculty of Graduate Studies and Research
in partial fulfillment of the requirements for the degree of
Master of Science

Department of Anatomy & Cell Biology
McGill University, Montréal, Canada
May, 2000

ABSTRACT

During myocardial infarction, significant myocardial cell loss occurs in a process termed "post-ischemic reperfusion injury", a two-step process where the myocardium first undergoes temporary conditions of ischemia caused by an occlusion of blood flow, followed by the re-establishment of blood flow to the previously hypoxic myocardium. It is believed that the excessive production of reactive oxygen intermediates, such as free radicals and pro-oxidants, during the reperfusion process is a major contributing factor to the observed cell death. In the present study, we sought to investigate the role of the pro-oxidant, hydrogen peroxide (H_2O_2), in triggering apoptosis in H9c2(2-1) cells, a clonogenic cell line derived from embryonic rat heart ventricles. Treatment with H_2O_2 caused decreased cell viability, along with the formation of an oligonucleosomal ladder and activation of the cysteine protease, caspase-3, hallmarks of apoptotic cell death. Moreover, we observed that elongation factor-1 alpha (EF–1α) protein levels underwent rapid and sustained increases upon treatment with toxic dosages of H_2O_2, whereas the effect was only transient with sublethal doses. Pre-treatment with a transcriptional inhibitor, actinomysin D did not abolish the oxidant-induced increase in EF–1α, and Northern blotting analysis revealed that EF–1α mRNA levels remained steady throughout the H_2O_2-treatment period, suggesting that the up-regulation of EF–1α is mediated post-transcriptionally. Moreover, a protective effect against H_2O_2 injury was effected by transient transfection of antisense EF–1α. A similar elevation in EF-1α protein levels was observed in heart tissues of transgenic mice undergoing *in vivo* oxidative stress, where the gene encoding the antioxidant, manganese superoxide dismutase (MnSOD), was inactivated by homologous recombination. As with the cell culture system, EF-1α mRNA levels did not mimic the change at the protein level, and remained unaltered. Thus, we demonstrate that there is a rapid up-regulation of EF–1α en route to apoptosis initiated by an oxidative insult *in vitro* and *in vivo*, and that this phenomenon may be a necessary early event in the induction of apoptosis.

RÉSUMÉ

Lors d'un infarctus du myocarde, une perte significative de cellules myocardiaques selon un processus à deux volets appellé "post-ischemic reperfusion injury". Dans un premier temps, un état temporaire d'ischemie est creé par l'occlusion du flot sanguin suivie par le réétablissement du flot dans le myocarde. Il semble que la production excessive de dérivé actif de l'oxygène, comme les radicaux libres et les pro-oxydants, durant le processus de réperfusion, est un facteur majeur contribuant à l'apparition de mort cellulaire. Dans la présente étude, nous avons investigué le rôle d'un pro-oxydant, le peroxide d'hydrogène (H_2O_2), dans l'induction de l'apoptose dans un modèle de cellules, les H9c2(2-1), une lignée cellulaire clonogénique dérivée de ventricule de rat embryonaire. Le traitement à l' H_2O_2 cause une diminution de la viabilité cellulaire, accompagné par la fragmentation internucléosomale de l'ADN et par l'activation de la cysteine protéase, caspase-3, tout deux, marqueur de l'apoptose. De plus, nous observons une augmentation rapide et soutenue de la protéine elongation facteur-1 alpha (EF−1α) suite à une exposition à des doses toxiques de H_2O_2. De plus, cet effet est transitoire pour des doses subléthales. Une prétraitement des cellules avec l'actinomycin D, un inhibiteur de transcription, n'inhibe pas l'augmentation de EF−1α par les oxydants. L'analyse de l'ARN messager par hybridation de type Northern montre que le niveau de EF−1α demeure constant suite au traitement par l'H_2O_2, ce qui suggère que la régulation positive de EF−1α à lieu à un niveau post-transcriptionnel. De plus, nous observons un effet protecteur contre l'H_2O_2 suite à la transfection transitoire d'un antisense-EF−1α. Une augmentation similaire de la protéine EF−1α est observée dans les tissues cardiaques de souris transgéniques soumis à un stress oxidatif, où le gène codant pour l'antioxidant, manganese superoxide dismutase (MnSOD), a été inactivé par recombination homologue. Comme pour le système de culture cellulaire, le niveau de l'ARN messager de EF−1α ne correspond pas au changement obtenu au niveau de la protéine, demeurant inchangé. Donc, nous démontrons dans ce travail, qu'il y a une régulation positive de EF−1α, initiée par la présence d'un stress oxydatif *in vitro* et *in vivo* menant à l'apoptose et que ce phénomène peut être un évenement précoce nécessaire à l'induction de l'apoptose.

ACKNOWLEDGEMENTS

I would like to acknowledge my supervisor, Dr. Eugenia Wang, for her support and guidance throughout both my undergraduate and my graduate training, and without whom this work could not have been completed.

My sincerest gratitude to Dr. Ting-Ting Huang and Dr. Charles Epstein of the University of California at San Francisco for generously providing us with the tissue samples of the MnSOD-knockout mice, and for their assistance and expertise in the post-experimental analyses.

I would also like to thank the various members of Dr. Wang's laboratory and the Bloomfield Center for their guidance and for making my graduate experiences enjoyable. In particular, my gratitude to Dr. Abdelnaby Khalyfa for generating the EF-1α-specific antibody, to Gregory Proestou for excellent technical assistance with the Northern blots and to Alan Moscovic for providing the "stuff of life" for my cells to grow in. In addition, I am grateful to Denis Bourbeau for invaluable support and for patiently coping with a young and inexperienced undergraduate student three years ago, and to Richard Marcotte and Chantale Cossette for providing the French translation of the abstract. I am also indebted to Mr. Bourbeau, Mr. Marcotte, Tara Moriarty and two anonymous reviewers for critical reading of the text and insightful comments. I thank Emmanuel Petroulakis, Bruno Ruest, Chantale Lacelle and Dr. Jie Pan for helpful technical discussions and assistance. And I also thank Ms. Lucia Badolato for keeping us all sane and smiling.

Finally, this work would not have been possible without the support of my family and friends abroad. Especially, to my friends, Randeep Khurana and Zuhair Fancy, for being "bad influences" on me, and for making life interesting, for eleven years and going. And to Stella Wen for her love and support during troubled times.

TABLE OF CONTENTS

LIST OF FIGURES AND TABLES

LIST OF FIGURES AND TABLES

LIST OF ABBREVIATIONS AND SYMBOLS

Å	:	Angstrom
aa-tRNA	:	aminoacyl transfer RNA
ADP	:	adenosine diphosphate
ANT	:	adenine nucleotide translocator
Apaf-1	:	apoptosis protease activating factor-1
ATP	:	adenosine triphosphate
bp	:	base pair
cDNA	:	complementary DNA
Cu/ZnSOD	:	copper/zinc superoxide dismutase
DMEM	:	Dulbecco's modified eagle's medium
EF	:	elongation factor
EF-1α	:	elongation factor-1 alpha
EF-1$\beta\gamma\delta$	:	elongation factor-1 beta/gamma/delta complex
eIF	:	eukaryotic initiation factor
FADD	:	Fas-associated death domain
FCS	:	fetal calf serum
GDP	:	guanosine diphosphate
GTP	:	guanosine triphosphate
H_2O_2	:	hydrogen peroxide
HRP	:	horse radish peroxidase
Ig	:	immunoglobulin
kb	:	kilobase
kDa	:	kilodalton
MnSOD	:	manganese superoxide dismutase
MPTP	:	mitochondrial permeability transition pore

MTT	:	3-(4,5-dimethylthiazol-2-yl)-2,5-diphenyltetrazolium bromide
O_2	:	oxygen
O_2^-	:	superoxide anion
OH^-	:	hydroxyl anion
OH•	:	hydroxyl radical
PARP	:	poly(ADP-ribose) polymerase
Pu	:	purine
Py	:	pyrimidine
mRNA	:	messenger RNA
rRNA	:	ribosomal RNA
tRNA	:	transfer RNA
ROI	:	reactive oxygen intermediate
SDS-PAGE	:	sodium dodecyl sulfate-polyacrylamide gel electrophoresis
SOD	:	superoxide dismutase
TBST	:	tris-buffered saline + 0.5% Tween-20
TUNEL	:	terminal dUTP nick-end labeling
UTP	:	uracil triphosphate
UTR	:	untranslated region
VDAC	:	voltage-dependent anion channel

LITERATURE REVIEW

1. The Free Radical Hypothesis of Ischemia-Reperfusion Injury

The pathology of ischemic heart disease is initiated by thrombosis of a coronary artery, creating an occlusion of blood flow to the myocardium. Coronary blockage results in a reduction of oxygen supply to the heart, which, if sufficiently prolonged and severe, can induce membrane damage, necrosis and cell loss (Jennings, 1960). Paradoxically, while rapid reoxygenation and re-establishment of blood flow to the ischemic myocardium is critical in preventing hypoxia-induced damage, the reperfusion event is also capable of exacerbating damage to the myocardium (Melrose, 1955; Jennings *et al.*, 1974). The additional injury inflicted upon the myocardium, independent of the ischemic event, is referred to as "reperfusion injury" (Hearse, 1977).

One of the proposed mechanisms by which reperfusion injury is effected is through the generation of toxic reactive oxygen intermediates (ROIs) (Hess *et al.*. 1984). The superoxide anion (O_2^-) and hydrogen peroxide (H_2O_2) constitute the majority of ROIs of relevance to the cell under physiological circumstances (McCord, 1985). In actuality, however, these molecules are relatively unreactive and only damaging to cells at high concentrations (Ferrari *et al.*, 1991). The primary danger associated with accumulation of O_2^- and H_2O_2 is the potential for the formation of the highly unstable hydroxyl radical (OH•), which can arise *via* Fenton chemistry (Fenton, 1894). When H_2O_2 reacts with a transition metal catalyst (Me^{N+}), the following reaction occurs, generating the hydroxyl radical:

$$Me^{N+} + H_2O_2 \longrightarrow Me^{(N+1)} + OH^- + OH\bullet$$

While copper and cobalt can participate in Fenton reactions, the high levels of intracellular iron suggest that it serves as the predominant Fenton transition metal catalyst *in vivo* (Imlay, 1988). The hydroxyl radical generated is a highly unstable molecule, and

reacts with various intracellular macromolecules at diffusion-limited rates, usually within 10^{-6} seconds and 14 Å from its site of generation (Kukreja, 1992).

Under normal circumstances, the cell possesses endogenous defense mechanisms in the form of antioxidant enzymes to respond to aberrant production of ROIs. Superoxide dismutase (SOD) catalyzes the dismutation of the O_2^- to H_2O_2, which in turn is detoxified to water by other antioxidants, such as catalase or glutathione peroxidase.

$$O_2 \xrightarrow{\text{SOD}} O_2^- \xrightarrow{\text{catalase}} H_2O_2 \longrightarrow H_2O$$

The premise of the "free radical theory of reperfusion injury" is that during reoxygenation of the myocardium, ROIs are generated at sufficiently high levels to overcome endogenous cellular antioxidant defense mechanisms. This condition is referred to as "oxidative stress", which, if sufficiently severe, ultimately leads to cell and tissue damage (McCord, 1985).

Much of the evidence implicating ROIs in the pathology of reperfusion injury has been indirect. Supplementation of antioxidants, such as superoxide dismutase and/or catalase, in the reperfusion medium has been shown by many (Ambrosio *et al.*, 1987; Ytrehus *et al.*, 1987; Jolly *et al.*, 1984; Mitsos *et al.*, 1986; Werns *et al.*, 1985, 1986), but not all groups (Forman *et al.*, 1988; Gallagher *et al.*, 1986; Przyklenk *et al.*, 1989; Richard *et al.* 1988; Uraizee *et al.*, 1987) to reduce infarct size and improve cardiac function following reperfusion. Catalase-overexpressing transgenic mice have reduced infarct sizes following ischemia-reperfusion as compared to non-transgenic and transgene-negative controls (Li *et al.*, 1997). Additionally, manganese superoxide dismutase-knockout mice die during early post-natal development due to dilated cardiomyopathies and ventricular wall thinning (Li *et al.*, 1995). The first report to directly describe heightened free radical production following reperfusion of the ischemic myocardium was provided by Zweier and coworkers, who used electron paramagnetic

resonance spectroscopy and electron spin trapping to quantitate an increase in free radical concentrations, from 4.7 ± 0.5 μM in control hearts to 11.4 ± 0.6 μM in hearts reperfused with oxygenated buffer for ten seconds (Zweier *et al.*, 1987a, 1987b, 1988). Similar evidence was later provided by several other independent groups (Kramer *et al.*, 1987; Baker *et al.*, 1988; Garlick *et al.*, 1987). The majority of ROI production occurs within the first ten minutes following re-establishment of blood flow (Bolli *et al.*, 1990).

2. Sources of Reactive Oxygen Intermediates (ROIs) in the Reperfused Myocardium

2.0. Introduction

The actual source of ROIs following reperfusion of the myocardium remains a controversial issue, and several sites have been postulated as sources of free radical generation (Flitter, 1993). In the following sections, three of these mechanisms, which have received the most attention in the literature, are reviewed (Figure 1).

2.1. Mitochondria

Under ischemic conditions, the adenine nucleotide pool is partially degraded, limiting intracellular ADP pools (Freeman *et al.*, 1982). In its absence, due to a lack of substrates for ATP generation, oxidative phosphorylation in the mitochondria is halted and the electron carriers in the electron transport chain become fully reduced (McCord, 1988). This condition promotes leakage of electrons from the respiratory chain which react with the oxygen in the cell, thereby generating O_2^-. During the ischemic event, given the low levels of O_2^- in the tissue, any minute, aberrant generation of free radicals caused by this phenomenon is detoxified by the resident antioxidant defense mechanisms (Ferrari *et al.*, 1985). Upon reintroduction of oxygen during reperfusion, however, the electrons which leak from the respiratory chain react with the over-abundantly available oxygen, generating O_2^- at levels beyond the defense capabilities of the intracellular antioxidants

(Turner *et al.*, 1980; Nohl, 1982). Consistent with this model, Ide *et al.*, (1999) have recently detected a 2.7-fold increase in O_2^- production by the mitochondrial fraction of failing hearts, concluding that ROIs generated during reperfusion could be of mitochondrial origin.

2.2. Xanthine Dehydrogenase / Xanthine Oxidase

While the principle is vaguely evident during mitochondrial generation of ROIs, the xanthine dehydrogenase/xanthine oxidase system, as characterized by McCord, is the classical example of the potential of an ischemic event to "prime" the ensuing damage initiated by reperfusion (McCord, 1985). Two events occur during the ischemic event. First, ATP is degraded into hypoxanthine, and ultimately, to xanthine (Saugstad *et al.*, 1980). Secondly, the enzyme xanthine dehydrogenase is converted, by a calcium-dependent limited proteolysis, to xanthine oxidase (Granger *et al.*, 1981). This modified enzyme, instead of functioning to reduce NAD^+, prefers an oxygen substrate, resulting in the generation of O_2^-. Thus, reperfusing the ischemic myocardium supplies the molecular oxygen used by xanthine oxidase in precipitating a burst of O_2^- and inducing oxidative stress. In some studies, xanthine oxidase inhibitors, such as allinopurinol, oxypurinol or tungsten, protect against cell loss induced by ischemia-reperfusion in cat, rodent, dog and human systems (Werns *et al.*, 1986; Wexler *et al.*, 1981; Johnson *et al.*, 1974; Downey *et al.*, 1988). However, several negative studies in similar systems have also been reported (Podzuweit *et al.*, 1986; Kehrer *et al.*, 1987; Reimer *et al.*, 1985). In addition, the distribution of xanthine oxidase seems to be highly species-specific, with undetectable xanthine dehydrogenase or xanthine oxidase enzymatic activity in the human, rabbit and pig myocardium (de Jorg *et al.*, 1990). This discrepancy has been explained by the detection of xanthine dehydrogenase and xanthine oxidase activity in the outlying endothelial cells, suggesting that the vasculature participates in ROI generation during reperfusion (Jarasch *et al.*, 1986).

2.3. Activated Neutrophils

Another potential source of extracellular ROIs is from activated neutrophils. Due to the inflammatory processes associated with myocardial infarction, neutrophils have been shown to invade the infarct site (Mullane *et al.*, 1984). Neutrophils possess, as an element of an all-purpose anti-bacterial and anti-microbial response mechanism, a membrane-associated NADPH-dependent oxidase, which functions as an efficient producer of O_2^- once activated by bacteria, mitogens or cytokines, a process designated as a "respiratory burst" (Barbior, 1978; Barbior, 1984). Romson first proposed a role for neutrophils as a source of free radicals during the course of reperfusion, by demonstrating that neutrophil depletion reduced infarct size to a similar extent as the administration of antioxidants (Romson *et al.*, 1983). Other groups have also demonstrated that leukocyte and platelet depletion enhances cardiac function following reperfusion (Ko *et al.*, 1991; Simpson *et al.*, 1988; Litt *et al.*, 1989). Finally, anti-inflammatory compounds have also been shown to severely limit infarct size following reperfusion (Mullane *et al.*, 1984). However, the controversy over the importance of neutrophils in the pathology of reperfusion injury has been fueled by questions concerning the speed at which they arrive at the myocardium. While Romson and coworkers demonstrated that neutrophil content in the myocardium increases 17-fold 24-hours following reperfusion (Romson *et al.*, 1983), Engler reported a lack of neutrophil accumulation in the heart five hours following ischemia (Engler *et al.*, 1983), although irreversible damage had already been inflicted upon the tissue. Manning showed that three hours following ischemia, the number of neutrophils were only marginally increased, and were found primarily localized marginated in the veins, with no detectable cells in cardiac tissues (Manning, 1988). Thus, the apparent lack of a "cause-and-effect relationship" between neutrophil accumulation and tissue injury has made it difficult to assess the contribution of neutrophils in reperfusion injury (Flitter, 1993).

Figure 1. **Schematic diagram of sources of ROIs in the myocardium.** Three widely studied sources of ROIs following reperfusion of the ischemic myocardium are the endothelium, cardiac myocytes, and invading polymorphonuclear leukocytes and neutrophils.

Figure 1

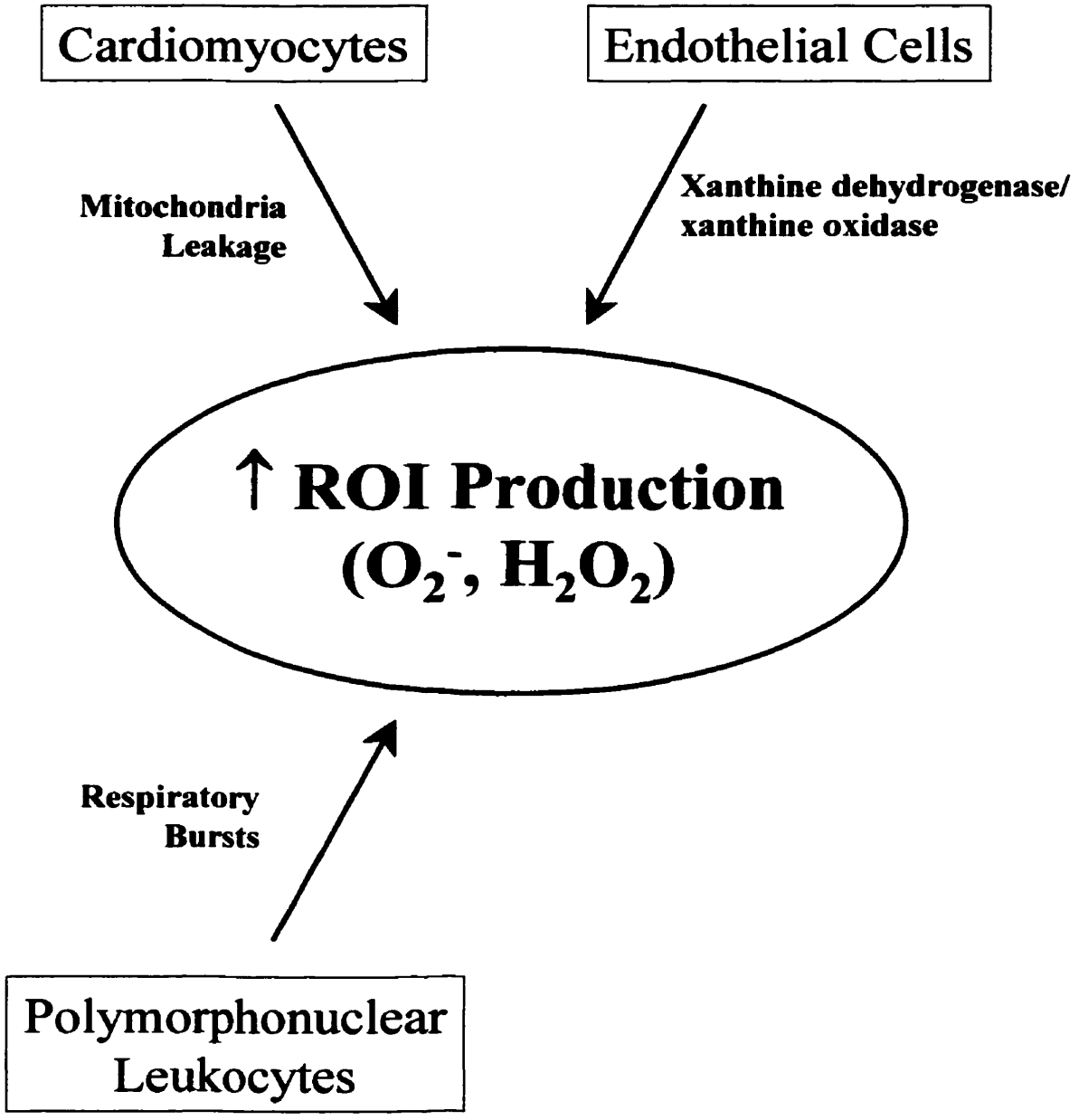
Cardiomyocytes
Endothelial Cells
Mitochondria Leakage
Xanthine dehydrogenase/ xanthine oxidase
↑ ROI Production
(O_2^-, H_2O_2)
Respiratory Bursts
Polymorphonuclear Leukocytes

3. Possible Mechanisms for Reactive Oxygen Intermediates-Induced Apoptosis

3.0. Introduction

Two distinguishable modes of cell loss occur in the myocardium following exposure to ROIs: necrosis and apoptosis (Saikumar *et al.*, 1998). Necrosis involves an uncontrolled breakdown of cellular and organellar structure, resulting in cell lysis and an inflammatory response. It occurs independent of cellular energy (Majno *et al.*, 1995). Apoptosis, on the other hand, is an active, adenosine triphosphate (ATP)-dependent, gene-driven, non-inflammatory, programmed cellular destruction process (Kerr *et al.*, 1972). Morphologically, while the former exhibits cell swelling and loss of membrane integrity, the latter is characterized by cell shrinkage, formation of membrane-enclosed apoptotic bodies, preservation of organelles and maintenance of membrane integrity (Yeh *et al.*, 1997; Haunstetter *et al.*, 1998). Phagocytosis of the apoptotic bodies by macrophages prevents the elicitation of an inflammatory response (Kerr *et al.*, 1972). Moreover, biochemically, apoptosis is characterized by fragmentation of the nuclear DNA into integer multiples of the internucleosomal length (approximately 180 bp) (Wyllie, 1980), and the *de novo* expression of a spectrum of apoptosis-specific genes (described below in sections 3.1-3.3).

Lennon and coworkers first demonstrated that ROIs are capable of inducing different modes of cell death in a dose-dependent manner. Excessive levels of ROIs are capable of inducing death in lymphocytes *via* necrosis, whereas lower doses induce death *via* apoptosis (Lennon *et al.*, 1991). The biochemical mechanisms by which ROI-induced apoptosis are still largely unknown (Clutton, 1997). However, with recent advances into understanding the genetic pathways involved in apoptosis, three common signaling pathways have emerged which may be applicable to free radical-induced apoptosis signaling (Dragovich *et al.*, 1998).

3.1. Mitochondria-Dependent Pathways of Apoptosis

One of the potential mechanisms by which free radicals induce apoptosis is through mitochondria-dependent pathways. *En route* to apoptosis, ROIs have been shown to induce a cascade of events at the mitochondria, which lead to programmed cell death. These events include (i) opening of the mitochondria permeability transition pore (MPTP), (ii) release of cytochrome c from the intermitochondria matrix, and (iii) activation of a family of apoptosis-related cysteine proteases, termed caspases (Zoratti *et al.*, 1995; Halestrap *et al.*, 1998; Cai *et al.*, 1998; Gross *et al.*, 1999).

3.1.1. Opening of the Mitochondrial Permeability Transition Pore (MPTP)

The mitochondria permeability transition pore (MPTP) is a megachannel proteinaceous complex which spans the intermitochondrial matrix. It consists of several inner and outer mitochondrial membrane proteins, including the adenine nucleotide translocator (ANT), the voltage-dependent anion channel (VDAC), the peripheral benzodiasepine receptor, cyclophilin D, hexokinase, creatine kinase and perhaps other unidentified components (Zoratti *et al.*, 1995). The MPTP functions primarily to control the efflux of mitochondrial matrix solutes with molecular masses of <1500 Da from the mitochondria to the cytoplasm, and to maintain a distinct mitochondrial matrix environment from that of cytoplasm (Zamzami *et al.*, 1998). Apoptosis induced by exogenous administration of the the superoxide anion producer, paraquat, has been shown to be preceeded by opening of the MPTP (Kroemer *et al.*, 1997), and subsequent mitochondrial depolarization, organellar swelling and uncoupling of oxidative phsophorylation. In addition, superoxide dismutase-knockout mice exhibited increased loss of mitochondrial permeability associated with increased cell loss (Williams *et al.*, 1998), hinting at a direct role of the superoxide anion in precipitating opening of the transition pore. The mechanism for the opening of the pore has been proposed by

Halestrap to involve oxidative stress-induced thiol modification of the ANT, which enhances binding with the mitochondrial matrix protein, cyclophilin D, allowing the ANT to undergo calcium-dependent conformational changes that result in the formation of a channel (Halestrap *et al.*, 1998). Accordingly, two distinct thiol groups on the ANT have been implicated in the process of enhancing channel formation (Petronilli *et al.*, 1994; Constantini *et al.*, 1996; Chernyak *et al.*, 1996)

3.1.2. Mitochondrial Release of cytochrome c

Opening of the MPTP serves to provide a channel for expulsion of key components of the mitochondrial electron transport chain which are necessary for activation of several downstream apoptotic executors. In particular, the intermitochondrial matrix protein, cytochrome c, has been shown to be ejected from the mitochondria following initiation of apoptosis (Liu *et al.*, 1996), and functions as an essential cofactor in the activation of a family of dowstream apoptosis-related proteases, termed caspases (Li *et al.*, 1997).

3.1.3. Activation of caspases

The caspase family is a family of cysteine proteases that function in the final executory pathways of programmed cell death by mediating proteolysis of a variety of intracellular proteins at specific aspartate residues. Among the many identified substrates are the poly(ADP-ribose) polymerase (PARP), lamin A, U1 70 kDa small nuclear ribonucleoprotein particle, actin, fodrin and Rb (Janicke *et al.*, 1996; Orth *et al.*, 1996; Casciola-Rosen *et al.*, 1996; Mashima *et al.*, 1995; Martin *et al.*, 1995; Kaufmann *et al.*, 1993). The first member of the caspase family, the interleukin-1β converting enzyme (ICE, now designated caspase-1), was initially identified by homology to the pro-apoptotic *C. elegans* protein, *ced-3* (Yuan *et al.*, 1993). Fourteen caspase family members

have since been identified, and it has been shown that caspase-3 and caspase-7 are the key effector caspases upon which most apoptotic signaling pathways appear to converge, and that their activation represents the final end stages of apoptotic execution. Overexpression of caspase-3 is sufficient to trigger apoptosis (Miura *et al.*, 1993), and caspase-3 knockout mice exhibit an embryonic lethal phenotype due to abnormal brain formation caused by the inability to diminish neuronal numbers during development (Kuida *et al.*, 1996).

Caspases are synthesized as proenzymes with variable prodomains and an enzymatic domain. Activation is initiated by post-translational cleavage within the enzymatic domain at specific aspartate residues, yielding large and small subunits, and subsequent association of two large and two small subunits into a heterotetrameric complex completes activation. Removal of the prodomain is not necessary for proteolytic activation, nor is its presence necessary for enzymatic activity (Salvesen *et al.*, 1997; Villa *et al.*, 1997). Since activation requires cleavage at specific aspartate residues, an ability unique to the caspase family, activation can only be mediated through autoactivation or by another caspase. Hence, the caspase family members exist in a biochemical cascade with a specific hierarchy.

At the mitochondria, the ejected cytochrome c participates in apoptosis induction by formation of a complex with apoptosis protease-activation factor-1 (Apaf-1) and procaspase-9, which, in a dATP- or ATP-dependent process, catalyzes the autoactivation of caspase-9 (Li *et al.*, 1997). Active caspase-9 subsequently activates caspase-3, precipitating cellular destruction.

Stridh *et al.* (1998) and Kluck *et al.* (1997) have demonstrated that H_2O_2 is capable of inducing translocation of cytochrome c from the mitochondria to the cytoplasm following two hours of oxidative stress in Jurkat lymphocytes and T lymphoblastoid CEM cells, respectively. In both studies, this was followed by caspase-3 activation. This observation was extended by von Harsdoft and coworkers to primary neonatal cardiac myocytes, where mitochondrial release of cytochome c and caspase-3

activation was also observed following H_2O_2 treatment (von Harsdorft *et al.*, 1999). Caspase activity was also detected by Turner *et al.* (1998) following initiation of apoptosis by H_2O_2 in a cardiac-derived cell line. Direct administration of pro-oxidants to cytoplasmic extracts which do not contain mitochondria, however, does not result in caspase activation, confirming that the activation of caspases and consequent induction of apoptosis, as induced by free radicals, occurs through mitochondria- (and most likely, cytochrome c-) dependent mechanisms (Hampton *et al.*, 1998).

3.1.4. The Role of the Bcl-2 Family

Another indication that free radicals initiate apoptosis through mitochondria-dependent pathways comes from studies of the Bcl-2 gene family (Gross *et al.*, 1999). The Bcl-2 proto-oncogene, the original founding member of the family, was discovered at a chromosomal breakpoint in B cell lymphomas characterized by the frequent t(14;18) translocation (Tsujimoto *et al.*, 1985; Bakhshi *et al.*, 1985). It is localized predominantly in the outer mitochondria membrane (Hockenbery, 1990), although it has also been detected in the endoplasmic reticulum and nuclear membrane (Chen-Levy *et al.*, 1990; Monaghan *et al.*, 1992). Its oncogenic potential derives from its ability to inhibit apoptosis induced by several stimuli (Hockenbery *et al.*, 1990; Jacobson *et al.*, 1993; Korsmeyer, 1992; McDonnell *et al.*, 1989).

Hockenbery and coworkers demonstrated that overexpression of the Bcl-2 gene is capable of protecting cells against exogenous administration of ROIs (Hockenbery *et al.*, 1993). The principle mechanism by which Bcl-2 exerts its anti-apoptotic role has been suggested to involve "guarding the mitochondrial gate" (Gross *et al.*, 1999). Yang *et al.* (1997), and Kluck *et al.* (1997) observed a decreased efflux of cytochrome c from the mitochondria following induction of apoptosis by DNA damaging agents in the presence of ectopic Bcl-2 levels. Accordingly, Shimizu and coworkers reported decreased caspase-

3 activation in Bcl-2-overexpressing cells (Shimizu *et al.*, 1996). Recently, Bcl-2 has been demonstrated to interact directly with components of the MPTP, specifically, VDAC and ANT, in order to regulate release of cytochrome c (Marzo *et al.*, 1998; Shimizu *et al.*, 1999). Thus, given the intimate relationship between the mechanism of Bcl-2 anti-apoptotic function and the mitochondria, the ability of Bcl-2 to inhibit free radical-induced apoptosis provides strong indirect evidence that pro-oxidants are capable of mediating programmed cell death through mitochondria-dependent processes.

3.2. Fas-Dependent Pathways of Apoptosis

The Fas receptor is a member of the tumor necrosis family of receptors which functions in transducing pro-apoptotic signals from the cell surface (Suda *et al.*, 1993). Binding of the receptor to the Fas ligand leads to the formation of a homotrimeric complex of the Fas receptor. Trimerization leads to the recruitment of the intracellular adaptor protein, Fas-associated death domain protein (FADD); the interaction is mediated by protein-protein association *via* an ~80 amino acid residue stretch, morbidly named the "death domain" (Itoh *et al.*, 1993; Chinnaiyan *et al.*, 1995). FADD subsequently interacts directly with caspase-8, leading to its autoactivation (Muzio *et al.*, 1996; Boldin *et al.*, 1996). This, in turn, causes activation of caspase-3 and apoptosis (Fernandes-Alnemri *et al.*, 1996).

FADD-knockout mice exhibit abnormal cardiac development, and FADD-null cardiac myocytes are resistant to several apoptosis-inducing agents (Yeh *et al.*, 1998), confirming that the Fas-mediated pathway of apoptosis is intact and relevant in cardiac myocyte apoptosis. Exposure to the intracellular oxidant, menadione, has been associated with an up-regulation of the Fas receptor (Caricchio *et al.*, 1999). And finally, reperfusion and reperfusion-associated free radical generation has also been related to increased levels of Fas mRNA (Tanaka *et al.*, 1994), implicating Fas-dependent processes as a

plausible mechanism by which oxidative stress-mediated cardiomyocyte apoptosis is achieved.

While increased expression of the Fas receptor is well established as an early event leading to myocardial cell loss during heart failure, less is known regarding the expression profile of its preferred ligand, the Fas ligand. Toyozaki and coworkers found that increased levels of soluble Fas ligand was present in the serum of patients undergoing myocarditis, a form of myocardial inflammation akin to events associated with reperfusion injury (Toyozaki *et al,* 1998). However, a separate laboratory has shown that the increase of the receptor during heart disease in humans is not mimicked by the ligand in all four functional stages (I through IV) of heart disease, and suggested that the increased incidences of apoptotic death was primarily achieved by increased levels of the Fas receptor, and not the Fas ligand (Nishigaki *et al.*, 1997). Part of the explanation for these contradicting results may be that expression of the Fas ligand is responsive to specific stimuli; for example, cardiac failure associated with increased plasma epinephrine levels was shown to be associated with increased levels of Fas ligand protein levels, whereas normal epinephrine levels did not generate the same increase (Romeo *et al.*, 2000). Potentially, different hormonal imbalances during heart disease would result in differential regulation of Fas ligand expression.

3.3. p53-Dependent Pathways of Apoptosis

Amongst the many intracellular targets of ROIs, its ability to inflict damage on DNA has been well documented. ROIs cause chromosome deletions, dicentrics and sister chromatid exchanges. Moreover, ROIs attack DNA at both the deoxyribose sugar residue and the nucleotide base, resulting in sugar fragmentation and base loss, respectively, resulting in single stranded breaks in the DNA backbone (Imlay *et al.*, 1988).

One of the key participants in guarding the genome and maintaining genomic stability against DNA damage is the tumor suppressor, p53 (Yonish-Rouach, 1996). p53

is a nuclear-localized, sequence-specific transcriptional transactivator. The amino-terminus of p53 functions as the transcriptional transactivation domain (Farmer *et al.*, 1992) and interacts directly with DNA containing the sequence 5'-PuPuPuC(A/T)(T/A)GPyPyPy-3' (El-Deiry *et al.*, 1992; Kern *et al.*, 1991). The ability to recognize damaged DNA is conferred by the carboxy-terminus (Lee *et al.*, 1995). Ordinarily, p53 exhibits a short half-life *in vivo*. In the presence of damaged DNA, however, p53 protein levels are increased by stabilization of pre-existing p53 protein and by up-regulation of p53 transcription (Kastan *et al.*, 1991; Kastan *et al.*, 1992).

The mechanisms by which DNA damage is recognized and p53 is stabilized are not fully understood (Ashkenas *et al.*, 1996). One proposed mechanism involves the DNA-dependent protein kinase (DNA-PK), which consists of a 350 kDa catalytic subunit associated with the proteins, Ku70 and Ku80. The Ku proteins bind directly to damaged DNA, and recruit and activate DNA-PK, which then functions to phosphorylate p53 (Anderson, 1993). Phosphorylation of p53 is thought to be the key signal in conferring a longer half-life to p53. Another potential molecule which signal to p53 in the presence of DNA damage is the poly(ADP ribose) polymerase (PARP). Like DNA-PK, PARP binds directly to sites of DNA damage, and mediates an ADP-ribose transfer onto various nuclear proteins . This function of PARP has been shown to be necessary for p53 up-regulation following DNA damage in cell culture systems (Whitacre *et al.*, 1995), although its significance is still under investigation. Strangely, the capacity for p53 up-regulation in response to DNA damage was shown to be unaltered in PARP-deficient mice (Wang *et al.*, 1995). Ultimately, it remains unclear as to whether these signaling molecules reflect one pathway to p53 induction, or represent multiple convergent pathways (Ashkenas *et al.*, 1996).

The first functional role ascribed to p53 following DNA damage was the induction of growth arrest at the restriction point (G1/S) of the cycle cycle, in order to allow for DNA repair (Diller *et al.*, 1990). This function involves activation of transcription of

several growth arrest-associated proteins, including the cyclin-dependent kinase inhibitor, p21 (El-Deiry *et al.*, 1993). Alternatively, in the face of irrepairable DNA damage, p53 functions as a pro-apoptotic factor, and can induce programmed cell death. Guillouf and coworkers demonstrated that introduction of p53 into p53-deficient cells was sufficient to induce apoptosis (Guillouf *et al.*, 1995). In the same study, it was revealed that both the growth arrest and the pro-apoptotic functions of p53 were simultaneously activated, and the two pathways existed independent of one another. This hypothesis was later corroborated by the ability of p21-null cells to undergo p53-dependent apoptosis (Deng *et al.*, 1995), again suggesting a distinctness between the two pathways.

The mechanism of p53-induced apoptosis remains poorly understood. Conflicting reports have been presented as to the dependence of p53-mediated transcriptional activation in the execution of apoptosis. Several groups have reported the ability of cells to undergo apoptosis in the absence of p53-induced transcriptional transactivation (Caelles *et al.*, 1994). Indeed, Haupt and coworkers reported the induction of apoptosis of HeLa cells by p53 lacking the transactivation domain (Haupt *et al.*, 1995). However, other groups have reported the ability of p53 to activate transcription of key pro-apoptotic factors. Miyashita and coworkers demonstrated that p53 functioned to up-regulate levels of Bax, a pro-apoptotic Bcl-2 homologue (Miyashita *et al.*, 1995). Moreover, p53 has also been shown to down-regulate levels of the anti-apoptotic protein, Bcl-2 (Hadler *et al.*, 1994). Given the capacity of Bcl-2 and Bax to heterodimerize (Oltvai *et al.*, 1993), it has been suggested that initiation of apoptosis may be controlled by the ability of p53 to orchestrate a Bax-Bcl2 equilibrium (Miyashita *et al.*, 1994). Another gene whose transcription is enhanced by p53 is Fas (Owen-Schaub *et al.*, 1995). Thus, there is likely considerable cross-talk between the cell surface, the mitochondria and the nucleus in the induction of apoptosis. Finally, Polyak and coworkers have suggested that p53 supports apoptosis by enhancing transcription of genes which serve to increase mitochondrial generation of intracellular ROIs, allowing the elevated levels of ROIs to act in the final

breakdown of cellular structures during the late stages of cell death (Polyak *et al.*, 1997). This would thus hint at the existence of a "vicious circle" in terms of free radicals and apoptosis, where oxygen radicals can act as both the initiator of apoptotic signaling pathways, as well as the effector molecule for mediating cellular damage (Polyak *et al.*, 1997; Wyllie, 1997). A schematic representation of all three pathways is presented in Figure 2.

4. Mechanism of Eukaryotic mRNA Translation

4.0. Introduction

Clearly, apoptosis is an active, gene-driven process, requiring *de novo* production of a myriad of initiators and executioners. In support of this concept, several reports have demonstrated that inhibition of macromolecular biosynthesis, such as inhibition of gene transcription and mRNA translation, can function to protect against programmed cell death (Wyllie *et al.*, 1984; Shi *et al.*, 1989).

The flow of genetic material from the nucleus to the synthesis of a protein from its precursor gene consists of three distinct steps: transcription of the template DNA strand into a complementary messenger RNA (mRNA), translation of the nucleotide sequence genetic code of the mRNA into an immature preproprotein polypeptide, followed by post-translational proteolysis and modification into mature, fully folded and functional proteins. In particular, the mechanism of the second stage, mRNA translation, is mediated by a large family of soluble protein factors, which function in three distinct stages: initiation, elongation and termination (Merrick, 1992). In this section, an overview of the biochemical mechanism of these three stages is provided, and the individual roles that key individual protein factors play during the process of mRNA translation are discussed.

Figure 2. **Apoptotic pathways in the myocardium.** The machinery involved in induction of apoptotic signals and execution of cellular destruction are complex. Three well-studied mechanisms capable of leading to apoptosis of cells in the myocardium include (i) mitochondrial-dependent pathways, (ii) Fas- (receptor)-dependent pathways, and (iii) p53-dependent pathways. The pathways are not completely distinct, but exhibit limited cross-talking.

Figure 2

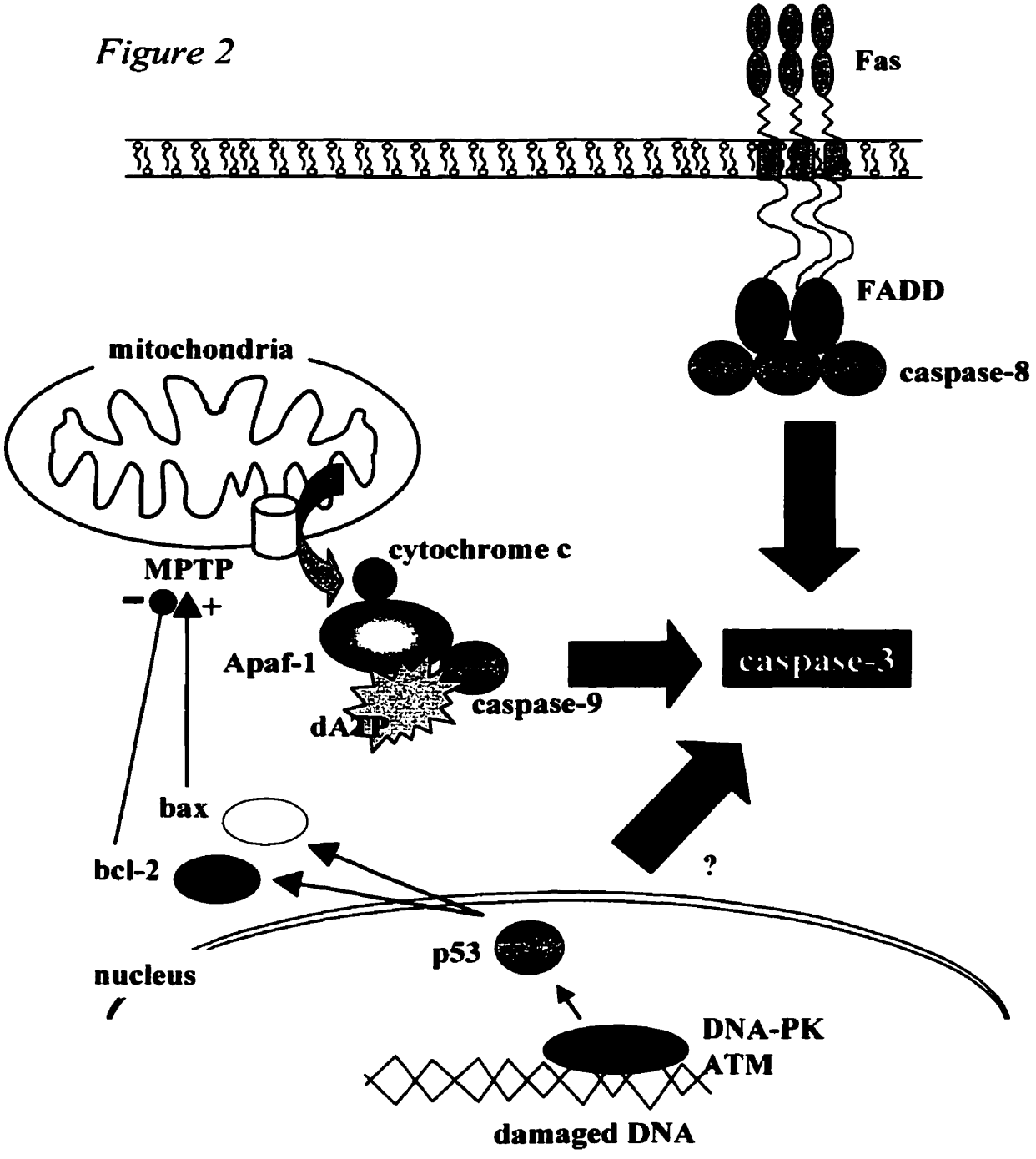
Fas
FADD
caspase-8
mitochondria
cytochrome c
MPTP
Apaf-1
caspase-9
dATP
caspase-3
bax
bcl-2
?
p53
nucleus
DNA-PK
ATM
damaged DNA

4.1. Initiation

The primary purpose of the initiation stage is to facilitate formation of the 80S ribosomal complex, the primary mediator of mRNA translation, at the AUG start codon of the mRNA (Bielka, 1985). The mechanism of initiation of mRNA translation begins by formation of the 43S pre-initiation complex, a conglomeration of a free 40S ribosomal subunit with a variety of initiation factors (eIFs). Amongst these factors are the initiation factor-2 (eIF-2), which functions to bind and recruit the first coded amino acid, methionine, which is conjugated to a tRNA molecule (met-tRNA) and GTP to the 40s ribosomal subunit (Nygard *et al.*, 1980). The eIF-2-met-tRNA-GTP structure is referred to as the ternary complex. The initiation factor-3 (eIF-3) also associates with the ribosomal subunit, functioning to maintain the 40S subunit in its native, free form., as opposed to in association with the 60s ribosomal subunit (Benne *et al.*, 1978).

The next stage involves recognition of the mRNA and association of the 40S ribosome subunit, events mediated by initiation factor-4F (eIF-4F), a complex of eIF-4E, eIF-4A and eIF-4G. The first of these subunits, eIF-4E, functions to recruit the entire eIF-4F complex to the mRNA by direct association with the 5'-guanosine cap of eukaryotic mRNAs (Sonenberg *et al.* 1977; Grifo *et al.*, 1983). The second subunit, eIF-4A, subsequently melts and unwinds the mRNA secondary structure by its single-stranded RNA-dependent ATPase and helicase activity (Lawson *et al.*, 1989; Ray *et al.*, 1985). Finally, the third subunit, eIF-4G, act to recruit the 40S ribosomal subunit to the mRNA cap based on its ability to associate with the eIF-3 already complexed with the ribosome (Hansen *et al.*, 1982; Grifo *et al.* 1983). As mentioned above, the 40S ribosome, in association with the three (and possibly more) initiation factors, localized at the 5'-guanosine cap of the mRNA strand, comprises the 43S pre-initiation complex.

Figure 3. **Schematic representation of the eukaryotic translation initiation.** Initiation of translation facilitates formation of the 80S ribosomal complex to the AUG start codon of the mRNA. The eIF-2-GTP-met-tRNA ternary complex associates with a free 40S ribosomal subunit (already in complex with eIF-3) forming the 43S preinitiation complex (1). The eIF-4F complex, consisting of eIF-4E, eIF-4A and eIF-4G, associates with the 5'-guanosine cap of the mRNA, an interaction mediated primarily by eIF-4E (2). eIF-4G mediates association with eIF-3 of the 43S preinitiation complex, recuiting the 40S ribosome to the mRNA (3). The ribosome-initiation factor complex scans the mRNA in a 5'-3' direction, aided by the mRNA unwinding action of eIF-4A (4). Upon recognition of the AUG start codon, GTP hydrolysis occurs (aided by eIF-5), releasing the initiation factors, allowing for association with the 60S ribosomal subunit and completing translational initiation (5). The ribosome stands poised to begin the elongation cycle. The diagram is adapted from Merrick, (1992).

Figure 3

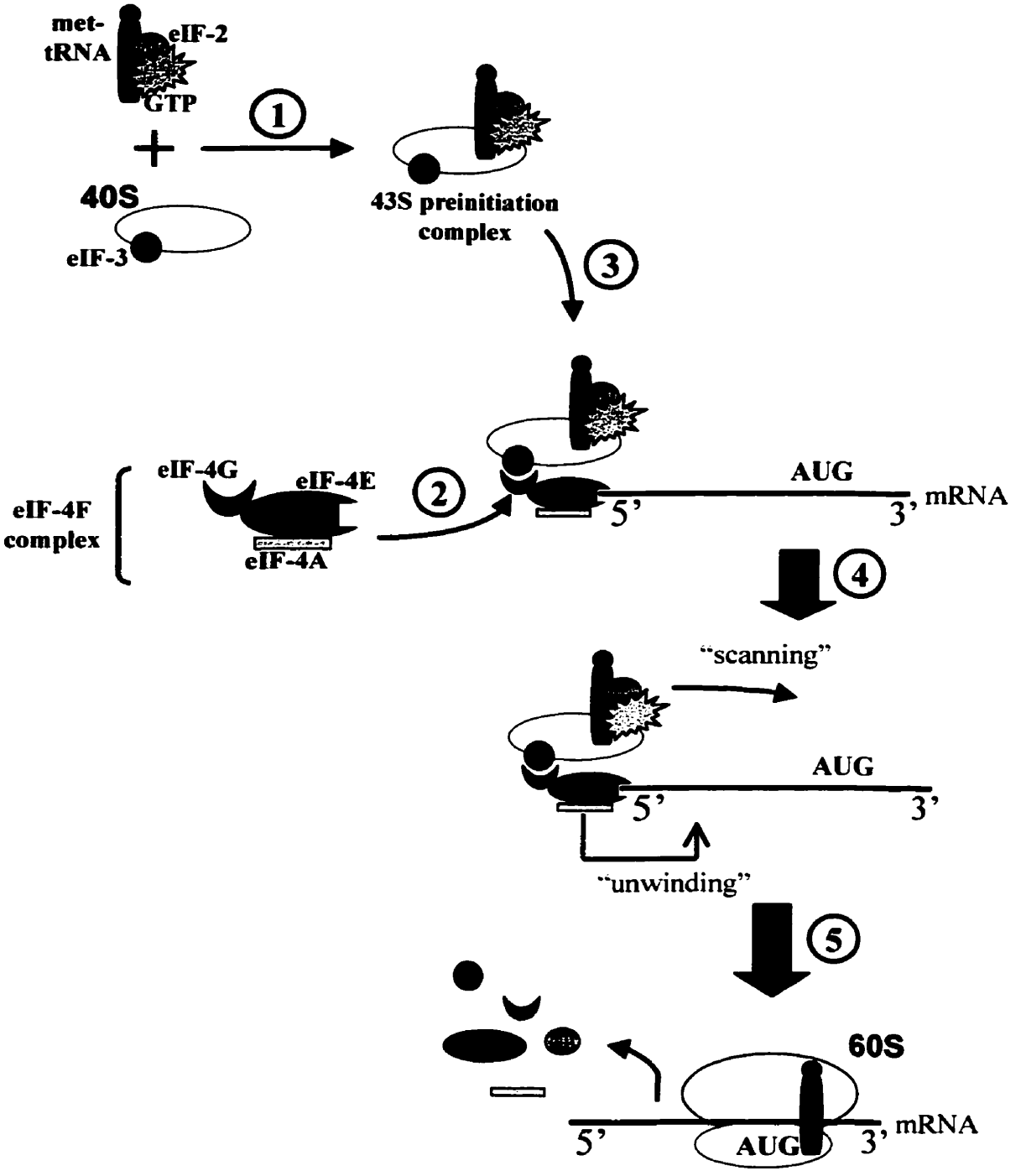
met-
tRNA
eIF-2
GTP
1
40S
eIF-3
43S preinitiation
complex
3
eIF-4F
complex
eIF-4G
eIF-4E
eIF-4A
2
AUG
5'
3', mRNA
4
"scanning"
AUG
5'
3'
"unwinding"
5
60S
5'
AUG
3', mRNA

At this point, the pre-initiation complex "scans" the mRNA in a 5'- to-3' direction until detection of the AUG "start" codon by the tRNA anticodon (Kozak, 1978, 1980, 1989, 1999). Upon recognition of the start codon, the GTP of the ternary complex is hydrolyzed, an event catalyzed by eIF-5, causing the release of the initiation factors from the ribosome (Ghosh *et al.*, 1989), and allowing for association with the 60s ribosomal subunit. The complex, now with a sedimentation coefficient of 80s, is poised for the elongation cycle. A schematic diagram of translation initiation is presented in Figure 3.

Formation of the 80s ribosome and hydrolysis of the ternary complex is associated with release of a GDP-eIF-2 binary complex (Begehi *et al.*, 1982; Pain *et al.*, 1983). Given eIF-2's heightened affinity for GDP over GTP, a nucleotide exchange factor is present to facilitate replacement of the GDP in favour of GTP. This role is mediated by a factor designated initiation factor-2B (eIF-2B) (Konieczny *et al.*, 1983). Indeed, "recharging" of eIF-2, thereby permitting it to form another ternary complex, represents the primary site of regulation of mRNA translation (Hershey, 1989). Cessation of protein synthesis can be effected by phosphorylation of eIF-2 at the serine-51 residue (Colthurst *et al.*, 1987). This has the effect of enhancing eIF-2 association with GDP and preventing eIF-2B-mediated nucleotide exchange (Rowlands *et al.*, 1988; Pain, 1988). Conversely, phosphorylation of eIF-2B enhances nucleotide exchange activity (Dholakia *et al.*, 1989a, 1989b). Thus, regulation of ternary complex formation, and therefore, of mRNA translation, can be regulated by an interplay of phosphorylation of eIF-2 and eIF-2B.

4.2. Elongation

Following successful intiation and recognition of the start codon, the elongation cycle serves to recruit appropriate amino acids (complexed to tRNAs) to the ribosome in a codon-dependent manner for transfer onto the growing polypeptide chain. According to the "half-site" model of Moazed and Noller, the 80S ribosome contains three sites for attachment of amino acid-tRNA complexes: the E-site is the exit site, the P-site is the

peptidyl-tRNA site and the A-site serves to allow binding of incoming aminoacyl-tRNAs. (Moazed *et al.*, 1986) Elongation factor-1 alpha (EF–1α) functions to bind to and recruit aminoacyl-tRNAs to the A-site of the ribosome in a GTP-dependent process (Nissen *et al.*, 1995). The structure, EF–1α-GTP-aminoacyl-tRNA, is also referred to as a ternary complex, although it is obviously distinct from the complex with the same name involved in initiation. Upon hydrolysis of GTP, the EF–1α-GDP complex is released from the ribosome. An enzymatic activity associated with the peptidyltransferase center of the large ribosomal subunit facilitates peptidyl-bond formation between the growing polypeptide in the P-site and the newly recruited amino acid in the A-site (Nygard *et al.*, 1990). This results in transfer of the polypeptide from the P-site to the A-site (Nyborg *et al.*, 1998). Next, the elongation factor-2 (EF-2), in another GTP-dependent process, moves the mRNA by three nucleotides to allow exposure of the next codon in the A-site, in a process designated "translocation" (Hershey, 1989). This also results in the shifting of the tRNA complexes, such that the growing peptide previously in the A-site is translocatd to the P-site, the "empty" tRNA previously in the P-site is translocated to the E-site, and the tRNA previously in the E-site is ejected from the ribosome (Nyborg *et al.*, 1998). A schematic diagram of the cycle is presented in Figure 4.

In an analogous reaction to the one involving the initiation factor, eIF-2, the EF–1α-GDP binary complex is "recharged" by the nucleotide exchange complex, consisting of elongation factor-1β, -1γ, and –1δ, which function to recycle the GDP-associated "off" form of EF–1α back to its active, "on" form, EF–1α-GTP. (Riis *et al.*, 1990; Janssen *et al.*, 1988; Iwasaki *et al.*, 1976) The cycle thus begins again by recruitment of an EF–1α-GTP-aminoacyl-tRNA complex to the now empty A-site. A schematic diagram of the elongation cycle is provided in Figure 4.

Figure 4. **Schematic representation of the eukaryotic elongation cycle.** Each successive round of the elongation cycle functions to add one amino acid onto the growing polypeptide chain being translated. EF–1α-GTP associates with an aminoacyl-tRNA (aa-tRNA) forming a ternary complex (1), and recruits it to the A-site of the ribosome (2). GTP hydrolysis occurs, resulting in release of the EF–1α-GDP binary complex (3). A peptide bond is formed between the recruited amino acid and the growing polypeptide chain resident in the P-site of the ribosome (4). Translocation is mediated by EF-2 in a GTP-dependent process (5), liberating the A-site, restarting the cycle at step 2. The EF–1α-GDP binary complex is made ready for another round of the cycle by a nucleotide exchange, replacing the GDP with GTP. The reaction is catalyzed by the exchange complex, EF-1βγδ (7). The diagram is adapted from Merrick, (1992).

Figure 4

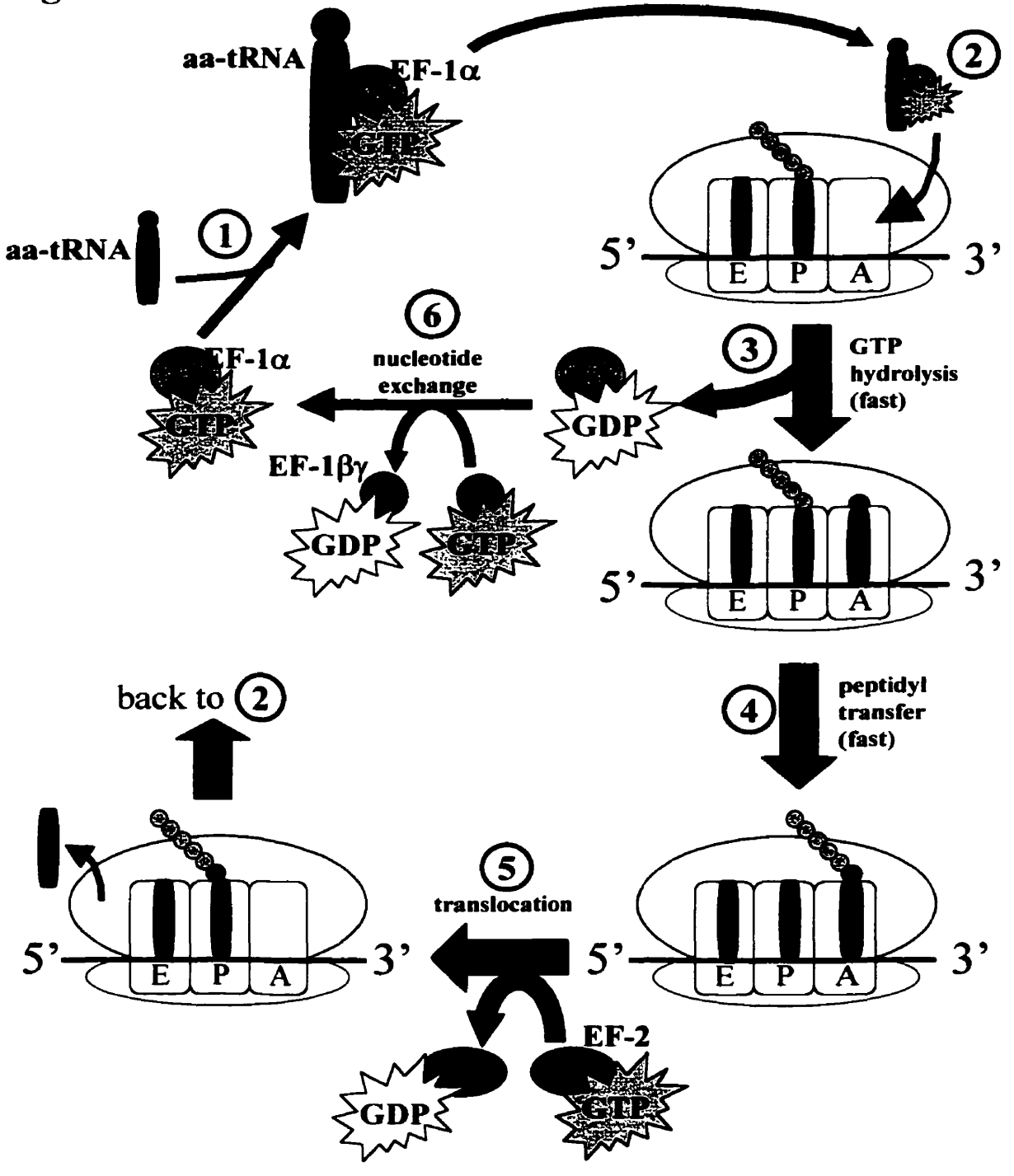
aa-tRNA
EF-1α
GTP
aa-tRNA
1
2
5'
E
P
A
3'
6
nucleotide
exchange
EF-1α
GTP
EF-1βγ
GDP
GTP
3
GTP
hydrolysis
(fast)
GDP
5'
E
P
A
3'
back to 2
4
peptidyl
transfer
(fast)
5
translocation
5'
E
P
A
3'
5'
E
P
A
3'
EF-2
GDP
GTP

4.3. Termination

Upon exposure of a "stop" codon (UAA, UGA, UAG) in the ribosomal A-site, a release factor (RF) associates, in a GTP-dependent manner, with the stop codon and catalyzes release of the peptide from the ribosome. It appears that an additional nucleotide adjacent to the stop codon is necessary for recognition of the release factor (Konecki *et al.*, 1977; Tate *et al.*, 1974). Release of the peptide causes dissociation of the ribosomal subunits, in readiness for another round of mRNA translation.

5. Elongation Factor-1 Alpha (EF–1α)

5.0. Introduction

One of the most well characterized components of the protein synthesis machinery is the elongation factor-1 alpha (EF–1α) (Negrutskii *et al.*, 1998). The reason for the disproportionate amount of information about this factor is due, in part, to its abundance in the cell (constituting > 1% of total soluble proteins), which has made biochemical analysis, even in the 1960's, reasonably easy. In the following section, a detailed review of the properties of this factor is provided. The first two parts give a historical review of EF–1α and its functional role in the cell. Next, the genetics of EF–1α is considered, with detailed analysis of the primary amino acid and nucleotide sequences, with emphasis on functional domains within the polypeptide. The section concludes with a discussion of the various pathways of regulation of EF–1α.

5.1. EF–1α Function in mRNA translation

The first elongation factor was isolated in 1963 in the prokaryotic organism, *E. Coli*, as a complex of two molecules which was shown to act as a carrier of aminoacyl-tRNAs to the ribosome during mRNA translation (Arlinghaus *et al.*, 1963;Nishizuka *et al.*, 1966). The complex, designated, elongation factor-T (for transfer) was later separated

into temperature unstable (Tu) and temperature stable (Ts) components. EF-Tu was later shown to be the factor which associates with GTP and aminoacyl-tRNA to form the ternary complex, and functioned in the recruitment of the complex to the ribosome (Miller *et al.*., 1970). Following association with the ribosome, the GTP is hydrolyzed to GDP. EF-Ts, in turn, functions as a nucleotide exchange factor, "recharging" EF-Tu with GTP, the driving force of the elongation cycle (Weissbach *et al.*, 1970).

Moving away from the prokaryote, Schweet and coworkers then isolated purified elongation factors from rabbit reticulocyte lysates, designated EF-1 and EF-2 (Arlinghaus *et al.*, 1963). Similar to the bacterial EF-T, EF-1 was also shown to be a complex of two distinct subunits, later designated EF−1α (equivalent to bacterial EF-Tu) and EF-1βγδ (equivalent to EF-Ts) (Ibuki *et al.*, 1968).

The ability of the EF−1α subunit to functionally substitute for EF-Tu, and to function in mRNA translation was demonstrated in a series of experiments in the 1970's. Moon and Weissbach first reported the ability of EF−1α to form ternary complexes, using a Millipore filtration system, which functioned to retain lone aminoacyl-tRNA, GTP and EF−1α components, but allowed the passage of ternary complexes (Moon *et al.*, 1972; Weissbach *et al.*, 1973) because of their altered conformational cork-screw structure (Nissen *et al.*, 1995). The ability of purified ternary complexes, consisting of the EF−1α component, to function in mRNA translation was subsequently assayed by incubation with ribosomes, poly-U tract mRNAs and radiolabelled phenylalanine-tRNA. It was observed that the presence of the ternary complex resulted in the production of the polyphenylalanine peptide, the coded amino acid for the UUU codon (Weissbach *et al*, 1973; Ibuki *et al.*, 1968; Nolan *et al.*, 1975). Through these experiments, the mechanism of EF−1α action was elaborated: GTP-bound EF−1α associates with the aminoacylated tRNA and recruits the ternary complex to the ribosome. Interaction with the ribosome promotes GTP hydrolysis and release of the EF−1α-GDP complex, which is recycled back to EF−1α-GTP by EF-1βγδ, allowing for association with another aminoacyl-tRNA,

the formation of another ternary complex and in another cycle of elongation (Ryazanov *et al.*, 1991).

5.2. EF–1α Function in Non-Protein Synthesis-Related Roles

Because of its abundance in the cell, and owing to the fact that its level of expression is in molar excess of its known ligands the mRNA translation machinery, other functions of EF–1α unrelated to the protein synthesis pathway are being intensely investigated. Among the best characterized of these non-canonical roles is the ability of EF–1α to function as an actin-binding and bundling-protein in *Dictyostelium discoideum* (Yang *et al.*, 1990; Dharmawardhane *et al.*, 1991). EF–1α cross-links actin filaments into square-packed, "checkerboard" patterns with 6.9 nm interfilament spacings, with each "checkerboard layer" separated at 10 nm intervals (Demma *et al.*, 1990). *In vivo* immunocytochemical studies have revealed that EF–1α is co-localized at intersection points of the actin filaments (Owens *et al.*, 1992). A similar role of actin bundling has been ascribed to EF–1α in the *Tetrahymena* (Kurasawa *et al.*, 1996), carrot (Yang *et al.*, 1993); algae (Collings *et al.*, 1994), rabbit (Bektas *et al.*, 1994) and mouse (Liu *et al.*, 1996). Due to the peculiar nature of EF–1α-mediated actin filament cross-linking and its ability to form square-packed bundles, it has been proposed that the altered cytoskeleton represents unique, intracellular "microenvironments", with properties more conducive to motility, anchorage or aminoacyl-tRNA channeling (Condeelis, 1995).

EF–1α has also been shown to affect the intracellular microtubule network, and has been postulated to function in regulating the dynamics of microtubule stability during mitosis. EF–1α forms complexes with α–, β–, and γ–tubulin and heat shock protein 70 (hsp70), a complex mimicking the components of the mitotic spindle microtubule organizing centers (Marchesi *et al.*, 1993). Moreover, EF–1α has been reported to have both microtubule destabilizing (Shiina *et al.*, 1994) and microtubule-bundling (Durso *et al.*, 1994) activity. Orchestration of these two opposing effects has been proposed to be

integral in mediating microtubule plasticity during the M phase of the cell cycle (Condeelis, 1995; Negrutskii *et al.*, 1998).

Recently, EF–1α has also been suggested to be a key player during the execution of the apoptotic pathway. Increased expression has been shown to confer increased susceptibility to serum deprivation-induced apoptosis in mouse 3T3 fibroblasts, while decreased expression confers decreased susceptibility (Duttaroy *et al.*, 1998). Also, increased expression of EF–1α mRNA levels has been detected in erythroleukemic cells undergoing p53-dependent apoptosis, and the EF–1α gene has been suggested to be directly activated by p53 itself upon the activation of programmed cell death (Kato, 1999; Kato *et al.*, 1997).

Other potential functions of EF–1α include participation in cellular transformation and metastasis (Tatsuka *et al.*, 1992; Taniguchi *et al.*, 1991), activation of phosphatidylinositol-4-kinase (Yang *et al.*, 1993) and ubiquitin-dependent proteolysis of N-terminus blocked proteins (Gonen *et al.*, 1995). The bacterial EF-Tu has recently been reported to function as a chaperone molecule to protect against heat shock-induced denaturation of cytosolic proteins (Caldas *et al.*, 1998). Whether this function applies to the eukaryotic EF–1α is still unknown.

5.3. EF–1α Primary Structure

Since the discovery of EF–1α and the elucidation of its function(s), several EF–1α cDNAs, approximately 1.8-1.9kb in length, have been isolated and characterized from numerous non-mammalian and mammalian species, including *Artemia salina* (van Hemert *et al.*, 1983), *Saccharomyces cerevisiae* (Nagata *et al.*, 1984), *Candida albicans* (Sundstrom *et al.*, 1990), *Stylonychia lemnae* (Bierbaum *et al.*, 1991), *Dictyostelium discoideum* (Yang *et al.*, 1990), *Mucor racemosus* (Linz *et al.*, 1986), *Drosophila melanogaster* (Hovermann *et al.*, 1988), *Xenopus laevis* (Krieg *et al.*, 1989), mouse (Lu *et al.*, 1992), rat (Ann *et al.*, 1992), rabbit (Cavallius *et al.*, 1992) and human (Brands *et al.*,

1986; Uetsuki *et al.*, 1989). The predicted molecular weight of the EF–1α protein varies between 48-52 kDa., depending on the species. Moreover, the human EF–1α genomic sequence has also been isolated from human fibroblasts. The gene consists of eight exons and seven introns, stretching a length of approximatly 3.5 kb (Uetsuki *et al.*, 1989). The EF–1α promoter was demonstrated to be a stronger promoter than the cytomegalovirus (CMV) and the adenovirus major late promoter (Mizushima *et al.*, 1990).

Analysis of EF–1α sequences from the isolated mammalian and non-mammalian cDNAs reveals a high degree of conservation of the primary nucleotide and amino acid sequences throughout evolution. For example, the primary amino acid sequence of the human EF–1α polypeptide exhibits 76% identity and 84% similarity to its most distant eukaryotic relative, the slime mold. Human and rabbit EF–1α are 100% identical (Merrick *et al.*, 1990). Moreover, the degree of inter-species conservation is heightened in EF–1α's functional domains (Riis *et al.*, 1990). For instance, comparison of human EF–1α sequences with its prokaryotic counterpart from *E. Coli.* reveals an overall 33% identity, but a 59% identity in the GTP-binding domain. A detailed dissection of the functional domains of EF–1α is presented in the following section.

5.4. EF–1α Functional Domains

Due to the interest in GTP-binding proteins and their role in cell signaling and oncogenesis, among the best characterized of EF–1α's functional domains is its GTP-binding domain. Analysis of nine functionally different members of the GTP-binding protein family has revealed a common motif. The consensus sequence consists of three consensus elements, GXXXXGK, DXXG, and NKXD, with spacing requirements of ~40-80 amino acids between the three elements (Dever *et al.*, 1987). X-ray crystallography has shown that these sequences are capable of forming the GTP-binding cleft, such that the first two elements form interactions with the phosphate portion of the GTP molecule, and the third element is involved in nucleotide specifity (Jurnak *et al.*,

1990; Nyborg *et al.*, 1990). In the EF–1α peptide in particular, the GTP-binding domain is found in the N-terminal region, ranging between amino acids 14-175, depending on the species (Dever *et al.*, 1987). As mentioned previously, the domain exhibits a high degree of conservation throughout evolution, and retains complete conservation at the primary amino acid sequence from yeast to man.

Another domain of EF–1α is the EF–1β-binding domain, which functions to facilitate nucleotide exchange. Work by van Damme and coworkers have demonstrated that a limited proteolyzed EF–1α protein lacking residues 288-461 in the C-terminus end lacked the ability to mediate association with EF–1β (van Damme *et al.*, 1992). However, 3D x-ray crystallography of its bacterial homologue, EF-Tu, has shown that EF-Ts associates extensively with the N-terminus of EF-Tu, with limited interaction with the C-terminus (Clark *et al.*, 1990). The conflicting reports may be due, as proposed by van Damme *et al.* (1992), to alterations in conformational structure of EF–1α following removal of C-terminal regions, which affect EF–1β association at the N-terminus.

EF–1α also associates with aminoacyl-tRNAs, in order to form the stable EF–1α-GTP-tRNA ternary complex. The ability of EF–1α to interact with aminoacyl-tRNA has been shown to reside in the N-terminal region, both by biochemical and structural studies (van Damme *et al.*, 1992). Especially important are residues lysine-208 and lysine-237, which were found to be important in mediating association with tRNA (van Noort *et al.*, 1984).

5.5. Non-Mammalian EF–1α Isoforms

Multiple copies of EF–1α exists in several different species. In the yeast *Saccharomyces cerevisiae*, two unlinked EF–1α genes are present in the genome, which both encode for identical and interchangeable proteins (Nagata *et al.*, 1984). The fungus *Mucor racemmous* possesses three EF–1α genes (Linz *et al.*, 1986). Again, the products of the three genes appear to be indistinguishable, and no function has been directly

attributed to the extra copies of EF–1α. Song *et al.* (1987) and Pingoud *et al.* (1990) have demonstrated that EF–1α gene dosage is directly proportional to translation fidelity, suggesting that the extra copies may contribute to reducing errors associated with mRNA translation.

In other species, EF–1α isoforms exhibit cell type-dependent or development-dependent patterns of expression. *Drosophila melanogaster* possesses two distinct EF–1α-like genes, F1 and F2, which encode for two non-identical proteins that are differentially expressed during development. F1 is a ubiquitous gene expressed in all cells, whereas F2 is restricted to the pupal stage of development (Walldorf *et al.*,. 1985). In *Xenopus laevis*, there are three active EF–1α genes, 42Sp50, EF–1αO, EF–1αS, which are all expressed in early development, but only the EF–1αS isoform is present in the adult (Dje *et al.*, 1990).

5.6. S1, the Mammalian EF–1α Isoform

In mammals, two EF–1α genes exist. The first gene, EF–1α, represents the house-keeping gene ubiquitously expressed early in mammalian development. A second EF–1α-like cDNA, S1, was isolated in 1991 in the rat (Ann *et al.*, 1991), and was shown to exhibit tissue-specific and developmental-specific expression pattern: S1 transcripts were detected only in post-development brain, heart and skeletal muscle tissues (Lee *et al.*, 1992; Lee *et al.*, 1993a). Specifically in the brain, S1 mRNA is localized to the neuronal sub-population of the organ, and is absent in the glial compartment (Lee *et al*, 1993b). Since its first identification, S1 cDNAs have also been isolated from mouse, rabbit and man (Lee *et al.*, 1995; Knudsen *et al.*, 1993; Kahns *et al.*, 1998).

S1, like EF–1α, encodes for a 50 kDa protein. It bears 72% homology with EF–1α at the primary nucleotide sequence level, and 92% identity at the amino acid level (Lee *et al.*, 1995). The GTP-, EF–1βγ-, and tRNA-binding domains present in EF–1α are completely conserved in S1. Accordingly, Kahn *et al.* have demonstrated that purified S1

protein is capable of stimulating *in vitro* mRNA translation (Kahns *et al.*, 1998). Whether S1 is able to participate in the other non-traditional roles of EF–1α is, at present, unknown.

5.7. EF–1α Regulation

Regulation of EF–1α mRNA and protein expression in the cell has been a topic of intense investigation. EF–1α expression is controlled largely by translational mechanisms. EF–1α belongs to a family of coordinately regulated proteins whose mRNAs bear a 5'-terminal oligopyrimidine (5'-TOP) sequence (Loreni *et al.*, 1993). The 5'-TOP sequence is a pyrimidine-rich stretch found in the 5'-terminal cap region of the untranslated region in these mRNAs, and has been shown to be necessary, although in itself insufficient, to regulate the efficiency of EF–1α mRNA translation (Levy *et al.*, 1991). Association of *trans*-binding factors to the 5'-TOP element causes redistribution of the mRNA, either into translation-inactive mRNA-ribonucleoprotein (mRNP) pools, or into translation-active polyribosome pools (Avni *et al.*, 1994; Avni *et al.*, 1997). One of the *trans*-binding factors has been recently identified as the La autoantigen, a 57 kDa RNA-binding protein implicated in translational initiation of poliovirus and immunodeficiency viruses (Pellizzoni *et al.*, 1996). This mode of regulation of EF–1α expression has been shown to be involved in growth factor stimulation and development. Upon mitogenic stimulation, mouse 3T3 fibroblasts raise intracellular EF–1α protein levels by recruitment of the pre-existing EF–1α mRNA to the actively translating polyribosome pool (Jeffries *et al.*, 1994). Also, dimunition of EF–1α levels in certain cell types during *Xenopus laevis* development has also been associated with redistribution of EF–1α mRNA levels to the translation-inactive mRNP pool (Loreni *et al*, 1993). Translation of 5'-TOP-bearing mRNAs, including EF–1α, is sensitive to, and can be inhibited by, the p70 S6 kinase inhibitor, rapamycin (Terada *et al.*, 1994).

6. H9c2(2-1) Cardiac Myoblast Cell Line

The H9c2(2-1) cardiac myoblast clonal cell line (Kimes *et al.*, 1976) was originally derived from embryonic rat heart ventricular tissue at 13 day gestation, using a "selective serial passage" technique described previously by Yaffe (1968). Using these protocols, fibroblasts and other non-cardiac cells were removed and the cardiac myoblast sub-population was enriched by differential attachment of cells to tissue culture dishes.

H9c2(2-1) cardiac myoblasts propagate as mononucleated myoblast cells under normal serum conditions, and represent undifferentiated cardiac precursor cells. While Kimes and Brandt reported that the cells can be induced to differentiate into multinucleated myotubes by reduction of serum conditions from 10% to 1%, and that fusion involves over 95% of cells in culture, the differentiated cells possess morphological and biochemical characteristics of skeletal myotubes, and not cardiac myocytes (Kimes *et al.*, 1976). No appearance of intercalated disks or specialized gap junctions were observed by electron microscopy, and multinucleated myotubes reminiscent of skeletal myotubes were observed. Moreover, differentiated H9c2(2-1) cultures possessed a skeletal muscle-specific isoform of creatine phosphokinase (Kimes *et al.*, 1976). However, Hoch and coworkers later reported cardiac-specific isoforms of Ca2+/calmodulin-dependent protein kinases in differentiated H9c2(2-1) cultures (Hoch *et al.*, 1998). Hescheler and coworkers have proposed that the discrepancy is caused by dedifferentiation of these cells into a mesodermal-derived myoblast precursor induced by adaptation of these cells to culture conditions, and thus, differentiated H9c2(2-1) myocytes represent an amalgamation of both skeletal and cardiac muscle phenotypes (Hescheler *et al.*, 1991).

Undifferentiated H9c2(2-1) cultures have been used extensively as an *in vitro* model of the myocardium for the study of reperfusion injury and the mechanisms involved in cell death. Treatment with the pro-oxidant H_2O_2 induces programmed cell death in H9c2(2-1) cardiac cells with apoptosis-associated caspase activation and DNA

fragmentation (Turner *et al.*, 1998). Introduction of heat shock protein 70 (hsp70) has been shown to confer protection against oxidative stress-induced cell death (Mestril *et al.*, 1994; Chong *et al*, 1998). Similarly, inhibition of poly(ADP-ribose) synthetase activity also protects again oxidative injury of H9c2(2-1) cultures (Gilad *et al.*, 1997).

7. Manganese Superoxide Dismutase (MnSOD)-Knockout Mice

Mice lacking the antioxidant, manganese superoxide dismutase (MnSOD), were generated by targeted disruption of exon 3 of the *Sod2* gene, by homologous recombination (Li *et al.*, 1995). The disruption resulted in the production of a shortened mRNA and loss of enzyme activity. Whereas heterozygous mice possessed 48.9-55% MnSOD activity relative to wildtype littermates, MnSOD activity was undetectable in homozygous mice. Consequently, while heterozygous animals survived with no abnormal phenotypes, homozygous animals die within 10-15 days following birth with a dilated cardiomyopathy, ventricular wall thinning, cardiomyocyte hypertrophy and metabolic acidosis (Li *et al.*, 1995). Electron micrographs indicated enlarged and swollen mitochondria. No evidence of motor disturbances or central nervous system failures were evident. Fibroblasts derived from MnSOD-knockout animals exhibited a heightened sensitivity to the O_2^- generator, paraquat (Huang *et al.*, 1997), and MnSOD-knockout mice exhibited increased oxidative damage to the iron-sulfur proteins in the mitochondria, as well as an increased loss of mitochondrial permeability and heightened incidences of cell death (Williams *et al.*, 1998).

Heterozygous $MnSOD^{+/-}$ mice appear unaffected by a ~50% reduction in MnSOD activity, and no major abnormalities inflicted heterozygous animals throughout its lifespan. Moreover, $MnSOD^{+/-}$ pulmonary tissues exposed to hyperoxic conditions (100% oxygen) for 75 hours or 90 hours did not develop any ultrastructural abnormalities, suggesting that 50% MnSOD activity is sufficient for normal development, aging and survival in a high oxygen environment (Tsan *et al.*, 1998).

8. Specific Aims of the Present Thesis

One of the primary focuses of Dr. Wang's laboratory has been the study of the intracellular roles of the elongation factor, EF–1α. Given the previously reported involvement of EF–1α in apoptotic induction, the principal aim of this project was to study the effects of oxidative stress-initiated apoptosis on EF–1α expression. To attain this objective, two systems were employed as models of the myocardium undergoing oxidative stress : 1) the H9c2(2-1) cardiac myoblast cell culture system following exposure to exogenous administration of H_2O_2, and 2) tissue samples obtained from MnSOD-knockout mice. The specific aims of the present thesis were to test the following hypotheses:

i) Induction of apoptosis of H9c2(2-1) cardiomyoblasts by administration of H_2O_2 is correlated with altered expression of the EF–1α protein,

ii) Abrogation of the alteration in EF–1α levels protects against H_2O_2-induced cytotoxicity in H9c2(2-1) cardiomyoblasts, and

iii) *In vivo* oxidative stress, as represented in transgenic mice lacking the antioxidant, MnSOD, is correlated with a similarly altered level of expression of EF-1α

MATERIALS AND METHODS

Materials

The H9c2(2-1) cardiac myoblast cell line (ATCC CRL 1446) was obtained from the American Type Culture Collection. Dulbecco's Modified Eagle Medium (DMEM), heat-inactivated horse serum (HS) and fetal calf serum (FCS) were purchased from Gibco BRL Life Technologies. Terminal transferase enzyme was purchased from Promega. Biotin-dUTP and streptavidin-FITC was obtained from Boehringer-Mannheim. TriZol reagent was obtained from Gibco BRL Life Technologies. Ponseau S solution was obtained from Sigma. Protein quantification assay reagent was obtained from Bio-Rad. All restriction enzymes were obtained from Pharmacia.

Plasmids

Plasmids containing the full length mouse EF–1α cDNA (pCCD29) and the human EF–1α promoter (pEF-BOS) were generous gifts of Dr. X. Lu (U. Ottawa, Canada) (Lu *et al.*, 1989) and Dr. Nagata (Osaka Bioscience Institute, Japan) (Mizushima *et al.*, 1990), respectively. The concentration and purity of the plasmid DNA was confirmed by spectrophotometry at 260 nm.

Antibodies

The EF–1α-specific antibodies were generated and provided by Dr. A. Khalyfa (McGill Univ.). The actin-specific antibody was purchased from Santa Cruz. Secondary goat anti-rabbit IgG $F(ab)_2$ fragments complexed to horseradish peroxidase were purchased from Cappel.

H9c2(2-1) cardiac myoblast cell cultures

Cell culture : Embryonic rat heart ventricle-derived H9c2(2-1) cardiomyoblasts were seeded in 100 mm culture dishes at a density of 250,000 cells per plate, and maintained in DMEM supplemented with 10% heat-inactivated FCS and penicillin-streptomycin (50 U/mL and 50 ug/mL, respectively), with media changes every two days. The cultures were incubated at 37 °C in the presence of 5% CO_2.

Induction of oxidative stress : To induce oxidative stress, the cultures were first washed twice with serum-free DMEM, and then exposed to 35 μM, 70 μM, 140 μM, 210 μM, 350 μM, 700 μM, 1.4 mM, 2.1 mM and 3.5 mM of H_2O_2 in serum-free DMEM at 37°C for 24h. In one set of samples, catalase was added at a concentration of 1 U/mL.

Assessment of cell viability : Cell viability following oxidative stress was assayed by a colorimetric assay based on the ability of the mitochondria in live but not dead cells to convert 3-(4,5-dimethylthiazol-2-yl)-2,5-diphenyltetrazolium bromide (MTT) to a blue end product, as previously described (Carmichael *et al.*, 1987). Following treatment, the cultures were incubated with 2 mg/mL MTT dissolved in phenol red-free DMEM for 4 h, followed by the addition of 0.5 mL DMSO to allow visualization of the final blue formazon product. The optical density was measured by an ELISA plate reader at 595 nm.

DNA laddering and Terminal dUTP Nick-End Labeling (TUNEL)

DNA laddering : H9c2(2-1) cell monolayers exposed to 700 μM H_2O_2 for 0, 1, 2, 3 and 4 days were washed in phosphate-buffered saline (PBS) (136 mM NaCl, 2.7 mM KCl, 8.1 mM Na_2HPO_4, and 1.5 mM KH_2PO_4), and scraped. Cells were collected by centrifugation at 6000 rpm for 1 min, and the cell pellet was lysed in 400 μL lysis buffer (100 mM NaCl, 25 mM EDTA, 10 mM Tris pH 7.4, 0.5% SDS and 0.4 mg/mL proteinase K) by overnight incubation at 56°C. Three phenol:chloroform (1:1) washes were performed to remove protein contaminants, and the DNA in the aqueous layer was

precipitated by addition of 40 µL 5 M sodium chloride (NaCl), and 1 mL 95% ethanol. The precipitate was resuspended in TE (10 mM Tris, 1 mM EDTA), and 5 µg of the extracted DNA was separated on a 1% agarose gel containing ethidium bromide, and visualized by UV transillumination.

Terminal dUTP Nick-End Labeling (TUNEL) : H9c2(2-1) cells were cultured in 8-chamber culture slide, followed by oxidative challenge by exposure to 175 µM, 350 µM and 700 µM H_2O_2 for 24 h. Following oxidative stress, the cells were fixed with 1:1 methanol : acetone for 30 min at –20°C. The cells were then subsequently rehydrated in 1x PBS at room temperature for 30 min, and incubated with 0.3 U/ µL terminal transferase and 10 µM biotin-dUTP for 1 h at 37°C in order to nick-end label fragmented DNA. The terminal transferase reaction was stopped by addition of 300 mM sodium chloride and 30 mM sodium citrate. The slides were washed three times with PBS, with gentle shaking. Subsequently, the cultures were incubated with streptavidin-FITC in a dilution of 1:15 for 30 min at 37°C, and subjected to three more washes in PBS. The stained nuclei were visualized by fluorescence microscopy.

Fluorometric caspase assay

Caspase-3 and caspase-8 activity was measured using a fluorometric assay modified from Nicholson *et al.*, (1995). Control and H_2O_2-treated H9c2(2-1) monolayer cultures were washed once with PBS and gently scraped. Cells were collected by centrifugation at 6000 rpm for 1 min, and the cell pellet was lysed by addition of 100 µL lysis buffer (100 mM HEPES, 10% sucrose, 5 mM dithiothreitol (DTT), 0.1% NP-40, 0.1% CHAPS). Crude lysates were allowed to sit on ice for 30 min before centrifugation at 10 000 rpm to remove insoluble elements. Ten micrograms of total soluble protein was assayed for caspase activity based on the ability to cleave fluorophore-conjugated peptides containing caspase-specific cleavage sites (DEVD-AFC for caspase 3, YMVD-AMC for caspase 8). Substrate cleavage leads to release of the free fluorophores, AFC or

AMC. Detection and quantitation of release of the fluorophores, AFC (excitation wavelength : 360, emission wavelength : 510) or AMC (excitation wavelength : 355 nm, emission wavelength : 460 nm), was performed by a BioRad fluorometer. In parallel samples, caspase-3 and caspase-8 inhibitors, Ac-DEVD-CMK and Ac-YMVD-CMK, respectively, were added at concentrations of 5 ng/μL.

Protein Extraction

Extraction of protein from H9c2(2-1) monolayers : H9c2(2-1) cell monolayers were washed with PBS and gently scraped. Cells were collected by centrifugation at 6000 rpm for 1 min, and the cell pellet was lysed by addition of 100 μL lysis buffer (100 mM Tris-HCl pH 7.4, 50 mM EDTA pH 8.0, 10 mM NaCl, 0.1% SDS) supplemented with protease inhibitors, aprotinin (10 ug/mL), pepstatin (1 ug/mL) and leupeptin (0.5 ug/mL), and allowed to sit on ice for 30 min. The crude lysate was passed through a $26^{3/8}$ gauge syringe, and spun down at 10 000 rpm for 1 min to pellet and remove the insoluble fraction. Protein concentration was assayed by a Bio-Rad protein assay reagent, according to manufacturer's protocols. Loading buffer was added to the protein extract, and heated to 100 °C for 2 min in order to fully denature proteins in preparation for electrophoresis.

Extraction of protein from tissue samples : Tissue samples were homogenized in 200 μL homogenization buffer (300 mM sucrose, 150 mM KCl, 30 mM Tris-HCl, 5 mM $MgCl_2$, 1.5 mM dithiothreitol (DTT), 1 mM EDTA and 1.5% Triton X-100) containing four protease inhibitors (10 μg/ml aprotinin, 2 μg/ml leupeptin, 10 μg/ml pepstatin and 2 mM phenylmethylsulfonyl fluoride (PMSF)) in a homogenizer. Crude lysate was transferred to a 1.5 mL Eppendorf tube, and allowed to sit on ice for 30 min. The lysate was then spun down at 10 000 rpm for 1 min to pellet and remove insoluble elements, and the supernatant was retained. Protein concentration was assayed by a Bio-Rad protein assay reagent, according to manufacturer's protocols. Loading buffer was added, and the samples were heated at 100 °C for 2 min to denature proteins.

Electrophoresis and Immunoblotting Analysis

Sodium dodecyl sulfate-polyacrylamide gel electophoresis (SDS-PAGE) was carried out on 10-12% gels using a discontinuous Laemmli system (Laemmli, 1970). For each assay of protein profile determination, 10 μg of total protein extract was loaded onto SDS-polyacrylamide gels, and electrophoresed at 35 mA. Proteins were electrophoretically transferred onto nitrocellulose support. Nitrocellulose membranes were stained with Ponceau S solution for 10 min at room temperature in order to visualize the total protein and the molecular weight markers, and subsequently destained with Tris-buffered saline (50 mM Tris-HCl, 500 mM NaCl) containing 0.5% Tween-20 (TBST) and blocked with 5% milk in TBST overnight at 4 °C. The membranes were probed with a primary antibody specific for EF–1α or actin for 3-4 hours at room temperature in TBST at 1:2,000 dilutions. The nitrocellulose blots were then washed three times with TBST for ten minutes each, followed by incubation with goat anti-rabbit immunoglobulin (IgG) conjugated to horseradish peroxidase (HRP) for one hour at room temperature in a 1:15,000. The membranes were rinsed again three times as described above. Nitrocellulose blots incubated with HRP-conjugated secondary antibodies were developed using enhanced chemiluminescence detection according to the manufacturer's protocols, and exposed to X-ray film.

Northern Blot Analysis

RNA was extracted from control and H_2O_2-treated H9c2(2-1) monolayers and from tissues using the Trizol reagent, using modified manufacturer's protocols (Chomczynski *et al.*, 1987). For RNA extraction from cell monolayers, cultures were washed with RNAse-free PBS, layered with 1 mL of Trizol reagent, and cells were collected in 1.5 mL Eppendorf tubes by gentle scraping. For RNA extraction from tissues samples, tissues were homogenized in 1 mL Trizol reagent in a Wheaton homogenizer, and transferred to a 1.5 mL Eppendorf tube. The mixtures were allowed to sit at room

temperature for 10 min to allow dissociation of nucleoprotein complexes. To induce phase separation, 200 μL chloroform was added, followed by centrifugation at 12,000 g for 15 min at 4 °C. The RNA-containing upper aqueous layer was collected, and subjected to a phenol-chloroform (1:1) wash. Again, the RNA-containing upper aqueous layer was collected, and RNA was precipitated by addition of 500 μL isopropanol, and room temperature incubation for 30 min. The samples were centrifuged at 12,000g for 15 min., and the supernatant was discarded. The pellet was washed in 1 mL ice-cold 70% ethanol, and then spun at 13 000 rpm for 10 min at 4°C. The RNA pellet was re-suspended in RNAse-free TE pH 8.0. The concentration of the RNA solution was determined by spectrophotometry at 260 nm, and the integrity of the RNA was confirmd by electrophoresis through a 0.8% agarose gel containing ethidium bromide.

Northern blot analysis to detect EF–1α mRNA and 18S rRNA levels was performed according to standard protocols (Sambrook et al, 1989). Five micrograms of cellular RNA from control and H_2O_2-treated H9c2(2-1) cells was separated on a denaturing 1% formaldehyde-agarose gel and transferred onto nylon membrane support by capillary transfer of nucleic acids. The membrane was subjected to prehybridization for 2 h in prehybridization solution (6X SSC, 2X Denhardt's reagent, 0.1% SDS), before hydridization with either a radiolabelled cRNA probe specific to the EF–1α 3'-untranslated region (3'-UTR) or with a radiolabelled DNA probe specific for the 18S rRNA for 16 h. at 42°C. The EF–1α-specific cRNA probe was constructed by *in vitro* transcription of a rat EF–1α cDNA in the presence of ^{32}P-UTP, as previously described (Lee *et al.*, 1992). The 18S rRNA-specific probe was constructed by random primed labelling using an 18S PCR product. The filter was then washed for thirty minutes at room temperature in 1X SSC, 0.1% SDS, followed by three washes of ten minutes at 68°C with the same solution. The membrane was then exposed to X-ray film for 24 h at –70°C.

Construction of Antisense EF–1α plasmid

The EF–1α promoter-containing plasmid, pEF-BOS (Mizushima et al., 1990), was linearized by EcoRI digestion for 2 h at 37 °C. The 1.7 kb EF–1α insert was excised from pCCD29 by digestion with EcoRI for 2 h at 37 °C. The insert was purified by a phenol:chloroform (1 :1) wash, followed by precipitation in 0.1x 5M NaCl and 2.5x 95% EtOH. Approximately 2 :1 ratios of insert-to-linearized pEF-BOS plasmid were ligated overnight at 14 °C using T4 ligase. Orientation of insertion of the 1.7 kb insert was tested by digestion with SspI.

Transient Transfection of Antisense EF–1α cDNA in H9c2(2-1) cells

DNA was introduced into H9c2(2-1) cells by calcium phosphate precipitation-mediated transfection using protocols adapted from Sambrook *et al.*, (1989). Fifteen micrograms of plasmid DNA (vector alone or antisense EF–1α) were mixed with 410 μL sterile low-TE solution (10 mM Tris pH 7.4, 5 mM EDTA pH 8.0) and 60 μL 2M $CaCl_2$, the latter added dropwise, in 15 mL polypropylene round-bottom tubes. The mixture was gently shaken. The DNA-$CaCl_2$ mixture was, then, slowly added, dropwise, atop 500 μL 2X HBS, gently shaken again, and allowed to sit at room temperature for 20 min in order to allow formation of calcium phosphate-DNA precipitates. Then, 3.5 mL of DMEM supplemented with 15% glycerol, and 5.5 mL of DMEM supplemented with 10% heat-inactivated FCS was added. The mixture was again shaken gently, and allowed to sit at room temperature for another 20 min. The resulting 10 mL solution was layered atop one 100 mm plate of H9c2(2-1) cells seeded at a density of 750,000 cells per 100 mm plate. Alternatively, 5 mL of the mixture was layered atop two 60 mm plates of H9c2(2-1) cells seeded at a density of 250,000 cells. The cultures were incubated at 37°C for 4 hrs, prior to washing with serum-free DMEM twice, and finally, incubation with DMEM supplemented with 10% fetal calf serum. Protein extracts were obtained, as described previously, 48 h following transfection, and probed with EF–1α-specific antiserum, in

order to test the efficacy of antisense inhibition of EF–1α expression. Parallel transfection of a plasmid constitutively expressing the β-galactosidase gene, followed by *in situ* β-galactosidase activity detection by X-gal staining (as described below) 48 h following transfection, was used to assess efficiency of transfection. All other assays were performed before 72 h following transfection.

Determination of Cytoprotective Effect of Antisense EF–1α

To determine any potential protective effects of lowered EF–1α levels on oxidative stress-induced apoptosis, a transient transfection system, described by Oral *et al.* (1999), was utilized. This technique has the advantage of limiting the scope of the assay only to those cells which have taken up the vector of interest, and overcomes the difficulties associated with variable efficiencies of transfection. H9c2(2-1) cells were co-transfected with 5 μg of a constitutively active β-galactosidase gene, along with either 10 μg of a full length antisense EF–1α cDNA under the control of the EF–1α promoter, or with 10 μg of an empty vector, by calcium phosphate precipitation. Two days following transfection, the cultures were left untreated or exposed to oxidative challenge by 24 h incubation with 700 μM H_2O_2. Beta-galactosidase activity was then assessed in the treated and untreated samples as follows: cell pellets were collected by gentle scraping, followed by centrifugation at 6000 rpm for 1 min. The pellets were then resuspended in 100 μL 0.25 M Tris-Cl pH 7.8 solution, and lysed by three cycles of freeze-thaw; rapid freezing was conducted in dry ice dissolved in 70% ethanol, and thawing was performed in a 37°C water bath. The crude lysate was then passed through a $28^{3/8}$ gauge syringe, and centrifuged at 10 000 rpm for 1 min to pellet the insoluble fraction; the supernatant was retained. Beta-galactosidase activity was assessed in a 300 μL reaction, containing 3 μL 100x Mg buffer, 66 μL 4 mg/mL ONPG, 201 μL 0.1M sodium phosphate solution pH7.5 and 30 μL of cell extract, and incubated at 37°C for 10 min. The reaction was stopped

with 500 μL 1M Na_2CO_3 , and the optical density (OD) of the samples at 420 nm was assessed by spectrophotometry. The percentage viability was calculated by the formula:

$$\% \text{ viability} = \frac{\text{OD (420 nm) after hydrogen peroxide treatment}}{\text{OD (420nm) medium control}}$$

As a confirmation, total β-galactosidase-positive cells were quantitated by direct counting of positively-stained cells following *in situ* staining for β-galactosidase activity. Monolayers were fixed with a 2% formaldehyde-0.2% glutaraldehyde solution for 5 min at room temperature, followed by staining with 1 mg/mL X-gal (5-bromo-4-chloro-3-indolyl-β-D-galactopyranoside) overnight at 37 °C. The cells were examined for positive blue staining in ten random fields using an inverted microscope.

RESULTS

H_2O_2 Induces Apoptosis of the H9c2(2-1) Cardiac Myoblast Cell Line

It is well established that pro-oxidants and reactive oxygen species, such as H_2O_2, are capable of inducing apoptosis in a variety of cell types, including primary cultures of neonatal cardiomyocytes (von Harsdorft *et al.*, 1999) and the cardiac-derived clonogenic cell line, H9c2(2-1) (Turner *et al.*, 1998). We confirm these previously reported observations of H9c2(2-1) susceptibility to H_2O_2-induced cytotoxicity; in our hands, using a colorimetric assay which detects mitochondrial respiration of viable cells in culture, we observed significant cell death following treatment with H_2O_2 at concentrations in excess of 700 μM for 24 hours. Lower concentrations of H_2O_2 (350 μM and below) had little effect on cell mortality (Figure 5, dark bars). When the H_2O_2-detoxifying antioxidant, catalase, is administered in conjunction with the H_2O_2 in the culture medium at a concentration of 10 U/mL, cell death was prevented, verifying a direct role of H_2O_2 in induction of cell death (Figure 5, light bars). The minute signals detected following treatment with lethal H_2O_2 doses represent unavoidable artifacts associated with the colorimetric cell viability assay, as it is difficult to completely remove the initial MTT dye from the cell culture wells prior to addition of the oxidizing agent initiating the color reaction proportional to the cell viability. Independent experiments, using a Trypan blue dye exclusion assay, showed ~0% viable cells with all H_2O_2 doses above 700 μM. The results shown are representative of two separate experiments.

Apoptosis is biochemically characterized by several hallmark events, one of which is the degradation of genomic DNA into an oligonucleosomal ladder consisting of DNA bands representing integer multiples of the internucleosomal DNA length (approximately 180 bp) (Wyllie, 1980). Thus, we next sought to assess whether H_2O_2-induced H9c2(2-1) cell death was accompanied by the formation of such an oligonucleosomal ladder, thereby confirming that the observed death was of an apoptotic

nature. H9c2(2-1) cells were treated with 700 μM H_2O_2 for four days, and the genomic DNA was separated on an agarose gel. We observed that after two days of treatment, the formation of a typical DNA ladder appeared, and persisted until 4 days post-treatment (Figure 6). A sample treated with 5 mM H_2O_2 for 4 days did not give the appearance of a DNA ladder, presumably because the mode of cell death was of a necrotic nature.

As further confirmation of an apoptotic mode of cell death, TUNEL staining, an *in situ* assay for DNA degradation, was also performed. Again, the appearance of a significant number of nuclei containing fragmented DNA was detected only in cultures exposed to toxic levels of H_2O_2 (700 μM); cells exposed to lower doses showed minimal effect, although we were still able to detect a small sub-population of cells which possessed fragmented nuclei (Figure 7).

Apoptosis is also characterized by the activation of a family of cysteine proteases, termed caspases, which function in the final executory stage of cell death, by mediating proteolysis of a variety of specific cellular substrates. Thus, caspase-3 and caspase-8 activity was assayed in control and H_2O_2-treated H9c2(2-1) cultures using a fluorogenic assay, which directly measures the ability of the cellular protein extracts to proteolytically cleave at caspase-specific cleavage sites, releasing a fluorophore. Following exposure to toxic levels of H_2O_2, significant caspase-3 activity was detected in the cellular homogenates. The specificity of this proteolytic activity was verified by the addition of a caspase-3 inhibitor, Ac-DEVD-CMK, in the reaction mixture, which nullified the detected caspase-3 activity (Figure 8). Conversely, no caspase-8 activity was detectable using the same cellular protein extracts, suggesting that caspase-8 is not activated upon oxidative stress-induced apoptosis, and that the observed caspase-3 activity is not due to an upstream proteolytic activation of caspase-8 (Figure 9).

Figure 5. **Mitochondrial respiration of H9c2(2-1) cardiac myoblasts following H_2O_2 treatment.** The ability of H9c2(2-1) cardiac myoblast mitochondria to reduce 3-(4,5-dimethylthiazol-2-yl)-2,5-diphenyltetrazolium bromide (MTT) to a formazon end product following treatment with various doses of H_2O_2 was assayed using a colorimetric assay, as described under "Materials and Methods". As indicated by the dark bars, mitochondrial respiration was only affected after 24 h treatments with concentrations of H_2O_2 of 1400 μM and above. A small signal represents an artifact associated with the MTT colorimetric assay. A trypan blue dye exclusion assay verified indicated ~0% cell viability following administration of H_2O_2 at doses above 700 μM. To confirm that H_2O_2 was indeed the cause of cytotoxicity in these experiments, when the antioxidant, catalase, was added to the medium at 10 U/mL, the effect on mitochondrial respiration was abrogated, as indicated by the light bars. The results shown are representitive of two separate experiments.

Figure 5

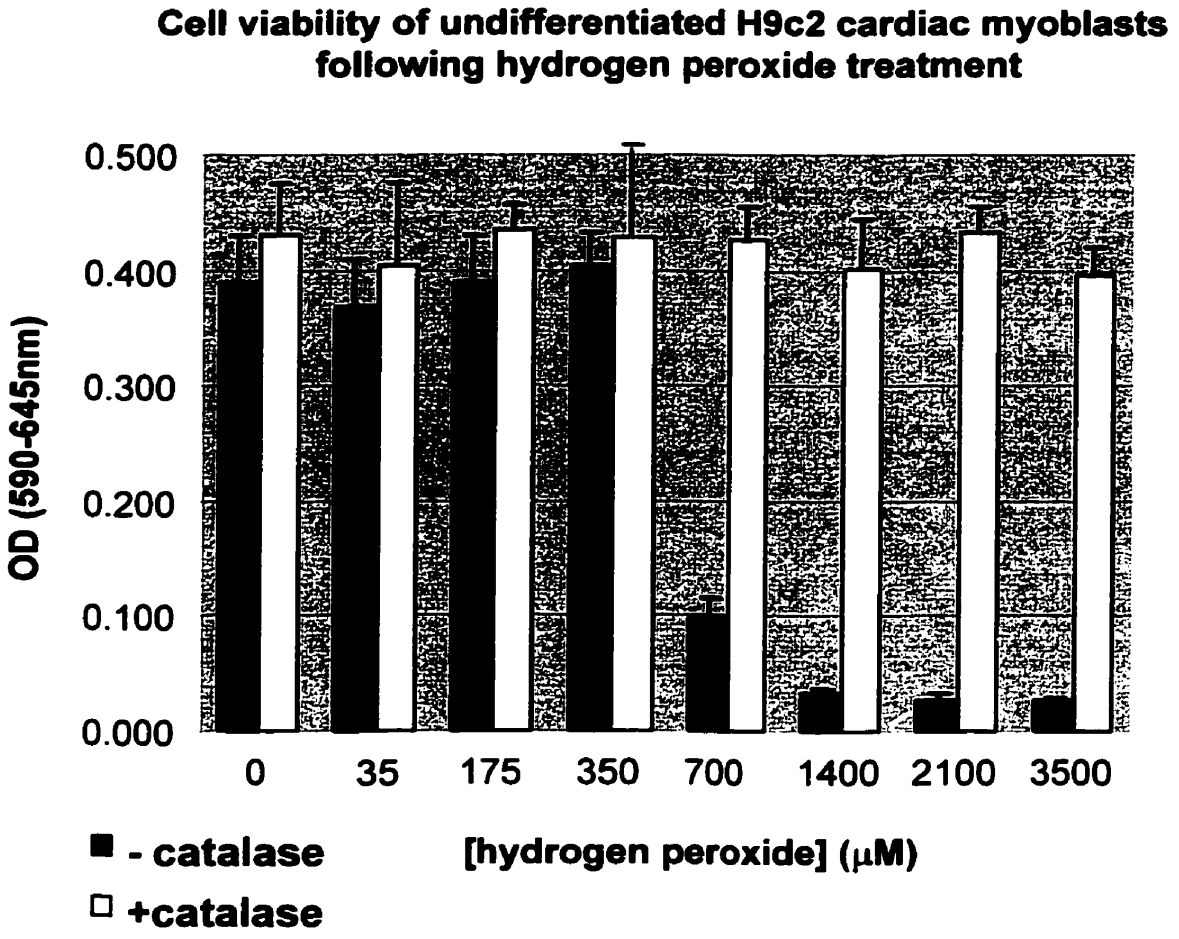
Cell viability of undifferentiated H9c2 cardiac myoblasts following hydrogen peroxide treatment
OD (590-645nm)
0.500
0.400
0.300
0.200
0.100
0.000
0
35
175
350
700
1400
2100
3500
- catalase
+catalase
[hydrogen peroxide] (μM)

Figure 6. **H9c2(2-1) cell death is accompanied by formation of DNA oligonucleosomal ladder.** DNA extracted from cells treated with 1 mM H_2O_2 for 0-4 days were separated on a 1.0% agarose gel, as described under "Materials and Methods". Note the gradual appearance of a DNA oligonucleosomal ladder beginning at 1 day following treatment, and increasing in intensity and prominence throughout the four days of treatment (lanes 1-5). Serum deprived mouse 3T3 fibroblasts provided a positive control (lane 6). H9c2(2-1) cultures treated at extremely high doses sufficient to induce necrosis, such as 5 mM H_2O_2, had an apparently intact DNA, identical to untreated samples (lane 7 versus lane 1).

Figure 6

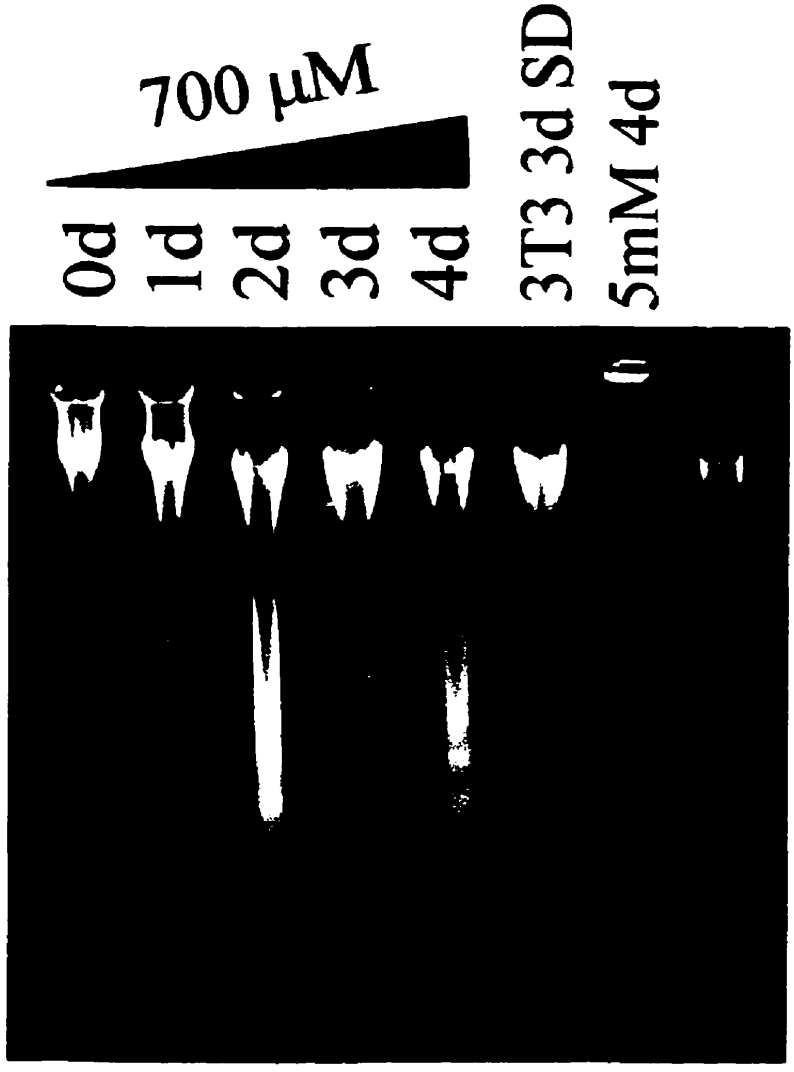

Figure 7. **H9c2(2-1) cell death is accompanied by *in situ* DNA degradation.** As an *in situ* indicator of apoptosis, H9c2(2-1) cells treated with various doses of H_2O_2 were TUNEL-labeled with FITC-conjugated antibodies and observed using fluorescence microscopy. As indicated, untreated cultures and cultures exposed to concentrations of 175 μM and 350 μM H_2O_2 (the three top panels) possessed very few apoptotic cells, although there was a small, sub-population which was brightly labeled (arrowheads). However, cultures treated with a concentration of 700 μM (bottom panel) possessed predominantly apoptotic cells and numerous brightly labeled nuclei (arrows).

Figure 7

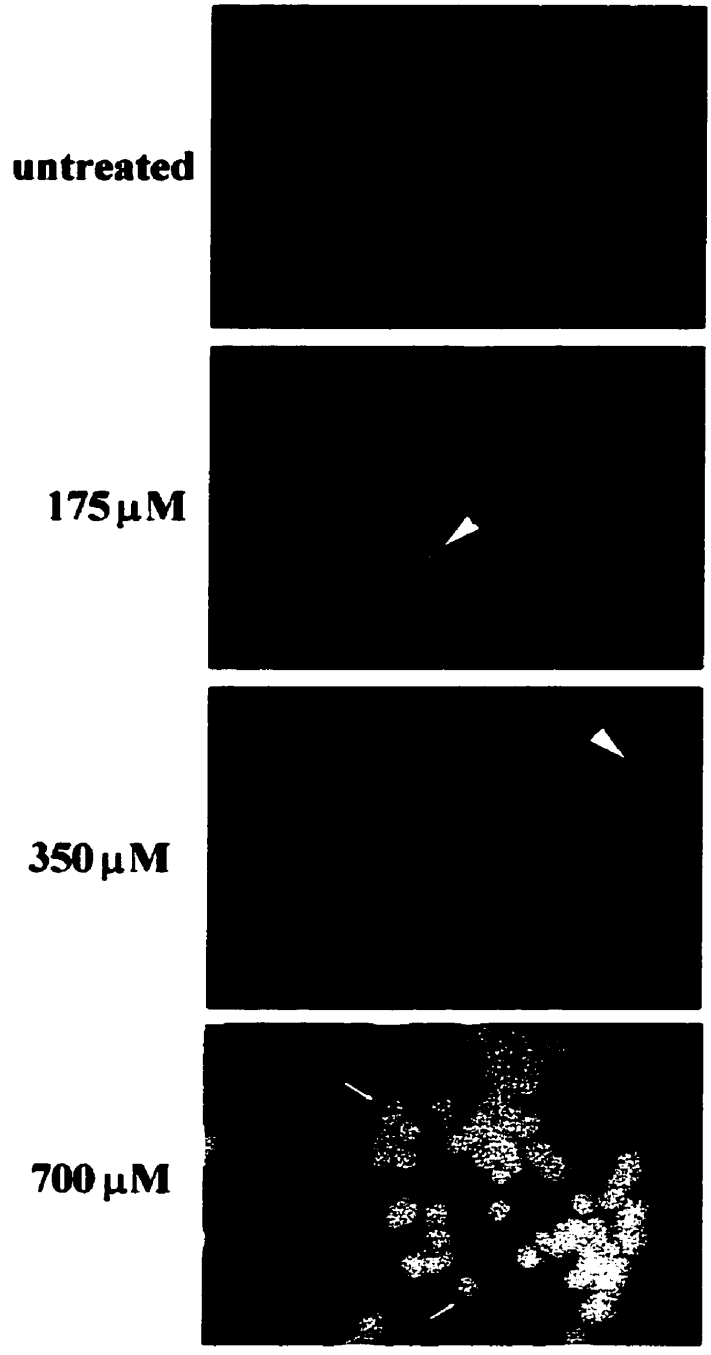

Figure 8. **Caspase-3 activity following induction of H9c2(2-1) apoptosis.** A fluorometric assay, based on the ability to cleave DEVD-AFC and release the AFC fluorophore (excitation λ: 360 nm, emission λ: 510 nm), was used to assess caspase-3 activity in H9c2(2-1) cardiomyoblast cell extracts at 0.5 h, 1 h, 1.5 h, 2 h and 4 h post-H_2O_2 treatment using a concentration of 700 μM. As indicated by the solid line, caspase-3 activity increased approximately 3.5-fold as compared to the non-treated control as a prelude to apoptotic cell death. As indicated by the dashed line the caspase-3 inhibitor, Ac-DEVD-CMK, added at concentrations of 5 ng/μL, completely inhibited the reaction, confirming the specificity of the detected proteolytic activity. The results are representitive of three separate experiments.

Figure 8

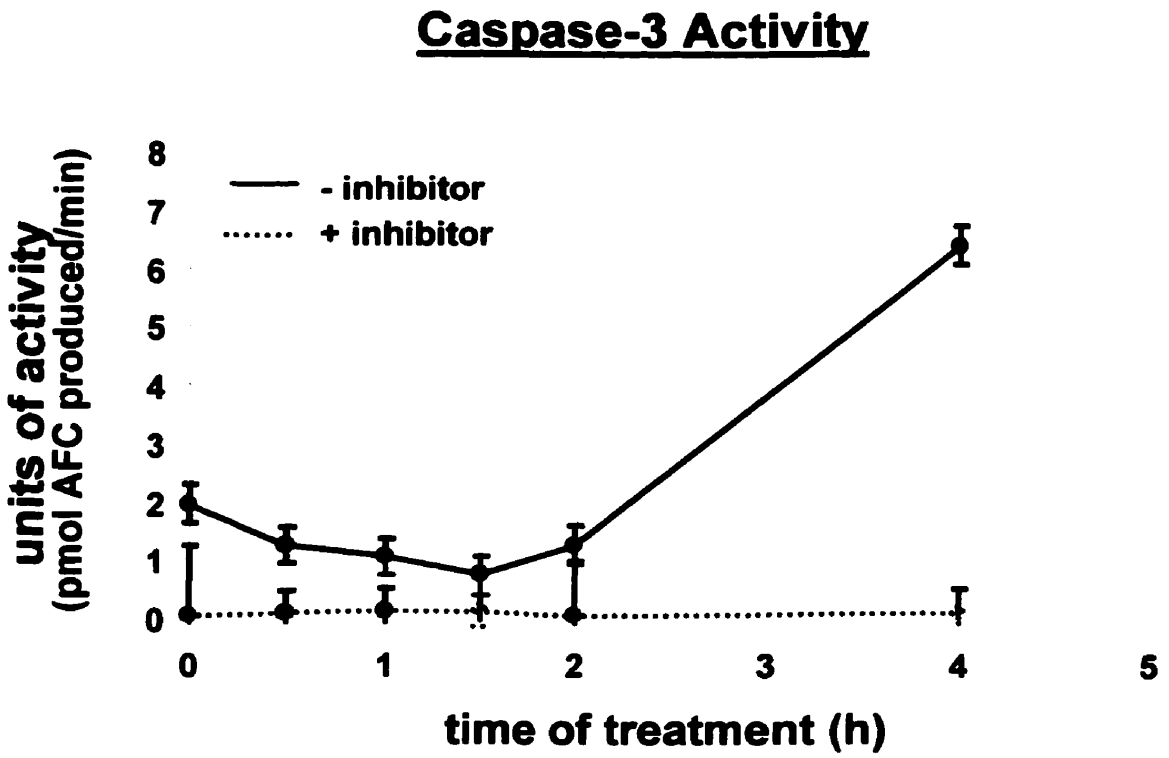
Caspase-3 Activity
units of activity
(pmol AFC produced/min)
- inhibitor
+ inhibitor
8
7
6
5
4
3
2
1
0
0
1
2
3
4
5
time of treatment (h)

Figure 9. **Caspase-8 activity following induction of H9c2(2-1) apoptosis.** A fluorometric assay, based on the ability to cleave YMVD-AMC and release the AMC fluorophore (excitation λ: 355 nm, emission λ: 460 nm), was used to assess caspase-8 activity in H9c2(2-1) cardiomyoblast cell extracts at 0.5 h, 1 h, 1.5 h, 2 h and 4 h post-H_2O_2 treatment using a concentration of 700 μM. As indicated by the solid line, there was negligible caspase-8 activity at all time points following oxidative stress. A similar lack of activity was observed when the caspase-8 inhibitor, Ac-YMVD-CMK was added at concentrations of 5 ng/μL, as indicated by the dashed line. The results are representitive of three separate experiments.

Figure 9

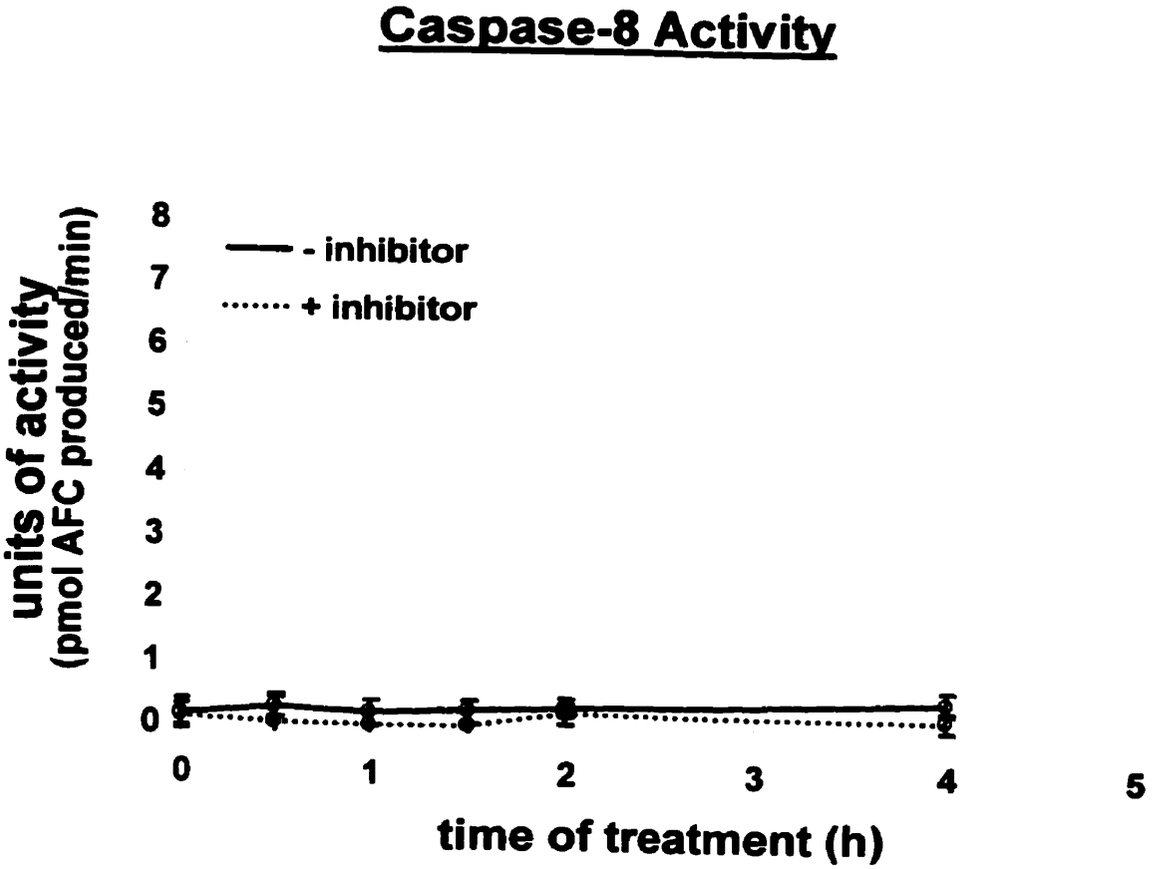
Caspase-8 Activity
units of activity
(pmol AFC produced/min)
8
7
6
5
4
3
2
1
0
- inhibitor
+ inhibitor
0
1
2
3
4
5
time of treatment (h)

H_2O_2 Induces Up-regulation of EF–1α protein

The peptide elongation factor, EF–1α, is traditionally known to participate in the elongation step of mRNA translation. A growing number of reports, however, indicate potential roles for EF–1α in apoptosis (Duttaroy *et al.*, 1998; Kato *et al.*, 1997). Thus, to assess whether EF–1α protein levels were affected during H_2O_2-induced apoptosis of H9c2(2-1) cells, protein extracts of control and H_2O_2-treated cultures were subjected to immunoblotting analysis using an EF–1α-specific antibody. Treatment of H9c2(2-1) cells with varying doses of H_2O_2 for 30 min revealed a dose-dependent up-regulation of EF–1α protein levels (Figure 10, Panel A). Actin protein levels were unaltered, suggesting that the increase was not a global event. Densitometric analysis of EF–1α band intensity, as standardized with the actin control, is presented in Figure 10, Panel B.

That EF–1α protein was elevated following both lethal (700 μM) and sub-lethal (350 μM) doses of H_2O_2 prompted further studies detailing the time-course kinetics of the EF–1α up-regulation under the two conditions. In both cases, sublethal and lethal doses of H_2O_2 induced a rapid increase in EF–1α protein levels, with elevated protein levels seen within just ten minutes following initiation of oxidative stress (Figure 11). By thirty minutes, both sublethal and lethal doses had achieved the elevation of EF–1α protein levels seen in the previous figure. However, beyond the sixty minutes time-point, EF–1α levels in cells treated with a sublethal dose (350 μM) were observed to return to normal levels (Figure 11, Panel A), while treatment with the lethal dose (700 μM) revealed more prolonged elevated levels of EF–1α, which persisted in excess of three hours (Figure 11, Panel B). Again, densitometric analysis also confirmed that cells treated with the lethal 700 μM H_2O_2 dose, unlike those treated with sub-lethal doses, have elevated EF–1α levels after three hours of treatment (Figure 10, Panels C and D, for 350 μM and 700 μM treatment, respectively). Therefore, sustained up-regulation of EF–1α expression may act as a necessary early event to the effecting of oxidative stress-induced H9c2(2-1) apoptotic death.

Figure 10. **EF-1α expression is up-regulated by H_2O_2 treatment in a dose-dependent manner.** Panel A, Immunoblotting analysis of EF-1α protein using an EF-1 α -specific antibody, HT7, performed as described under "Materials and Methods", revealed a dose-dependent elevation of EF–1α protein levels following thirty minute treatments of H9c2(2-1) cultures with increasing doses of H_2O_2 ranging from 50 μM to 5 mM. Panel B, Densitometric tracing of the EF–1α band intensities from Panel A is represented quantitatively as a graph.

Figure 10

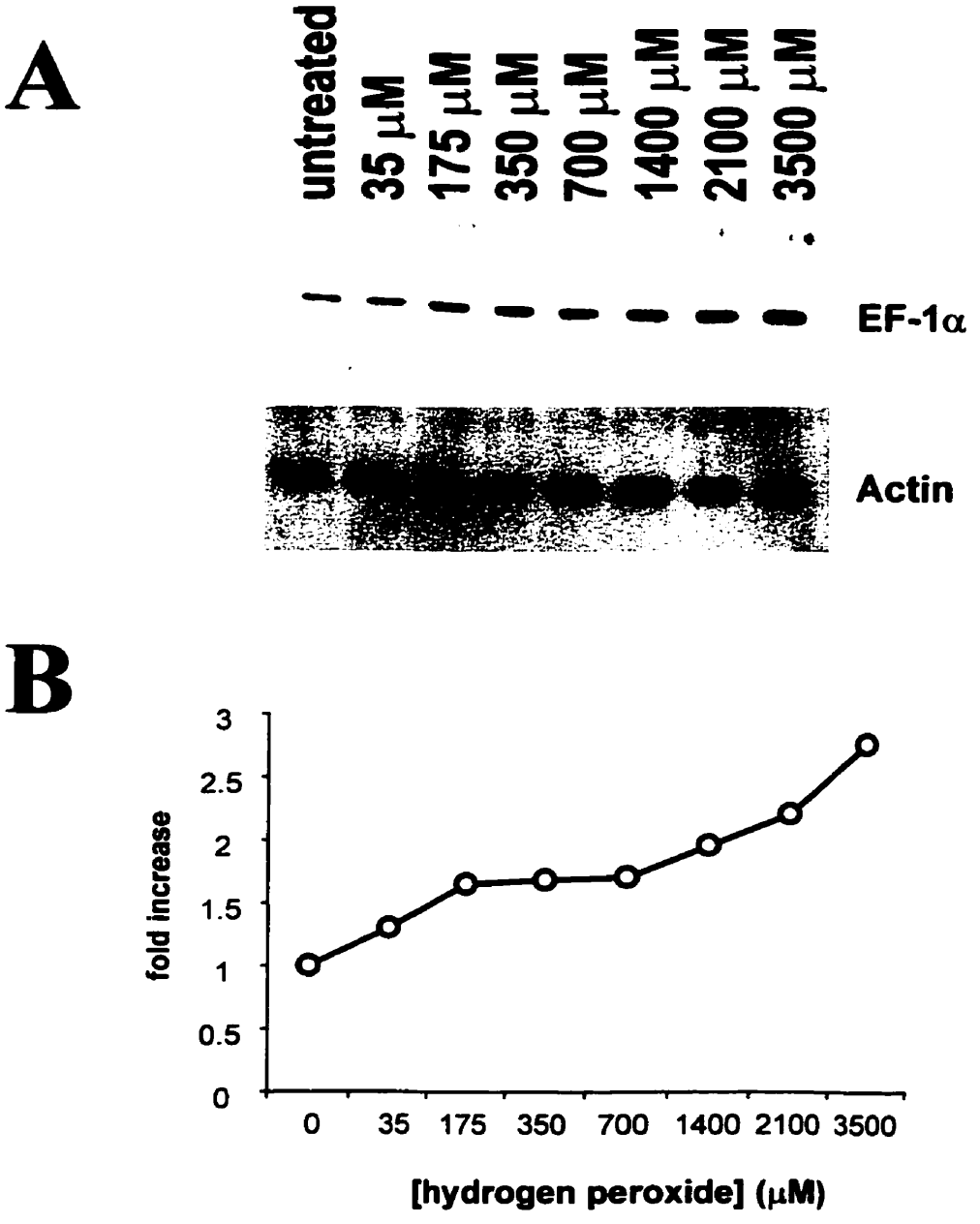
A
untreated
35 µM
175 µM
350 µM
700 µM
1400 µM
2100 µM
3500 µM
EF-1α
Actin
B
fold increase
3
2.5
2
1.5
1
0.5
0
0
35
175
350
700
1400
2100
3500
[hydrogen peroxide] (µM)

Figure 11. **H_2O_2 treatment at sub-lethal doses induces transient elevation of EF-1α protein levels, whereas lethal doses induce sustained elevation of EF-1α.** Panel A, A kinetic study of EF-1α protein following treatment of H9c2(2-1) cultures with a sub-lethal dose of H_2O_2 was performed. Total cellular protein was obtained 5 min., 10 min., 20 min., 30 min., 1 hour and 3 hours after treatment with 350 μM of H_2O_2, and subjected to immunoblotting with an EF-1 α-specific antibody, as described under "Materials and Methods". Immunoblot analysis revealed a transient up-regulation of EF-1 α protein, with the final levels of EF-1α falling back to that of the initial, control sample. Panel B, An analagous kinetic study of EF-1 α protein following treatment of H9c2(2-1) cultures with the lethal dose of 700 μM H_2O_2 using identical time points as described in Panel A revealed a more sustained and prolonged up-regulation of EF-1 α protein levels. Panels C & D, Densitometric tracing of the EF-1 α band intensities from Panels A & B, standardized with an internal actin control, are represented quantitatively as a graph.

Figure 11

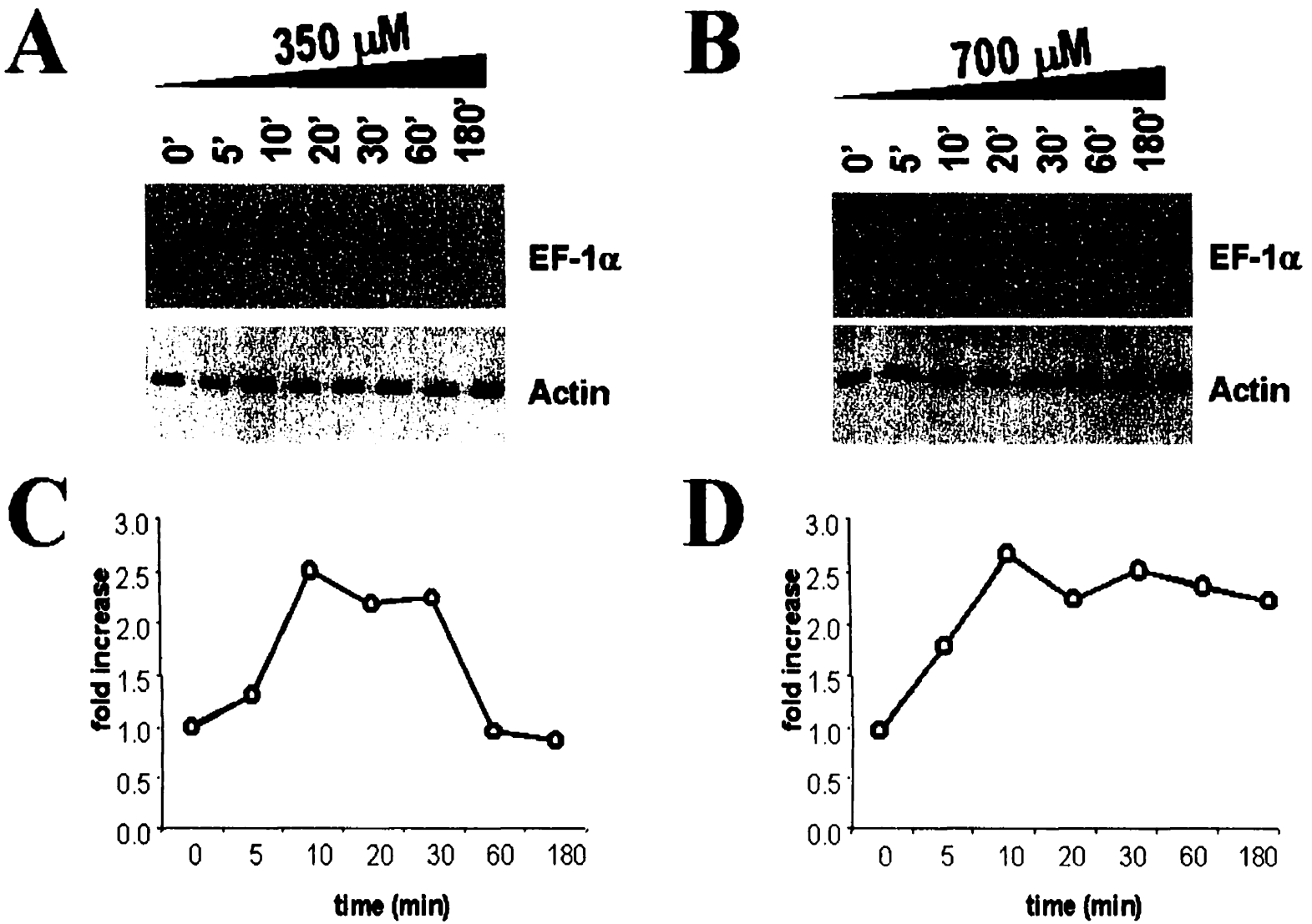
A
350 µM
0' 5' 10' 20' 30' 60' 180'
EF-1α
Actin
B
700 µM
0' 5' 10' 20' 30' 60' 180'
EF-1α
Actin
C
fold increase
3.0
2.5
2.0
1.5
1.0
0.5
0.0
0 5 10 20 30 60 180
time (min)
D
fold increase
3.0
2.5
2.0
1.5
1.0
0.5
0.0
0 5 10 20 30 60 180
time (min)

EF−1α up-regulation is mediated post-transcriptionally

The rapidity of the response to H_2O_2 (in both cases, effecting an increase in EF−1α protein within ten minutes) prompted investigation as to whether the up-regulation was mediated at the transcriptional or post-transcriptional level. H9c2(2-1) cultures were pre-treated with a transcriptional inhibitor, actinomysin D, and/or a translational inhibitor, cycloheximide, for thirty minutes, prior to addition of 700 μM H_2O_2, in combination with either actinomysin D and/or cycloheximide for another thirty minutes. We again witnessed the increase in EF−1α protein levels when H9c2(2-1) were treated with H_2O_2 alone (Figure 12, compare lane 1 to lane 5). In the presence of a translational inhibitor, cycloheximide, the H_2O_2-induced up-regulation of EF−1α was completely abolished (compare lane 2 to lane 6, and lane 4 to lane 8), demonstrating that the increase in EF−1α following oxidative challenge requires active protein synthesis. However, in the presence of a transcriptional inhibitor, actinomysin D, the up-regulation of EF−1α was not suppressed (compare lane 3 to lane 7), which suggests that *de novo* gene transcription is not necessary for the elevation of EF−1α protein levels, and that such an increase is most probably effected post-transcriptionally.

Classically, gene regulation at the translational level is discernible by fluctuating protein levels concomitant with an absence of change in the mRNA levels. Thus, to further gain insight into the mechanism of H_2O_2-induced EF−1α up-regulation, Northern blot analysis was performed to address whether any changes in EF−1α message levels occurred at various time points following H_2O_2 treatment. Using similar time points as depicted in Figure 11, it was found that, unlike the protein fluctuations, the EF−1α message levels were static throughout the entirety of the three hours of oxidative stress (Figure 13, Panel A). Densitometric analysis, depicting the EF−1α message standardized with the internal 18S rRNA control, reinforce the Northern analysis that EF−1α message levels did not mimic the increase observed in the protein levels (Figure 13, Panel B).

Figure 12. **H_2O_2-induced up-regulation of EF-1α does not require *de novo* gene transcription.** The effect of pre-treatment of H9c2(2-1) cultures with either transcriptional inhibitor, actinomysin D (5 μg/mL) or protein synthesis inhibitor, cycloheximide (50 μg/mL) on H_2O_2-induced elevation of EF-1α levels was examined. There was minimal effect on EF-1 α levels by the actinomysin D and/or cycloheximide alone (lanes 1-4). When incubated with H_2O_2 alone, there was, again, an elevation of EF-1 α levels (compare lane 1 versus lane 5), which was abolished with pre-treatment with cycloheximide (lane 6) or with cycloheximide and actinomysin (lane 8). However, when H9c2(2-1) cultures were pre-treated with actinomysin D, the up-regulation of EF-1 α is still evident (lane 7).

Figure 12

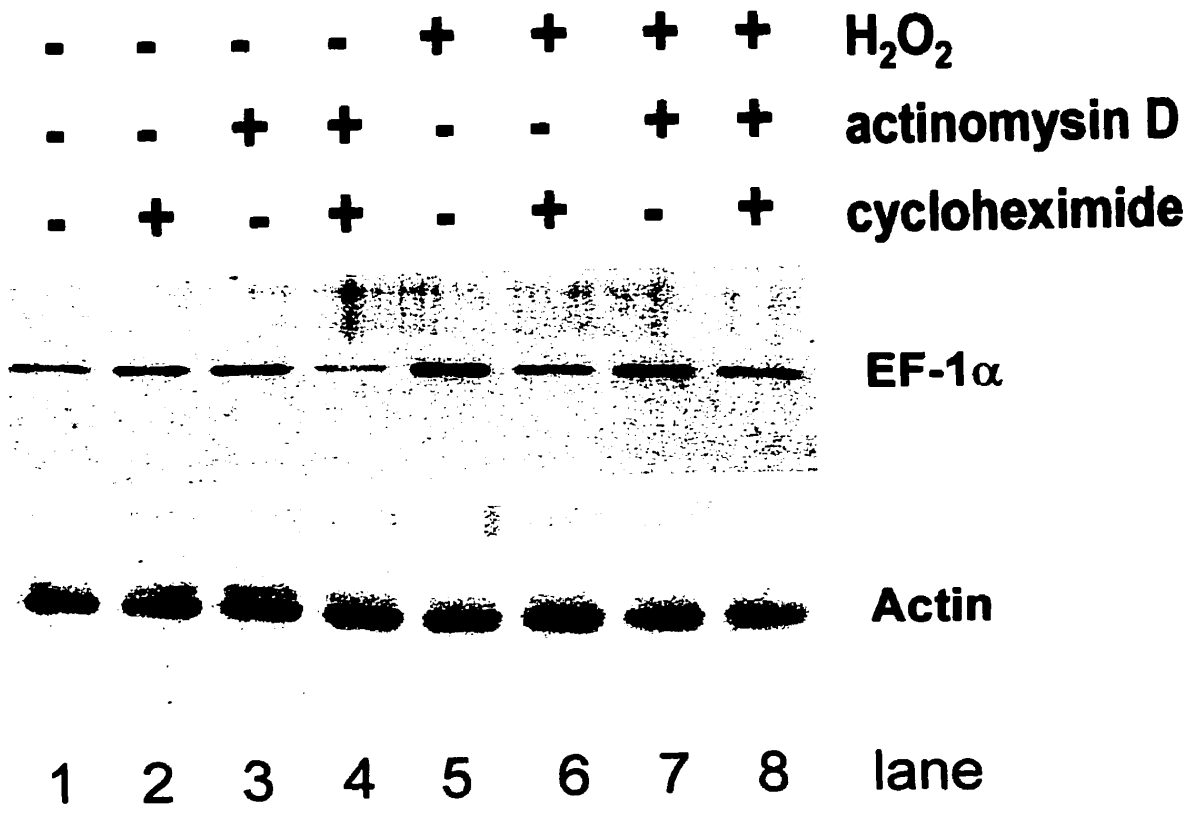
- - - - + + + + H2O2
- - + + - - + + actinomysin D
- + - + - + - + cycloheximide
EF-1α
Actin
1 2 3 4 5 6 7 8 lane

Figure 13. **H_2O_2 does not alter EF-1α mRNA levels in H9c2(2-1) cells.** Panel A, Total cellular RNA was obtained 0 min, 10 min, 20 min, 30 min, 1 hour and 3 hours after treatment with a lethal dose of H_2O_2 (700 μM), and processed for Northern blot analysis, as described in "Materials and Methods". EF-1α mRNA levels showed no significant fluctuations, unlike those witnessed for protein levels (Figure 10). Panel B, Densitometric analysis of EF-1A band intensity in Panel A, standardized with an internal 18S rRNA control, are represented quantitatively as a graph.

Figure 13

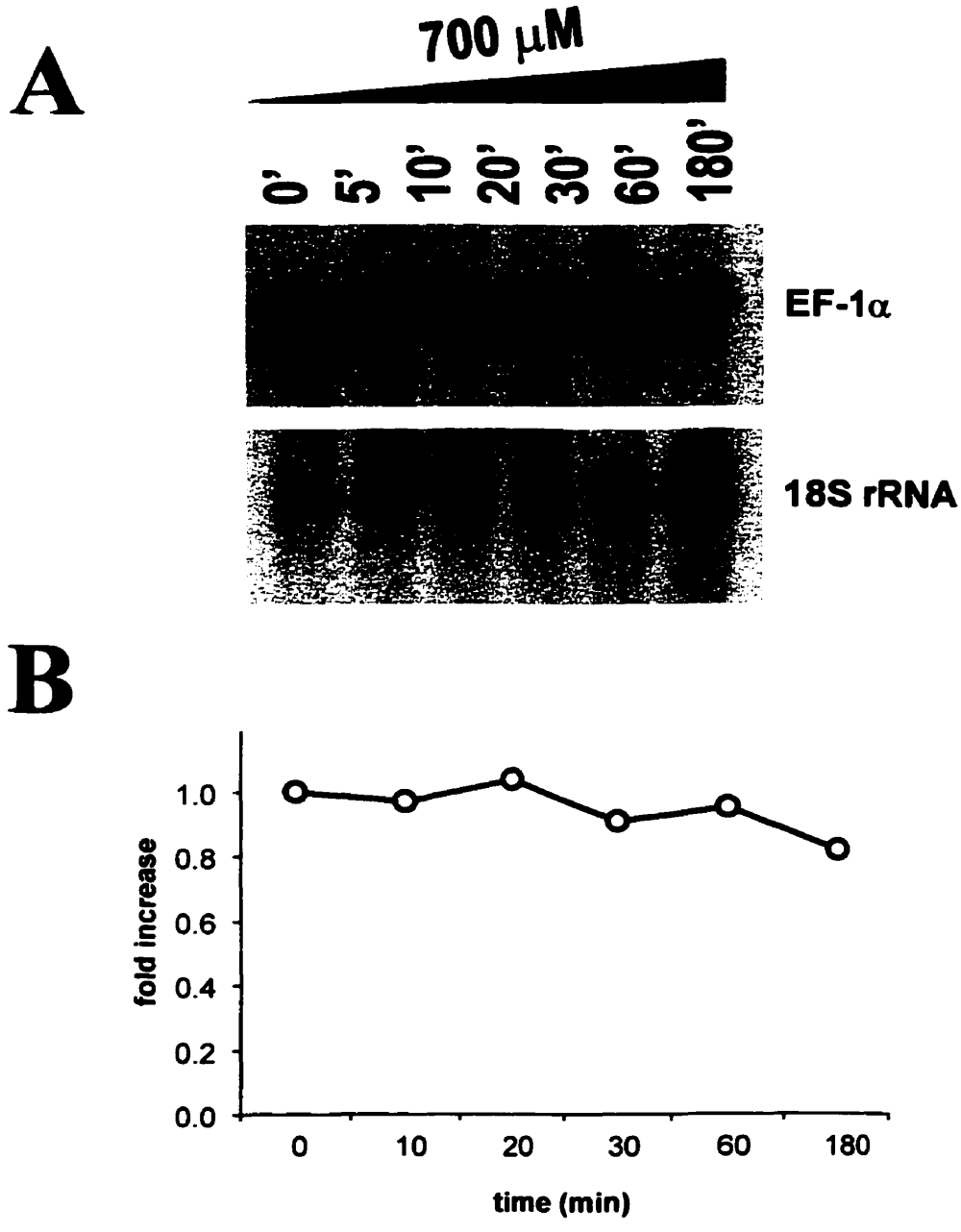
A
700 μM
0'
5'
10'
20'
30'
60'
180'
EF-1α
18S rRNA
B
fold increase
1.0
0.8
0.6
0.4
0.2
0.0
0
10
20
30
60
180
time (min)

Indeed, three hours following oxidative challenge, there appears to be a modest down-regulation of the EF–1α message. Regardless, this further confirms the hypothesis that the oxidant is increasing the cellular EF–1α levels by affecting the translational mechanism.

Antisense-EF–1α confers a protective effect against oxidative stress

Decreased expression of EF–1α in H9c2(2-1) cultures was mediated by transient transfection of a full length antisense EF–1α cDNA. The promoter which was chosen to drive production of the antisense EF–1α transcript was the EF–1α promoter itself, and not the cytomegalovirus promoter, since the EF–1α promoter has been reported to one of the strongest known mammalian promoters, as assessed in promoter-reporter assays (Mizushima *et al.*, 1990). Thus, a plasmid bearing a full length EF–1α cDNA oriented in the antisense direction under the control of the EF–1α promoter was constructed (designated EF-BOS-AS), and transiently transfected into H9c2(2-1) cell cultures to mediate a specific down-regulation of total cellular EF–1α levels.

The efficacy of the transfection of the EF-BOS-AS plasmid in down-regulating total cellular EF–1α protein levels was assessed by immunoblot analysis using an EF–1α-specific antibody. Forty-eight hours following transfection, levels of EF–1α protein were significantly decreased in cultures transfected with an antisense EF–1α construct, as compared to the mock transfected control. EF–1α levels in parallel cultures transfected with an empty vector control were unaffected (Figure 14, Panel A). Densitometric analysis indicated that the percentage repression of EF–1α expression was 40% (Figure 14, Panel B), consistent with the transfection efficiency, as assessed by *in situ* β–galactosidase staining (Figure 14, Panel C, white arrows).

The assessment of cell viability following transient transfection of any given gene of interest is marred by variabilities in the transfection efficiency, which results in the

presence of different cell sub-populations in the culture *i.e.* those transfected, and those not transfected. To limit the scope of the cell viability assay only to those cells which had been successfully transfected and taken up the newly introduced plasmid, a β-galactosidase co-transfection system was employed, as described in Oral *et al.* (1999). A constitutively active CMV-β-galactosidase plasmid was co-transfected along with the vector of interest, followed by assessing the β-galactosidase activity of the culture after induction of apoptosis. Since dead β-galactosidase-positive cells lyse thereby leaving viable cells attached, assaying for β-galactosidase activity of the remaining adherent cells has been shown to be a reasonably accurate measure of cell viability, and for determination of the cytoprotective effects of a transiently expressed gene of interest.

Thus, using this system, we next assessed cell viability of cultures transfected with the vector alone control and with the antisense EF−1α cDNA following induction of apoptosis at varying doses of H_2O_2. Again, as previously indicated in Figure 5, we observed no effect on cell viability following exposure to H_2O_2 levels of 350 μM and below. However, at concentrations of 525 μM, the antisense transfected cultures exhibited a moderate resistance to H_2O_2-induced cell death, as compared to cultures transfected with an empty control vector (72.3% ± 0.9%, compared to 55.5% ± 9.9%). The effect is more dramatic at the H_2O_2 concentration of 700 μM, where again, transfection of the antisense EF−1α cDNA is able to confer resistance to cell death (53.7% ± 2.7% as compared to 27.0% ± 6.1%) (Figure 15). Therefore, while the cytoprotective effect of diminished EF−1α levels is not absolute, diminution of its surge following H_2O_2 expsoure does have a partial protective effect against H_2O_2-mediated cytotoxicity, suggesting that the up-regulation of EF−1α following oxidative stress may have some functional physiological relevance in the initiation or execution of the apoptotic program.

Figure 14. **Transfection of antisense-EF-1α diminishes EF-1α protein levels in proportion to transfection efficiency.** To prevent the up-regulation of EF-1α, a full length antisense-EF-1α was transfected into H9c2(2-1) cells by calcium phosphate precipitation. Panel A, Immunoblotting analysis of EF-1α protein levels 48 hours post-transfection. EF-1α levels were significantly decreased in cultures transfected with an antisense-EF-1α cDNA (AS), relative to a mock transfected culture (MOCK) and a culture transfected with an empty vector control (VA). Panel B, Densitometric analysis indicates that the EF-1α band intensity following transfection is 60%. Panel C, Consistent with the 40% reduction of total EF-1α protein, *in situ* β-galactosidase staining revealed approximately 30-40% transfection efficiency. Positively stained cells are indicated by white arrows.

Figure 14

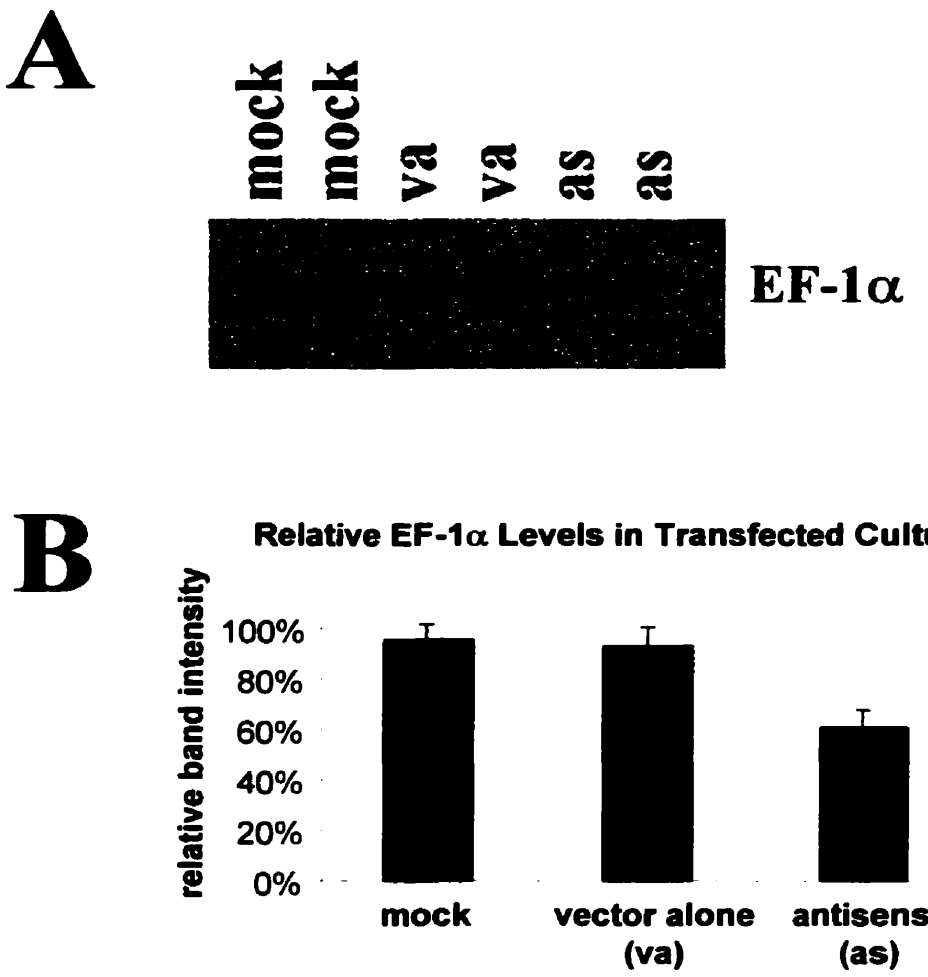
A
mock
mock
va
va
as
as
EF-1α
B
Relative EF-1α Levels in Transfected Cultures
relative band intensity
100%
80%
60%
40%
20%
0%
mock
vector alone (va)
antisense (as)
C

Figure 15. **Transfection of antisense-EF-1α confers a protective effect against H_2O_2.** The effects of the introduction of an antisense-EF-1α cDNA on H_2O_2-induced apoptosis was assayed using a transient transfection reporter-cytotoxicity assay, as described by Oral *et al.* (1999). The assay normalizes cell death with transfection efficiency, limiting the assessment of cytotoxicity only to those cells which had been successfully transfected. We observed a dose-depenent protective effect following transfection of an antisense-EF-1α cDNA, compared to that of cells transfected with an empty vector control. At H_2O_2 levels below 350 μM, there was negligible effect on cell viability. However, at concentrations of 535 μM and above, the antisense-EF-1α conferred a protective effect against H_2O_2-induced cytotoxicity, relative to the vector alone control, raising cell viability from 55.5% to 72.3% for cultures treated with 525 μM H_2O_2, and from 27% to 53.7% for cultures treated with 700 μM H_2O_2.

Figure 15

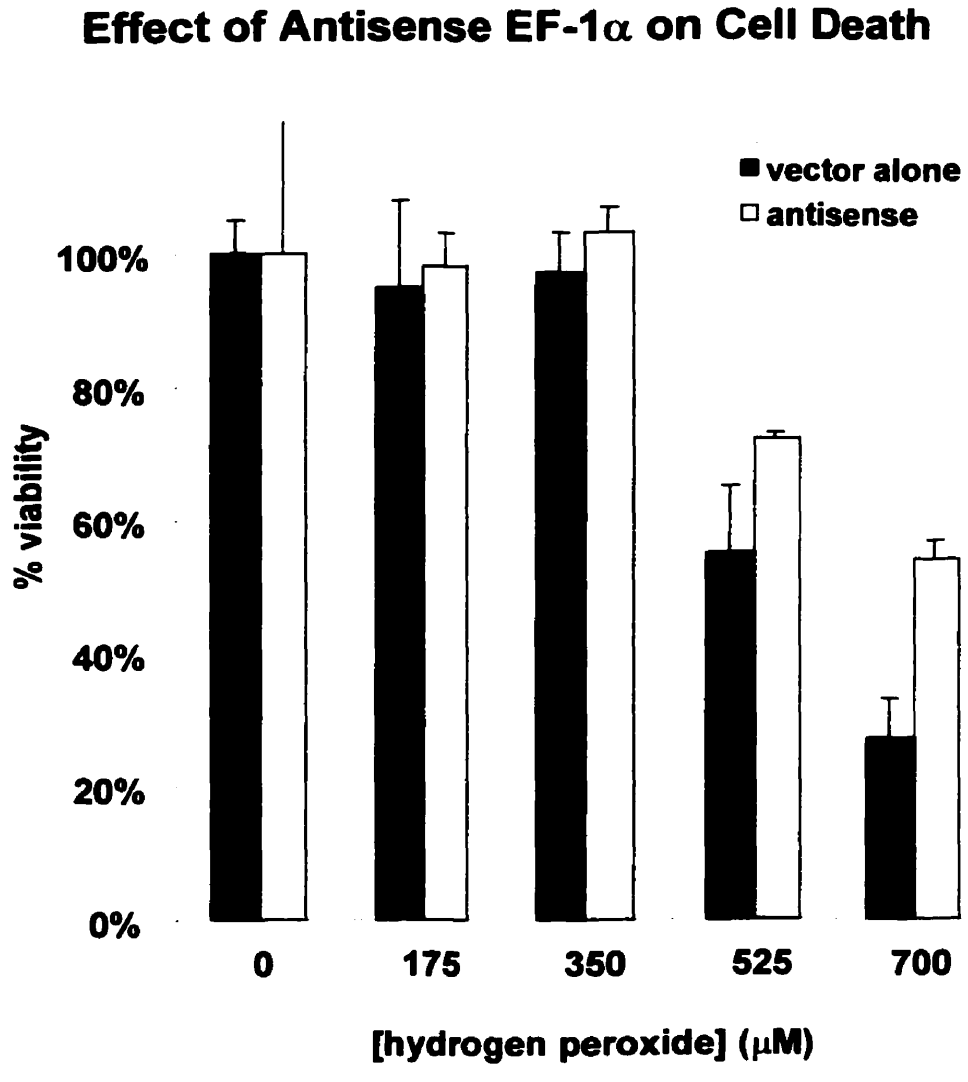
Effect of Antisense EF-1α on Cell Death
vector alone
antisense
% viability
100%
80%
60%
40%
20%
0%
0
175
350
525
700
[hydrogen peroxide] (μM)

EF-1α Protein Expression in MnSOD-Knockout Mice

In order to assess alterations in EF–1α expression during oxidative stress in *in vivo* situations, cardiac tissue samples were obtained from 14-15 day old mice in which the gene encoding for the antioxidant, manganese superoxide dismutase, was inactivated by homologous recombination (generous gifts of Dr. Ting-Ting Huang and Dr. Charles Epstein). Wildtype tissues were also obtained as controls. The homozygous mutant mice exhibit dilated cardiomyopathy, metabolic acidosis and ventricular wall thinning, culminating in death within fifteen days following birth (Li et al., 1995).

Analysis of EF–1α levels in four wildtype animals and five homozygous mutant animals revealed that while EF–1α levels were consistently low in four wildtype animals, EF–1α levels were elevated in three of five mutant animals (Figure 16, Panel A). This change was confirmed by densitometric analysis where three mutant animals were observed to possess a two-fold increase in EF–1α levels as compared to the wildtype controls (Figure 16, Panel B).

A retrospective analysis of the precise ages of the animals revealed that the three homozygous animals exhibiting elevated EF–1α levels shared a common age of 14 days old, whereas the remaining two mutant animals were 15 days old. In comparison, a mixture of 14-day old and 15-day old animals comprised the wildtype animals (Table 1). Thus, homozygous mutant animals aged at 14 days post-birth all shared the common characteristic of elevated EF–1α levels when compared to wildtype controls, whereas homozygous animals aged at 15 days post-birth did not exhibit a similar phenotype. A densitometric analysis of EF–1α band intensity in animals pooled based on age is presented in Figure 17.

Figure 16. **EF-1α protein expression is elevated in MnSOD-knockout mouse hearts.** Heart tissue samples were obtained from four wildtype mice and five homozygous mutant mice whose gene encoding for MnSOD had been inactivated by homologous recombination. All mice were aged between 14 and 15 days old. Panel A, Western immunoblotting analysis of tissue samples using an EF-1α-specific antibody revealed low EF-1α levels in all four wildtype controls, and elevated expression in three of five mutant animals. Panel B, Densitometric analysis assessing EF-1α band intensity.

Figure 16

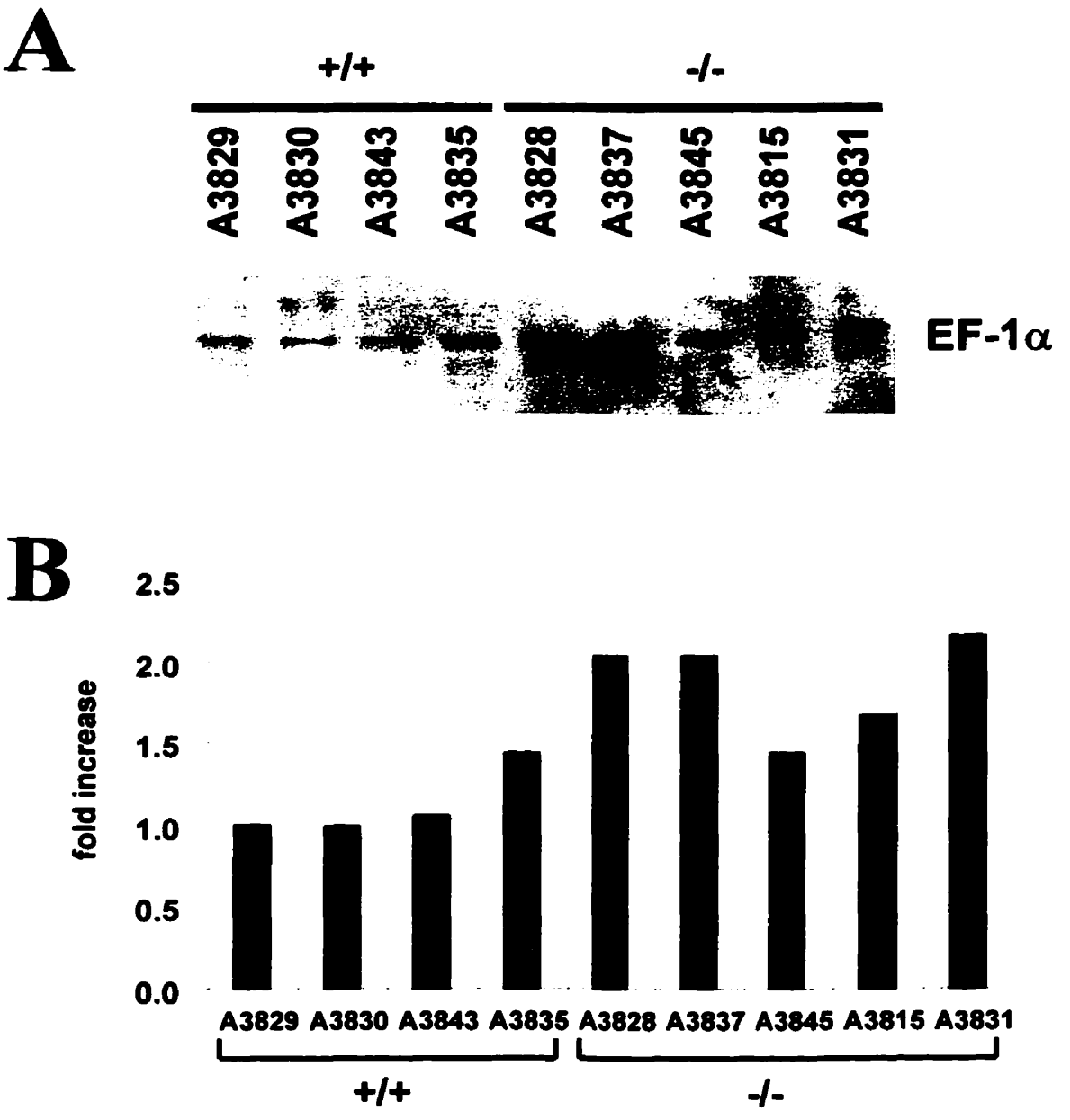
A
+/+
-/-
A3829
A3830
A3843
A3835
A3828
A3837
A3845
A3815
A3831
EF-1α
B
fold increase
2.5
2.0
1.5
1.0
0.5
0.0
A3829 A3830 A3843 A3835 A3828 A3837 A3845 A3815 A3831
+/+
-/-

Table 1. **Retrospective analysis of precise mouse age in comparison to genotype and EF-1α levels.** Following Western immunoblotting analysis using an EF-1α-specific antibody, a retrospective analysis of the age of each mouse was performed and compared to genotype and fold-increase of EF-1α protein.

Table 1. **Retrospective analysis of precise mouse age in comparison to EF-1α levels.**

animal code	genotype	age	fold increase of EF-1α
A3829	+/+	14 days	1.00[1]
A3830	+/+	15 days	1.00
A3843	+/+	15 days	1.11
A3835	+/+	14 days	1.45
A3828	-/-	14 days	2.06
A3837	-/-	14 days	2.02
A3845	-/-	15 days	1.43
A3815	-/-	15 days	1.52
A3831	-/-	14 days	2.11

[1] the EF-1α levels of the animal A3829 (+/+) was arbitrarily designated as 1.00

Figure 17. **Densitometric analysis of EF-1α band intensity of heart samples pooled based on age.** Densitometric analysis assessing EF-1α band intensity was performed following separation of animals based on precise age. Homozygous mutant animals aged 14 days old (n=3) possessed a two-fold increase in EF-1α band intensity compared to wildtype controls (n=4). Conversely, homozygous mutant animals aged 15 days old (n=2) did not exhibit significantly elevated EF-1α levels.

Figure 17

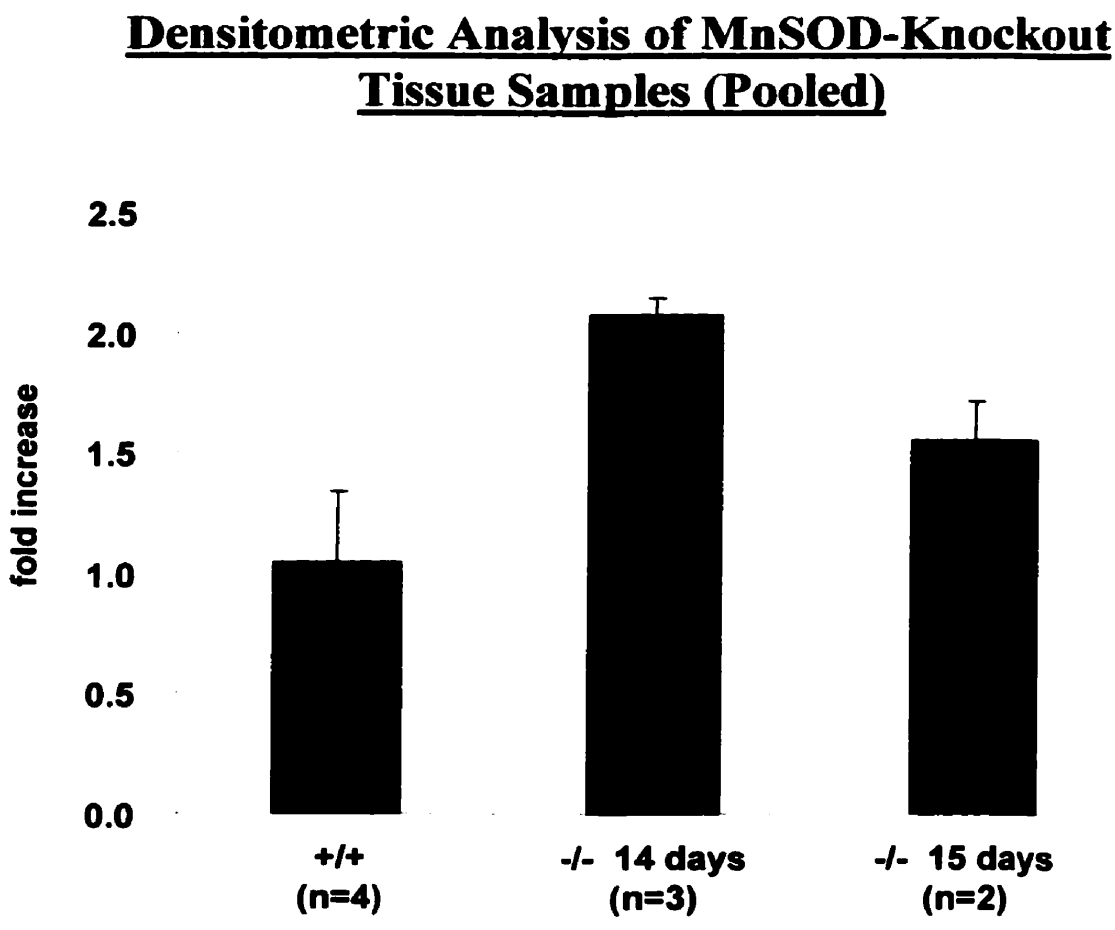
Densitometric Analysis of MnSOD-Knockout Tissue Samples (Pooled)
fold increase
2.5
2.0
1.5
1.0
0.5
0.0
+/+ (n=4)
-/- 14 days (n=3)
-/- 15 days (n=2)

EF-1α mRNA Expression in MnSOD-Knockout Mice

EF−1α mRNA levels were assessed by Northern blot analysis and found to be consistent in abundance in all nine animals tested (Figure 18, Panel A), again demonstrating that fluctuations observed in EF−1α protein levels occurred independent of mRNA changes. Confirmation of the stable mRNA levels was provided by densitometric analysis (Figure 18, Panel B).

Figure 18. **EF-1α mRNA expression is not altered in MnSOD-knockout mouse hearts.** Heart tissue samples were obtained from four wildtype mice and five homozygous mutant mice whose gene encoding for MnSOD had been inactivated by homologous recombination. All mice were aged between 14 and 15 days old. Panel A, Northern blot analysis of tissue samples using an EF-1α-specific probe revealed no alterations in EF-1α mRNA levels in all nine animals tested. Panel B, Densitometric analysis assessing EF-1α band intensity.

Figure 18

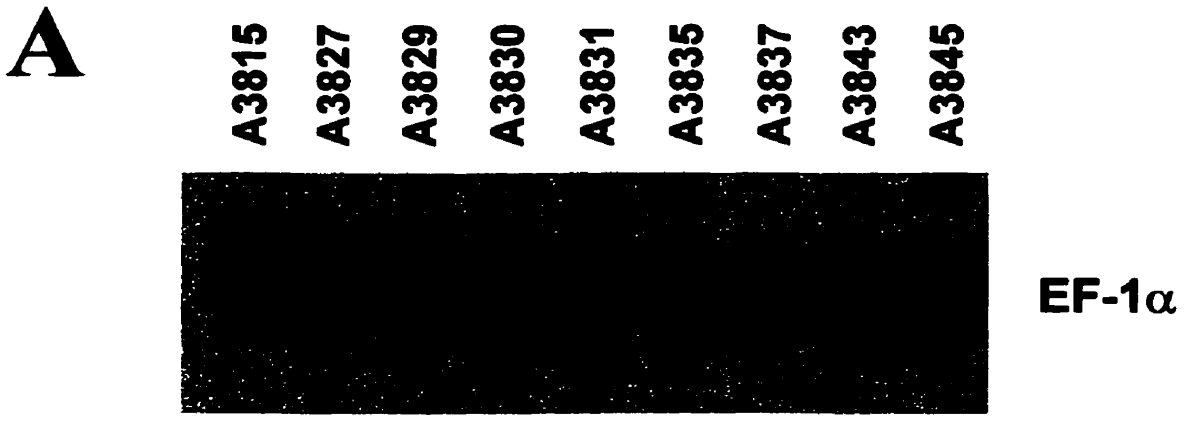
A
A3815
A3827
A3829
A3830
A3831
A3835
A3837
A3843
A3845
EF-1α

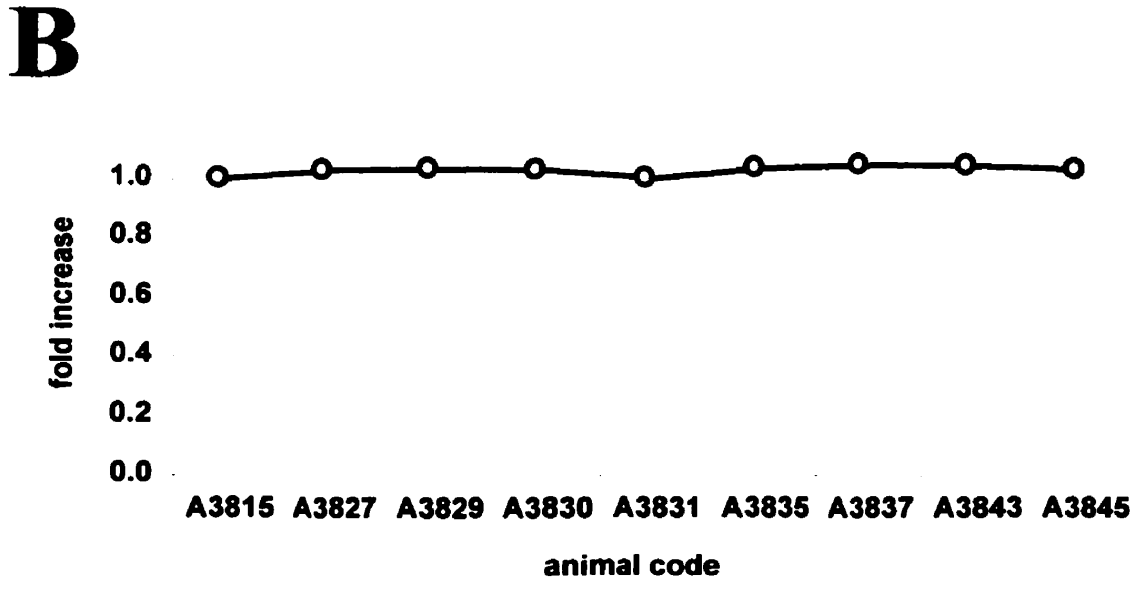
B
fold increase
1.0
0.8
0.6
0.4
0.2
0.0
A3815 A3827 A3829 A3830 A3831 A3835 A3837 A3843 A3845
animal code

DISCUSSION

The potential for free radicals and pro-oxidants to induce apoptosis and reduce cell numbers in the myocardium is of direct relevance in myocardial dysfunction, including artherosclerosis and reperfusion injury. However, understanding of the intracellular signaling mechanisms by which H_2O_2 and other pro-oxidants induce the apoptotic program remains limited. In attempts to investigate the molecular processes underlying cardiac reperfusion injury, many investigators have turned to *in vitro* cell culture models to simulate the processes involved in pro-oxidant-induced apoptosis.

Lennon and coworkers first reported that several cytotoxic agents, including hydrogen peoxide, could induce apoptosis in a dose-dependent manner in lymphocytes (Lennon *et al.*, 1991). Recently, this observation was extended to primary neonatal cardiomyocyte cultures. Concomitant with apoptosis of cardiac myocytes, ROIs also activated cytochrome c translocation from the mitochondria, caspase-3 activation and DNA fragmentation, all hallmarks of apoptotic cell death (von Harsdorft *et al.*, 1999). The development of a cardiac-derived cell line by Kimes and Brandt (1976), designated H9c2(2-1), has further facilitated the study of the mechansism of free radical-induced cell death in the myocardium, by avoiding the demanding technical protocols and costly expenses associated with primary cultures of neonatal cardiomyocytes.

Given previous reports indicating a role of the peptide elongation factor, EF–1α, in apoptotic proceses (Duttaroy *et al.*, 1998; Kato *et al.*, 1997), the current project was undertaken to investigate the effect of oxidative stress on the expression of the peptide elongation factor, and to assess its role in the ensuing induction of apoptosis. Two systems were used to emulate models of the myocardium undergoing oxidative stress: 1) the H9c2(2-1) cardiac-derived cell line when oxidatively challenged by exposure to H_2O_2, and 2) cardiac tissue samples obtained MnSOD-null transgenic mice. While these two paradigms are fundamentally dissimilar in that they represent over-abundancies of two

different oxygen intermediates, there are also several similarities which serve as a basis for comparison between these two models. Both MnSOD-knockout mice and catalase-knockout mice have been shown to exhibit similar abnormal cardiac phenotypes, including ventricular wall thinning and increased apoptotic incidences of cardiomyocytes (Li *et al.*, 1995). However, ultimately, neither molecules mediate their effects directly, but rather by the generation of the hydroxyl anion, and blockage of the Fenton reactions can ameliorate the effects of both species. In essence, both O_2^- and H_2O_2 reflect intermediates in the same series of reactions, leading to the hydroxyl radical, the true mediator of cellular damage. Therefore, insofar as these systems represent models of *in vitro* and *in vivo* oxidative stress in the myocardium, they were used to explore the effects of exposure to ROIs on apoptotic induction and on the expression of EF-1α.

Mechanism of Reactive Oxygen Intermediates-Induced Caspase Activation

Turner *et al.* (1998) previously demonstrated that the H9c2(2-1) cardiac myoblast cell line can undergo apoptotic cell death when exposed to toxic levels of H_2O_2. Concomitant with DNA fragmentation, caspase-3 activity was detected during the end stages of cellular demise. The mechanism by which caspase-3 activation is achieved, however, was not subjected to investigation. von Harsdorft *et al.* (1999), using primary neonatal cardiomyocytes, reported the ejection of cytochrome c as an early step to caspase-3 activation, suggesting that the mitochondria is involved in apoptotic executionary pathways. To complement these findings, here, we show that caspase-3 activation in H_2O_2-treated H9c2(2-1) cells is not accompanied by caspase-8 activity. Thus, we define an absent role in receptor-mediated signaling pathways in apoptotic signaling as induced by ROIs. This could be an indication that mitochondrial-dependent events represent the sole pathway involved in the execution of apoptosis following exposure to ROIs. To verify such a hypothesis, caspase-9-specific and caspase-8-specific inhibitors could be administered in culture in conjunction with H_2O_2 to assess which

inhibitor is capable of protecting aginst ROI-induced cytotoxicity. In theory, if the mitochondrial-dependent apoptotic pathway represents the lone pathway functioning following oxidative stress, caspase-9 inhibitors would be able to block apoptotic pathways virtually completely, while caspase-8 inhibitors would have negligible effect.

Translational Control of EF–1α Expression Following Oxidative Stress

In this study, we provide evidence describing an elevation in expression of the peptide elongation factor, EF–1α, in two situations of oxidative stress, *i.e.* following treatment of a cardiac-derived cell line with the pro-oxidant, H_2O_2, and in cardiac tissue samples obtained from mice lacking the antioxidant, MnSOD. Furthermore, we present evidence that the mode of up-regulation is mediated post-transcriptionally, as the EF–1α mRNA levels remain constant under conditions of oxidative stress. Moreover, in the H9c2(2-1) culture system, the elevation in EF–1α protein occurred without the need for *de novo* gene transcription. To our knowledge, this is only the second instance in which levels of expression of a protein have been shown to be regulated at the translational level following oxidative stress with H_2O_2. Regulation of ferritin and transferrin receptor mRNA translation has been shown previously to be regulated by altered binding capabilities of the iron regulatory protein (IRP) to the iron response elements (IREs) in the 5'-UTRs, following oxidative stress.

That EF–1α protein levels are elevated *via* translational mechanisms is not altogether surprising. The EF–1α protein belongs to a family of coordinately regulated proteins, which includes ribosomal proteins, elongation factor-2 and insulin-like growth factor-1, whose mRNAs bear a 5'-terminal oligopyrimidine (5'-TOP) tract in the 5'-untranslated region (Loreni *et al.*, 1993). The 5'-TOP, a pyrimidine-rich stretch located at the terminal cap, functions to dictate efficiency of translation by regulating distribution of the mRNA into translation-inactive mRNA-ribonucleoprotein pools or into translation-

active polyribosome pools. As such, this form of gene regulation allows rapid responses, bypassing the necessity of *de novo* gene transcription by simply recruiting pre-existing mRNA to the actively translating compartment. The advantage of this phenomenon may lie in the potential rapidity of the responses, necessary especially in the immediate early responses seen in the initial phases of apoptosis, where a quick up-regulation of the protein synthesis machinery is needed in order to start synthesizing apoptotic executioner proteins. We hypothesize that this is also the case under conditions of oxidative stress, where there is a redistribution of the EF–1α mRNA to the actively translatable pool upon treatment with H_2O_2, and that this process is dependent upon the 5'-TOP sequence.

Three experiments using the H9c2(2-1) cell culture system could be performed to address this hypothesis. The first set of experiments would involve reporter assays by high effiency transient transfection of a reporter gene under the control of the 5'-TOP *cis*-element into H9c2(2-1) cultures. Quantitation of the activity of the reporter gene (which would be proportional to the efficiency at which the reporter gene product is produced) prior to and following H_2O_2 administration would allow for assessment of the effects of oxidative challenge on translation of any mRNAs bearing the 5'-TOP element. In conjunction, a second test of the role of the 5'-TOP tract would be to assess the efficacy of the immunosuppresant, rapamycin, in inhibiting EF–1α up-regulation following oxidative stress. Rapamycin is a potent inhibitor of the p70 S6 kinase, which functions up-stream of activation of translation of 5'-TOP-bearing mRNAs (Proud, 1996). If the polypyrimidine tract is, indeed, the *cis*-element involved in mediating activation of EF–1α translation, rapamycin should be sufficient in abrogating the increase. And finally, assessment of EF–1α mRNA levels in separated mRNP and polyribosome pools by Northern blot analysis would allow for the visualization of any "pool-to-pool" movement of EF–1α mRNA following oxidative challenge. Taken together, these experiments would permit a definitive demonstration that the mechanism of EF–1α up-regulation

following oxidative stress is mediated at the translational level, and is controlled by the 5'-TOP tract.

Increased EF–1α in MnSOD-Knockout Transgenic Mice

In addition to the *in vitro* cell culture model, elevated levels of EF–1α were also detected in transgenic mice lacking the antioxidant, MnSOD, a system which represents an *in vivo* model of oxidative stress. In comparison to four wildtype animals where EF-1α levels were low, EF–1α was elevated in all three 14-day old homozygous animals tested (2.06-fold increase, SD = 0.05). The effect was also present, although less significant, in the two 15-day old homozygous animals tested (1.48-fold increase, SD = 0.06). In the meanwhile, in all nine animals, EF-1α mRNA remained constant.

Why is the elevation of EF–1α at 14-days post-birth more pronounced than at 15-days post-birth? The explanation may lie, in part, in the life span of the mutant animals. Fifteen days represents the absolute maximum life span of these mice lacking the MnSOD antioxidant, with no animals ever having been documented to survive beyond this barrier (T.-T. Huang, C.J. Epstein, personal communication). Therefore, it may be that such a late stage prior to death reflects the final self-destructive processes of the cell in its extreme late stage of cell death, where all cellular components, even components of the apoptotic machinery, are actively being destroyed, and literally everything, bar none, is being steadfastly disassembled. On the other hand, fourteen days may represent a time point at which apoptotic signaling pathways are still intact and apoptotic initiators and executioners are still functioning to signal and execute pro-apoptotic signals. One such molecule may be EF–1α, and as such, its expression may remain elevated at the earlier time point. If such a hypothesis is correct, a corollary would be that other structural components and housekeeping genes of the cell would also be more prone to a global down-regulation in 15-day old animals in comparison to 14-day old animals. As such, immunoblots for housekeeping genes such as actin could be performed to judge the

effects of the 14-to-15-day transition on the diminution of such ubiquitous proteins in the cell. Moreover, total cellular proteins could also be quantified by extraction by TCA precipitation, and total quantities measured in order to compare total protein content in 14-day *versus* 15-day old animals. Again, if the effect is global and represents total and end-stage breakdown of cellular and tissue structure, total protein content should diminish in 15-day old tissue samples relative to its 14-day old counterpart.

Alternatively, it may be that the 14-to-15-day transition results in the loss of the pro-apoptotic cells containing elevated EF-1α levels, and that which remains in 15-day old mouse hearts are cells with unusually strong antioxidant capabilities able to better resist oxidative stress. As such, these cells would be less affected by their lack of MnSOD, not be undergoing oxidative stress, and thus, would not possess elevated EF-1α levels. In order to test such a hypothesis, primary cultures of cardiomyocytes from 14-day old and 15-day old hearts could be assayed for their resistance to an O_2^- generator, such as paraquat. If this theory is true, the 15-day old primary cultures would be less affected in such an *in vitro* assay. Also, immunoblotting analyses on the primary cultures would be able to test whether elevation of EF-1α is altered in 14-day old *versus* 15-day old cardiomyocytes following oxidative exposure.

Speculative Roles of EF−1α in Oxidative Stress-Induced Apoptosis

So what is the role of the elevated EF-1α following oxidative stress? In fact, can we be certain that the up-regulation is of physiological relevance at all? The ability of diminished EF−1α levels (by transfection of an antisense-EF−1α) to confer a partial protective effect against cell death argues that the increase of EF−1α abundance is a functionally relevant one to the initiation or execution of apoptosis. That the antisense protection is not total suggests that, not surprisingly, other factors are necessary in the induction of apoptosis upon exposure to oxidative stress, and that EF-1α does not stand at an upstream juncture of a single pro-apoptosis pathway. Indeed, the revelation that a

significant population of cells in any given system undergo apoptosis regardless of the lowered EF-1α levels achieved by the antisense transfection suggests that in some cases apoptosis can occur independent of alterations in EF-1α expression. These findings are consistent with Duttaroy *et al.* (1998) who observed that mouse 3T3 fibroblasts stably transfected with antisense EF–1α showed decreased susceptibility to serum deprivation-induced apoptosis, while cells stably transfected with sense EF–1α showed increased susceptibility. The lack of a total protective effect was also noted by this group. Furthermore, others have demonstrated in a p53-deficient erythroleukemic cell line that a p53-dependent induction of EF–1α mRNA expression occurred prior to cell death (Kato *et al.*, 1997; Kato, 1999).

The question, therefore, turns to one of why EF–1α is increased when cells are dying, and what is its role? While both studies mentioned above demonstrated a need for EF–1α in the execution of the apoptotic program, neither has been able to clarify its exact role. Given that apoptosis is an active, gene-driven process, one possible explanation for the observed increase in EF–1α may be to support *de novo* synthesis of proteins needed to fuel apoptotic processes. Consistent with this premise is the observed delay from EF-1α protein up-regulation (maximal at 30-60 minutes post-H_2O_2 exposure) to caspase-3 activation (maximal at 3 hours post-H_2O_2 exposure). The rise in EF-1α levels precedes caspase-3 activity because elevated EF-1α levels are needed in order to generate the caspase enzyme, among with its many other partners in the execution of apoptosis. The fact that EF-1α can be regulated post-transcriptionally, thus allowing its rapid up-regulation, and that caspase gene expression is regulated transcriptionally, provides the mechanism by which this chronology of events can be possible.

Previous reports demonstrating that inhibition of macromolecular biosynthesis is capable of preventing apoptosis in some cases lends credence to the hypothesis that EF-1α may function to generate apoptotic executioner proteins during apoptosis (Wyllie *et al.*, 1984; Shi *et al.*, 1989). However, this hypothesis is confounded by the ability of

transcriptional and translational inhibitors, such as actinomysin D and cycloheximide, themselves, to induce apoptosis at sufficiently high doses (Martin *et al.*, 1990) . In addition, it has been well documented that there is a global shut-down of protein synthesis following cerebral reperfusion, mediated by phosphorylation of the initiation factor 2α (eIF2α) (DeGracia *et al.*, 1996). Moreover, eIF-2α has also been recognized as a substrate for caspase-3 following induction of apoptosis (Satoh *et al.*, 1999). Since these inhibitory measures function to prevent the formation of the 43S preinitiation complex needed for recognition of the 5'-cap during mRNA translation at a step up-stream of EF−1α function, its effects would, thus, supercede any effects of increased EF−1α abundance on mRNA translation. Therefore, while increased EF−1α following oxidative stress may participate to some degree in the production of apoptosis-related proteins, it is unlikely that the function of EF−1α during apoptosis is limited exclusively to protein synthesis processes.

An alternative function of EF−1α during apoptosis which may have a profound impact on cellular function, as proposed by Kato (1999), relates to its effects on the cytoskeleton. Microinjection of EF−1α in fibroblasts has been shown to destabilize microtubule structures (Shiina *et al.*, 1994). Moreover, EF−1α's well characterized role in actin bundling (Demma *et al.*, 1990; Dharmawardhane *et al.*, 1991) could be responsible for formation of specialized actin structures following oxidative stress, such as stress fibres. Thus, EF−1α's versatile position at a critical juncture between essential housekeeping homeostatic functions, such as protein synthesis, and the regulation of cell fluidity by cytoskeletal reorganization, has led to suggestions that EF−1α may play a part in effecting damage to the cytoskeleton, especially to the microtubule and actin filament networks, during execution of apoptosis. Its ability to destabilize the intracellular cytoskeletal architecture may be a critical event in the orderly dismantling of the cell associated with programmed cell death.

Future Prospects

From these theories emerge one key question to be resolved: What are the cytoskeletal effects, if any, of altered expression of EF−1α during oxidative stress-induced apoptosis? And thus, would interference with the associated pro-apoptotic function(s) of EF−1α be a viable treatment option for cardiac dysfunction?

Specific effects of EF−1α under-expression on the cytoskeletal architecture upon apoptotic stresses can be assessed by immunocytochemical studies of intracellular actin or tubulin distribution in H_2O_2-treated antisense-EF−1α-transfected H9c2(2-1) cell cultures, as compared to structures in transgene-negative or vector alone controls. While the region of the EF-1α peptide responsible for microtubule association and severing have not yet been identified, a putative actin-association domain has been described (Owens *et al.*, 1992). Oxidative challenge of cultures transfected with an EF-1α cDNA bearing a specific disruption in this domain, followed by assessment of actin distribution patterns by immunocytochemistry, could be performed to ascertain the importance of EF-1α-actin association during apoptosis. Furthermore, the domain necessary for the microtubule-associated functions of EF-1α can also be identified, and similar experiments could be performed to determine the role of EF-1α-mediated microtubule modulation in apoptosis, as well.

The second question, an assessment of the efficacy of introduction of antisense-EF−1α as a viable treatment option, could be answered using gene therapy techniques, using adenoviral carriers. One approach would be to supplement reoxygenated reperfusion medium with antisense-EF−1α-adenoviruses, and determine whether it can protect against reperfusion-induced infarct size and cell loss. An alternate methodology would involve gene therapy trials on mice engineered to be constitutively subjected to *in vivo* oxidative stress, such as the MnSOD-knockout mice described in this report (Li *et al.*, 1995). Infection of viruses bearing an antisense-EF−1α which can abrogate the oxidative stress-associated EF−1α elevation can be tested on its ability to significantly

delay mortality in these mice. Any prolongation of life beyond the expected 10-15 days of homozygous MnSOD-null mice would be a tremendous achievement.

In the end, the results presented within this thesis represent an attempt to elucidate one specific mechanistic aspect associated with oxidative stress-initiated apoptotic cell death. Hopefully, better understanding of the mechanism by which EF-1α facilitates the process of apoptosis could, therefore, allow for the development of treatment options for reperfusion-associated myocardial infarctions by minimizing oxidative stress-induced apoptosis.

WORKS CITED

Ambrosio, G., Weisfeldt, M.L., Jacobus, W.E., Flaherty, J.T. Evidence for a reversible oxygen radical-mediated component of reperfusion injury: reduction by recombinant human superoxide dismutase administered at the time of reflow. *Circulation* (1987) 75, 282-291.

Anderson, C.W. DNA damage and the DNA-activated protein kinase. *Trends Biochem Sci* (1993) 18, 433-437.

Ann, D.K., Lin, H.H., Lee, S., Tu, Z-J., Wang, E. Characterization of the statin-like S1 and rat elongation factor 1α as two distinctly expressed messages in rat. *J Biol Chem* (1992) 267, 699-702.

Ann, D.K., Moutsatsos, I.K., Nakamura, T., Lin, H.H., Mao, P-L., Lee, M-J., Chin, S., Liem, R.K.H., Wang, E. Isolation and characterization of the rat chromosomal gene for a polypeptide (pS1) antigenically related to statin. *J Biol Chem* (1991) 266, 10429-10437.

Arlinghaus, R., Favelukes, G., Schweet, R. A ribosome-bound intermediate in polypeptide synthesis. *Biochem Biophys Res Comm* (1963) 11, 92-96.

Ashkenas, J., Warb, Z. Proteolysis and the biochemistry of life-or-death decisions. *J Exp Med* (1996) 183, 1947-1951.

Avni, D., Biberman, Y., Meyuhas, O. The 5' terminal oligopyrimidine tract confers translational control on TOP mRNAs in a cell type- and sequence context-dependent manner. *Nucleic Acids Res* (1997) 25, 995-1001.

Avni, D., Shama, S., Loreni, F., Meyuhas, O. Vertebrate mRNAs with a 5'-Terminal pyrimidine tract are candidates for translational repression in quiescent cells: characterization of the translational *cis*-regulatory element. *Mol Cell Biol* (1994) 14, 3822-3833

Bagchi, M.K., Bannerjee, A.C., Roy, R., Chakrabarty, I., Gupta, N.K. Protein synthesis in rabbit reticulocytes: characteristics of co-eIF-2 protein complex. *Nucleic Acids Res* (1982) 10, 6501-6510.

Baker, J.E., Felix, C.C., Olinger, G.N., Kalyanaraman, B. Myocardial ischemia and reperfusion: direct evidence for free radical generation by electron spin resonance spectroscopy. *Proc Natl Acad Sci USA* (1988) 85, 2786-2789.

Bakhshi, A., Jensen, J.P., Goldman, P., Wright, J.J., McBride, O.W., Epstein, A.L., Korsmeyer, S.J. Cloning the chromosomal breakpoint of t(14;18) human lymphomas: clustering around JH on chromosome 14 and near a transcriptional unit on 18. *Cell* (1985) 41, 899-906.

Barbior, B.M. The respiratory burst of phagocytes. *J Clin Invest* (1984) 73, 599-601.

Barbior, R.M. Oxygen-dependent microbial killing by phagocytes. *N Engl J Med* (1978) 298, 659-721.

Bektas, M., Nurten, R., Gurel, Z., Sayer, Z., Mermek, E. Interaction of eukaryotic elongation factor 2 with actin: a possible link between protein synthetic machinery and cytoskeleton. *FEBS Lett* (1994) 356, 89-93.

Benne, R., Hershey, J.W.B. The mechanism of action of protein synthesis initiation factors from rabbit reticulocytes. *J biol Chem* (1978) 253, 3078-3087.

Bielka, H. Properties and spatial arrangement of components in preinitiation complexes of eukaryotic protein synthesis. *Prog Nucleic Acid Res Mol biol* (1985) 32, 267-289.

Bierbaum, P., Donhoff, T., Klein, A. Macromolecular and micromolecular configurations of a gene encoding the protein synthess elonation factor EF–1α in *Stylonychia lemnae*. *Mol Microbiol* (1991) 5, 1567-1575.

Boldin, M.P., Goncharov, T.M., Goltsev, Y.V., Wallach, D. Involvement of MACH, a novel MORT1/FADD-interacting protease, in Fas/APO-1-and TNF receptor-induced cell death. *Cell* (1996) 85, 803-815.

Bolli, R., McCay, P.B. Use of spin traps in intact animals undergoing myocardial ischaemia/reperfusion: a new approach to assessing the role of oxygen free radicals in myocardial "stunning" *Free Rad Res Comm* (1990) 9, 169-180.

Brands, J.H., Maassen, J.A., van Hemert, F.J., Amons, R., Moller, W. The primary structure of the alpha subunit of human elongation factor 1. Structural aspect of guanine-nucleotide binding sites. *Eur J Biochem* (1986) 155, 167-171.

Caelles, C., Helmberg, A., Karin, M. p53-dependent apoptosis in the absence of transcriptioinal activation. *Nature* (1994) 370, 220-223.

Cai, Y., Yang, J., Jones, D.P. Mitochondrial control of apoptosis: the role of cytochrome c. *Biochim Biophys Acta* (1998) 1366, 139-149.

Caldas, T.D., El Yaagoubi, A., Richarme, G. Chaperone properties of bacterial elongation factor EF-Tu. *J Biol Chem* (1998) 273, 11478-11482.

Caricchio, R., Kovalenko, D., Kaufmann, W.K., Cohen, P.L. Apoptosis provoked by oxidative stress inducer menadione (vitamin K(3) is mediated by the Fas/Fas ligand system. *Clin Immunol* (1999) 93, 65-74.

Carmichael, J., DeGraff, W.G., Gazdar, A.F., Minna, J.D., Mitchell, J.B. Evaluation of a tetrazolium-based semiautomated colorimetric assay: assessment of chemosensitivity testing *Cancer Res* (1987) 47, 936-942.

Casciola-Rosen, L., Nicholson, D.W., Chong, T., Rowan, K.R., Thornberry, N.A., Miller, D.K., Rosen, A. Apopain/CPP32 cleaves proteins that are essential for cellular repair: a fundamental principle of apoptotic death. *J Exp Med* (1996) 183, 1957-1964.

Cavallius, J., Merrick, W.C. Nucleotide sequence of rabbit elongation factor-1 alpha cDNA. *Nucleic Acids Res* (1992) 20, 1422

Chen-Levy, Z., Cleary, M.L. Membrane topology of the Bcl-2 proto-oncogenic protein demonstrated *in vivo*. *J Biol Chem* (1990) 265, 4923-4933.

Chernyak, B.V., Bernardi, P. The mitochondrial permeability transition pore is modulated by oxidative agents through both pyridine nucleotides and glutathione at two separate sites. *Eur J Biochem* (1996) 238, 623-630.

Chinnaiyan, A.M., O'Rouke, K., Tewari, M., Dixit, V.M. FADD, a novel death domain-containing protein, interacts with the death domain of Fas and initiates apoptosis. *Cell* (1995) 81, 505-512.

Chomczynki, P., Sacchi, N. Single-step method of RNA isolation by acid guanidium thiocyanate-phenol-chloroform extraction. *Anal Biochem* (1987) 162, 152-159.

Chong, K-Y., Lai, C-C., Lille, S., Chang, C., Su, C-Y. Stable overexpression of the constitutive form of heat shock protein 70 confers oxidative proection. *J Mol Cell Cardiol* (1998) 30, 599-608.

Clark, B.F.C., Kjeldgaard, M., la Cour, T.F.M., Thirup, S., Nyborg, J. Structural determination of the functional sites of *E. coli* elongation factor Tu. *Biochim Biophys Acta* (1990) 1050, 203-208.

Clutton, S. The importance of oxidative stress in apoptosis. *Br Med Bull* (1997) 53, 662-668.

Collings, D.A., Wasteneys, G.O., Miyazaki, M., Williamson, R.E. Elongation factor 1α is a component of the subcortical actin bundles of characean algae. *Cell Biol Int* (1994) 18, 1019-1024.

Condeelis, J. Elongation factor 1α, translation and the cytoskeleton. *Trends Biochem Sci* (1995) 20, 169-170.

Constantini, P., Chernyak, B.V., Petronilli, V., Bernardi, P. Modulation of the mitochondrial permeability transition pore by pyridine nucleotides and dithiol oxidation at two separate sites. *J Biol Chem* (1996) 271, 6746-6751.

Cothurst, D.R., Campbell, D.G., Proud, C.G. Structure and regulation of eukaryotic initiation factor eIF-2: sequence of the site in the α subunit phosphorylated by the haem-controlled repressor and by the double-stranded RNA-activated inhibitor. *Eur J Biochem* (1987) 166, 357-363.

de Jorg, J.W., van der Meer, P., Nieukoop, A.S., Huizer, T., Stroeve, R.J., Bos, E. Xanthine oxidoreductase activity in perfused hearts of various species, including humans. *Circ Res* (1990) 67, 770-773.

DeGracia, D.J., Neumar, R.W., White, B.C., Krause, G.S. Global brain ischemia and reperfusion: modifications in eukaryotic initiation factors associated with inhibition of ranslation initiation. *J Neurochem* (1996) 67, 2005-2012

Demma, M., Warren, V., Hock, R., Dharmawardhane, S., Condeelis, J. Isolation of an abundant 50,000-Dalton actin filament bundling protein from *Dictyostelium* amoebae. *J Biol Chem* (1990) 265, 2286-2291.

Deng, C., Zhang, P., Harper, J.W., Elledge, S.J., Leder, P. Mice lacking p21/PCII/WAF1 undergo normal development, but are defective in G1 checkpoint control. *Cell* (1995) 82, 675-684.

Dever, T.E., Glynias, M.J., Merrick, W.C. GTP-binding domain: three consensus sequence elements with distinct spacing. *Proc Natl Acad Sci USA* (1987) 84, 1814-1818.

Dharmawardhane, S., Demma, M., Yang, F., Condeelis, J. Compartmentalization and actin binding properties of ABP-50: the elongation factor-1 alpha of *Dictyostelium*. *Cell Motil. Cytoskel* (1991) 20, 279-288.

Dholakia, J.N., Francis B.R., Haley, B.E., Wahba, A.J. Photoaffinity labelling of the rabbit reticulocyte guanine nucleotide exchange factor and eucaryotic initiation factor 2 with 8-azindopurine nucleotides: identification of GTP- and ATP-binding domains. *J Biol Chem* (1989b) 264, 20638-20642.

Dholakia, J.N., Wahba, A.J. Mechanisms of the nucleotide exchange reaction in eucaryotic polypeptide chain initiation. *J Biol Chem* (1989a) 264, 546-550.

Diller, L., Kassel, J., Nelson, C.E., Gryka, M.A., Litwak, G., Gebhardt, M., Bressac, B., Ozturk, M., Baker, S.J., Vogelstein, B., Friend, S.H. p53 functions as a cell cycle control protein in osteosarcomas. *Mol Cell Biol* (1990) 10, 5772-5781.

Dje, M.K., Mazabraud, A., Viel, A., le Maire, M., Denis, H., Crawford, E., Brown, D.D. Three genes under different developmental control encode elongation factor-1 alpha in *Xenopus laevis*. *Nucleic Acids Res* (1990) 18, 3489-3493.

Downey, J.M., Hearse, D.J., Yellon, D.M. The role of xanthine oxidase during myocardial ischaemia in several species including man. *J Mol Cell Cardiol* (1988) 20 (suppl II), 55-63.

Dragovich, T., Rudin, C.M., Thompson, C.B. Signal transduction pathways that regulate cell survival and cell death. *Oncogene* (1998) 17, 3207-3213.

Durso, N.A., Cyr, R.J. A calcoduin-sensitive interaction between microtubules and a higher plant homolog of elongation factor–1α. *Plant Cell* (1994) 6, 893-905.

Duttaroy, A., Bourbeau, D., Wang, X-L., Wang, E. Apoptosis can be accelerated or decelerated by overexpression or reduction of the level of elongation factor–1α. *Exp Cell Res* (1998) 238, 168-176.

Eddy, L.J., Stewart, J.R., Jones, H.P., Engerson, T.D., McCord, J.M., Downey, J.M. Free radical-producing enzyme, xanthine oxidase, is undetectable in human hearts. *Am J Physiol* (1987) 253, H709-H711.

El-Deiry, W.S., Kern, S.E., Pietenpol, J.A., Kinzler, K.W., Vogelstein, B. Definition of a consensus binding site for p53. *Nature Gen* (1992) 1, 45-49.

El-Deiry, W.S., Tokino, T., Velculencu, V.E., Levy, D.B., Parsons, R., Trent, J.M., Lin, D., Mercer, E.W., Kinzler, K.W., Vogelstein, B. WAF1, a potential mediator of p53 tumour suppression. *Cell* (1993) 71, 817-825.

Engler, R.L., Schmid Schonbein, G.W., Pavelec, R.S. Leucocyte capillary plugging in myocardial ischaemia and reperfusion in the dog. *Circulation* (1983) 62, 1016-1023.

Farmer, G., Bargonetti, J., Zhu, H., Friedman, P., Prywes, R., Prives, C. Wild-type p53 activates transcription in vitro. *Nature* (1992) 358, 83-86.

Fenton, H.J.H. Fenton chemistry. *J Chem Soc* (1894) 65, 899-910.

Fernandes-Alnemri, T., Armstrong, R.C., Krebs, J., Srinivasula, S.M., Wang, L., Bullrich, F., Fritz, L.C., Trapani, J.A., Tomaselli, K.J., Litwack, G., Alnemri, E.S. *In vitro* activation of CPP32 and Mch3 by Mch4, a novel human apoptotic cysteine protease containing two FADD-like domains. *Proc Natl Acad Sci USA* (1996) 93, 7464-7469.

Ferrari, R., Ceconi, C., Curello, S., Cargnoni, A., Pasini, E., De Guili, F., Albertini, A. Role of oxygen free radicals in ischemic and reperfused myocardium. *Am J Clin Nutr* (1991) 53, 215S-222S.

Ferrari, R., Ceconi, C., Curello, S., Guarnieri, C., Caldarera, C.M., Albertini, A., Visioli, O. Oxygen-mediated myocardial damage during ischaemia and reperfusion: role of the cellular defences against oxygen toxicity. *J Mol Cell Cardiol* (1985) 17, 937-945.

Flitter, W.D. Free radicals and myocardial reperfusion injury. *Br Med Bull* (1993) 49, 545-555.

Forman, M.B., Puett, D.W., Cates, C.U., McCroskey, D.E., Beckman, J.K., Greene, H.L., Virmani, R. Glutathione redox pathway and reperfusion injury effect of n-acetylcysteine on infarct size and entricular function. *Circulation* (1988) 78, 202-213.

Freeman, B.A., Crapo, I.D. Biology of disease: Free radicals and tissue injury. *Lab Invest* (1982) 47, 412-426.

Gallagher, K.P., Buda, A.J., Pace, D., Gerren, R.A., Shlafer, M. Failure of superoxide dismutase and catalase to alter size of infarction in conscious dogs after three hours of occlusion followed by reperfusion. *Circulation* (1986) 73, 1137-1142.

Garlick P.B., Davies, M.J., Hearse, D.J., Slater, T.F. Direct detection of free radicals in the reperfused rat heart using electron spin resonance spectroscopy. *Circ Res* (1987) 61, 757-760.

Ghosh, S., Chevesich, J., Maitra, U. Further characterization of eucaryotic initiation factor 5 from rabbit reticulocytes. *J Biol Chem* (1989) 264, 5134-5140.

Gilad, E., Zingarelli, B., Salzman, A.L., Szabo, C. Protection by inhibition of poly(ADP-ribose) synthetase against oxidant injury in cardiac myoblasts *in vitro*. *J Mol Cell Cardiol* (1997) 29, 2585-2597.

Gonen, H., Smith, C.E., Siegel, N.R., Kahana, C., Merrick, W.C., Chakraburtty, K., Schwartz, A.L., Ciechanova, A. Protein synthesis elongation factor EF-1 alpha is essential for ubiquitin-dependent degradation of certain N alpha-acetylated proteins and may be substituted for by the bacterial elongation factor EF-Tu. *Proc Natl Acad Sci USA* (1995) 91, 7648-7652.

Granger, D.N., Rutilio, G., McCord, J.M., Superoxide radicals in feline intestinal ischaemia. *Gastroenterology* (1981) 81, 282-291.

Grifo, J.A., Tahara, S.M., Morgan, M.A., Shitkin, A.J., Merrick, W.C. New initiation factor activity required for globin mRNA translation. *J Biol Chem* (1983) 258, 5804-5810.

Gross, A., McDonnell, J.M., Korsmeyer, S.J. BCL-2 family members and the mitochondria in apoptosis. *Genes Dev* (1999) 13, 1899-1911.

Guillouf, A., Grana, X., Selvakumaran, M., De Luca, X.A., Giordano, A., Hoffman, B., Liebermann, D.A. Dissection of the genetic programs of p53-mediated G1 growth arrest and apoptosis: blocking p53-induced apoptosis unmasks G1 arrest. *Blood* (1995) 85, 2691-2698.

Hadler, S., Negrini, M., Monne, M., Sabbioni, S., Croce, C.M. Down regulation of bcl-2 by p53 in breast cancer cells. *Cancer Res* (1994) 54, 2095-2097.

Halestrap, A.P., Kerr, P.M., Javadov, S., Woodfield, K-Y. Elucidating the molecular mechanism of the permeability transition pore and its role in reperfusion injury in the heart. *Biochim Biophys Acta* (1998) 1366, 79-94.

Hampton, M.B., Fadeel, B., Orrenius, S. Redox Regulation of the caspasees during apoptosis. *Ann Rev NY Acad Sci* (1998) 854, 328-335.

Hansen, J., Etchison, D., Heshey, J.W.B., Ehrenfeld, E. Association of cap binding protein with eucaryotic initiation factor 3 in initiation factor preparations from uninfected and poliovirus infected HeLa cells. *J Virol* (1982) 42, 200-207.

Haunstetter, A., Izumo, S. Apopsosis: Basic mechanisms and implications for cardiovascular disease. *Circ Res* (1998) 82, 1111-1129.

Haupt, Y., Rowan, S., Shaulian, E., Vousden, K.H., Oren, M. Induction of apoposis in HeLa cells by trans-activation deficient p53. *Genes Dev* (1995) 8, 2170-2183.

Hearse, D.J. Reperfusion of ischaemic myocardium. *J Mol Cell Cardiol* (1977) 9, 607-616.

Hershey, J.W.B. Protein phosphorylation controls translation rates. *J Biol Chem* (1989) 264, 20823-20826.

Hescheler, J., Meyer, R., Plant, S., Krautwurst, D., Rosenthal, W., Schultz, G. Morphological, biochemical, and electrophysiological characterization of a clonal cell (H9c2) line from rat heart. *Circ Res* (1991) 69, 1476-1486.

Hess, M.L., Manson, N.H. Molecular oxygen, friend and foe. *J mol Cell Cardiol* (1984) 16, 969-985.

Hoch, B., Haase, H., Schulze, W., Hagemann, D., Morano, I., Krause, E-G., Karczewski, P. Differentiation-dependent expression of cardiacδ-CaMKII isoforms. *J Cell Biochem* (1998) 68, 259-268.

Hockenbery, D.M., Nunez, G., Milliman, C., Schreiber, R.D., Korsmeyer, S.J. Bcl-2 is an inner mitochondrial membrane protein that blocks programmed cell death. *Nature* (1990) 348, 334-336.

Hockenbery, D.M., Oltvai, Z.N., Yin, X-M., Milliman, C.L., Korsmeyer, S.J. Bcl-2 functions in an antioxidant pathway to prevent apoptosis. *Cell* (1993) 75, 241-251.

Hoevermann, B., Richter, S., Waldorf, U., Cziepluch, C. Two genes encode related cytoplasmic elongation factor 1 alpha in *Drosophila melanogaster* with continuous and stage specific expression. *Nucleic Acid Res* (1988) 16, 3175-3194.

Huang, T-T., Yasunami, M., Carlson, E.J., Gillespie, A.M., Reaume, A.G., Hoffman, E.K., Chan, P.H., Scott, R.W., Epstein, C.J. Superoxide-mediated cytotoxicity in superoxide dismutase-deficient fetal fibroblasts. *Arch Biochem Biophys* (1997) 344, 424-432.

Ibuki, F., Moldave, K. The effect of guanosine triphosphate, other nucleotides, and aminoacyl transfer ribonucleic acid on the activity of transferase I and on its binding to ribosomes. *J Biol Chem* (1968) 243, 44-50.

Ide, T., Tsutsui, H., Kinugawa, S., Utsumi, H., Kang, D., Hattori, N., Uchida, K., Arimura, Ki., Egashira, K., Takeshita, A. Mitochondrial electron transport complex I is a potential source of oxygen free radicals in the failing myocardium. *Circ Res* (1999) 85, 357-63.

Imlay, J.A., Linn, S. DNA damage and oxygen radical toxicity. *Science* (1988) 240, 1302-1309.

Itoh, N., Nagata, S. A novel protein domain required for apoptosis: mutational analysis of human Fas antigen. *J Biol Chem* (1993) 74, 845-853.

Iwasaki, K., Motoyoshi, K., Nagata, S., Karizo, Y. Purification and properties of a new polypeptide chain elongation factor,EF−1βγ from the pig liver. *J Biol Chem* (1976) 251, 1843-1845.

Jacobson, M.D., Burnett, J.F., King, M.D., Miyashita, T., Reed, J.C., Raff, M.C. Bcl-2 blocks apoptosis in cells lacking mitochondrial DNA. *Nature* (1993) 361, 365-369.

Janicke, R.U., Walker, P.A., Lin, X.Y., Porter, A.G. Specific cleavage of the retinoblastoma protein by an ICE-like protease in apoptosis. *EMBO J* (1996) 15, 6969-6978.

Jarasch, E.D., Bruder, G., Heid, H.W. Significance of xanthine oxidase in capillary endothelial cells. *Acta Physiol Scand* (1986) 548, 39-46.

Janssen, G.M.C., Moller, W. Kinetic studies on the role of elongation factors 1β and 1γ in protein synthesis. *J Biol Chem* (1988) 263, 1773-1778

Jeffries, H.B.J., Thomas, G., Thomas, G. Elongation factor−1α is selectively translated following mitogenic stimulation. *J Biol Chem* (1994) 269, 4367-4372.

Jennings, R.B., Ganote, C.E. Structural changes in myocardium during acute ischemia. *Circ Res* (1974) 34-35(Suppl. III), 156-172.

Jennings, R.B., Sommers, H.M., Smyth, G.A., Flack, H.A., Linn, H. Myocardial necrosis induced by temporary occlusion of a coronary artery in the dog. *Arch Pathol* (1960) 70, 68-78.

Johnson, J.L, Rajagopalan, K.V., Cohen, H.J. Molecular basis of the biological function of molybdenum: effect of tungsten on xanthine oxidase and sulfite oxidase in the rat. *J Biol Chem* (1974) 249, 859-866.

Jolly, S.R., Kane, W.J., Bailie, M.B., Abrams, G.D., Lucchesi, B.R. Canine myocardial reperfusion injury: its reduction by the combined administration of superoxide dismutase and catalase. *Circ Res* (1984) 54, 277-285.

Jurnak, F., Heffron, S., Schick, B., Delaria, K. Three-dimensional models of the GDP and GTP forms of the guanine nucleotide domain of *Escherichia coli* elongation factor Tu. *Biochim Biophys Acta* (1990) 1050, 209-214.

Kahns, S., Lund, A., Kristensen, P., Knudsen, C.R., Clark, B.F.C., Cavallius, J., Merrick, W.C. The elongation factor 1 A-2 isoform from rabbit: cloning of the cDNA and characterization of the protein. *Nucleic Acid Res* (1998) 26, 1884-1890.

Kastan, M.B., Zhan, Q., El-Deiry, W.S., Carrier, F., Jacks, T., Walsh, W.V., Plunkett, B.S., Vogelsetin, B., Fornace, A.J. A mammalian cell cycle checkpoint pathway utilizing p53 and GADD45 is defective in ataxia-telangiectasia *Cell* (1992) 71, 587-597.

Kato, M.V. The mechanism of death of an erythroleukemic cell line by p53: involvement of the microtubule and mitochondria. *Leuk Lymphoma* (1999) 33, 181-186.

Kato, M.V., Sato, H., Nagayoshi, M., Ikawa, Y. Upregulation of the elongation factor–1α gene by p53 in association with death of an erythroleukemic cell line. *Blood* (1997) 90, 1373-1378.

Katstan, M.B., Onyekwere, O., Sidransky, D., Voglstein, B., Craig, R.W. Participation of p53 protein in the cellular response to DNA damage. *Cancer Res* (1991) 51, 6304-6311.

Kaufmann, S.H., Desnoyers, S., Ottaviano, Y., Davidson, N.E., Poirier, G.G. Specific proteolytic cleavage of poly(ADP-ribose) polymerase: an early marker of chemotherapy-induced apoptosis. *Cancer Res* (1993) 53, 3976-3985.

Kehrer, J.P., Piper, H., Sies, H. Xanthine oxidase is not responsible for reoxygenation injury in isolated-perfused rat heart. *Free Rad Res Commun* (1987) 3, 69-78.

Kern, S.E., Kinzler, K.W., Bruskin, A., Jarosz, D., Friedman, P., Prives, C., Vogelstein, B. Identification of p53 as a sequence-specific DNA binding protein. *Science* (1991) 252, 1708-1711.

Kerr, J.F., Wyllie, A.H., Currie, A.R. Apoptosis: a basic biological phenomenon with wide-ranging implications in tissue kinetics. *Br J Cancer* (1972) 26, 239-257.

Kimes, B.W., Brandt, B.L. Properties of a clonal muscell cell line from rat heart. *Exp Cell Res* (1976) 98, 367-381.

Kluck, R.M., Bossy-Wetzel, E., Green, D.R., Newmeyer, D.D. The release of cytochrome c from mitochondria: A primary site for Bcl-2 regulation of apoptosis. *Science* (1997) 275, 1132-1136.

Knudsen, S.M., Frydenberg, J., Clark, B.F.C., Leffers, H. Tissue-dependent variation in the expression of elongation factor–1α isoforms: isolation and characterization of a cDNA encoding a novel variant of human elongation factor 1α. *Eur J Biochem* (1993) 215, 549-554.

Ko, W., Hawes, A.S., Lazenby, W.D., Calvano, S.E., Shin, Y.T., Zelano, J.A., Antonacci, A.C., Ison, O.W., Krieger, K.H. Myocardial reperfusion injury: platelet-activating factor stimulates polymorphonuclear leukocyte hydrogen peroxide production during myocardial reperfusion. *J Thorac Cardiovasc Surg* (1991) 102, 297-308.

Konecki, D.S., Aune, K.C., Tate, W.P., Caskey, C.T. Characterization of reticulocyte release factor. *J Biol Chem* (1977) 252, 4515-4520.

Konieczny, A., Safer, B. Purification of the eucaryotic initiation factor 2-eukcaryotic initiation factor 2B complex and characterization of its guanine nucleotide exchange activity during protein synthesis initiation. *J Biol Chem* (1983) 258, 3402-2408.

Korsmeyer, S.J. Bcl-2 initiates a new category of onocogenes: regulators of cell death. *Blood* (1992) 80, 879-886.

Kozak, M. Role of ATP in binding and migration of 40s ribosomal subunits. *Cell* (1980) 22, 459-467.

Kozak, M. How do eukaryotic ribosomes select initiation regions in messenger RNA? *Cell* (1978) 15, 1109-1123.

Kozak, M. The scanning model for translation: an update. *J Cell Biol* (1989) 108, 229-241.

Kozak, M. Initiation of translation in prokaryotes and eukaryotes. *Gene* (1999) 234, 187-208.

Kramer, J.H. Arroyo, C.M., Dickens, B.F., Weglicki, W.B. Spin trapping evidence that graded myocardial ischemia alters post-ischemic superoxide production. *Free Rad Biol Med* (1987) 3, 153-159.

Krieg, P., Varnum, S.M., Worington, M., Melton, D.A. The mRNA encoding elongation factor-1 alpha is a major transcript at the midblastulation transition in *Xenopus. Dev Biol* (1989) 133, 93-100.

Kroemer, G., Zamzami, N., Susin, S.A. Mitochondrial control of apoptosis. *Immunol Today* (1997) 18, 45-51.

Kuida, K., Zheng, T.S., Na, S., Kuan, C., Yang, D., Karasuyama, H., Rakic, P., Flaell, R.A. Decreased apoptosis in the brain and premature lethality in CPP32-deficient mice. *Nature* (1996) 384, 368-372.

Kukreja, R.C., Hess, M.L. The oxyen free radical system: from equations through membrane-protein interactions to cardiovascular injury and protection. *Cardiovasc Res* (1992) 26, 641-655.

Kurasawa, Y., Hanyu, K., Watanabe, Y., Numata, O. F-actin bundling activity of *Tetrahymena* elongation factor 1α is regulated by Ca2+/calmodulin. *J Biochem* (1996) 119, 791-798.

Laemmli, U.K. Cleavage of structural proteins during the assembly of the head of bacteriophage T4. *Nature* (1970) 227, 680-685.

Lawson, T.G., Lee, K.A., Maimone, M.M., Abramson, R.D., Dever, T.E., Merrick, W.C., Thach, R.E. Dissociation of double stranded polynucleotide helical structures by eukaryotic initiation factors as revealed by a novel asay. *Biochemistry* (1989) 28, 4729-4734.

Lee, S., Ann, D.K., Wang, E. Cloning of human and mouse brain cDNAs encoding for S1, the second member of the mammalian elongation factor-1 alpha gene family: analysis for a possible evolutionary pathway. *Biochem Biophys Res Comm* (1995) 203, 1371-1377.

Lee, S., Elenbaas, B., Levine, A., Griffith, J. p53 and its 14 kDa C-terminal domain recognize primary DNA damage in the form of insertion/deletion mismatches. *Cell* (1995) 81, 1013-1020.

Lee, S., Francoeur, A-M., Liu, S., Wang, E. Tissue-specific expression in mammalian brain, heart, and muscle of S1, a member of the elongation factor–1α gene family. *J Biol Chem* (1992) 267, 24064-24068.

Lee, S., Stollar, E., Wang, E. Localization of S1 and elongation factor–1α mRNA in rat brain and liver by non-radioactive in situ hybridization. *J Histochem Cytochem* (1993) 41, 1093-1098.

Lee, S., Wolfraim, L., Wang, E. Differential expression of S1 and elongation factor–1α during rat development. *J Biol Chem* (1993) 238, 24453-24459.

Lennon, S.V., Martin, S.J., Cotter, T.G. Dose-dependent induction of apoptosis in human tumour cell lines by widely diverging stimuli. *Cell Prolif* (1991) 24, 203-214.

Levy, S., Avni, D., Hariharan, N., Perry, R.P., Meyuhas, O. Oligopyrimidine tract at the 5' end of mammalian ribosomal protein mRNAs is required for their translational control. *Proc Natl Acad Sci USA* (1991) 88, 3319-3323.

Li, G., Chen, Y., Saari, J.T., Kang, Y.J. Catalase-overexpressing transgenic mouse heart is resistant to ischemia-reperfusion injury. *Am J Physiol* (1997) 273, H1090-H1095.

Li, P., Nijhawan, D., Budihardjo, I., Srinivasula, S.M., Ahmad, M., Alnemri, E.S., Wang, X. Cytochrome c and ATP-dependent formation of Apaf-1/Caspase-9 complex initiates an apoptotic protease cascade. *Cell* (1997) 91, 479-489.

Li, Y., Huang, T.T., Carlson, E.J., Melov, S., Ursell, P.C., Olson, J.L., Noble, L.J., Yoshimura, M.P., Berger, C., Chan, P.H., Epstein, C.J. Dilated cardiomyopathy and neonatal lethality in mutant mice lacking manganese superoxide dismutase. *Nature Gen* (1995) 11, 376-381.

Linz, J.E., Katayama, C., Sypherd, P.S. Three genes for the elongation factor-1 alpha in *Mucor racemous*. *Mol Cell Biol* (1986) 6, 593-600.

Litt, M.R., Jeremy, R.W., Weisman, H.F., Winkelstein, J.A., Becker, L.C. Neutrophil depletion limited to repefusion reduces myocardial infarct size after 90 minutes of ischemia: evidence for neutrophil-mediated reperfusion injury. *Circulation* (1989) 80, 1816-1827.

Liu, G., Edmonds, B.T., Condeelis, J. pH, EF–1α and the cytoskeleton. *Trends Cell Bio* (1996) 6, 168-171.

Liu, X., Kim, C.N., Yang, J., Jemmerson, R., Wang, X. Induction of apoptotic program in cell-free extracts: requirement for dATP and cytochrome c. *Cell* (1996) 86, 147-157.

Loreni, F., Francesconi, A., Amaldi, F. Coordinate translational regulatio in the syntheses of elongation factor 1α and ribosomal proteins in *Xenopus laevis*. *Nucleic Acids Res* (1993) 21, 4721-4725.

Lu, X.A., Werner, D. The complete sequence of mouse elongation factor-1 alpha (EF-1 alpha) mRNA. *Nucleic Acid Res* (1989) 17, 442

Majno, G., Joris, I. apoptosis, oncosis, and necrosis: an overview of cell death. *Am J Pathol.* (1995) 146, 3-15.

Manning, A.S. Reperfusion-induced arrhythmias: do free radicals play a critical role? *Free Rad Biol Med* (1988) 4, 305-316.

Marchesi, V.T., Ngo, N. *In vitro* assembly of multiprotein complexes containing α, β, and γ tubulin, heat shock protein HSP70, and elongation factor 1α. *Proc Natl Acad Sci* (1993) 90, 3028-3032.

Martin, S.J., Lennon, S.V., Bonham, A.M., Cotter, T. Induction of apoptosis (programmed cell death) in human leukemic HL-60 cells by inhibition of RNA or protein synthesis. *J Immuno* (1990) 145, 1859-1867.

Martin, S.J., O'Brien, G.A., Nishioka, W.J., McGahon, A.J., Mahboubi, A., Saido, T.C., Green, D.R. Proteolysis of fodrin (non-erythroid spectrin) during apoptosis. *J Biol Chem* (1995) 270, 6425-6428.

Marzo, I., Brenner, C., Zamzami *et al.*, Jurgensmeier, J.M., Susin, S.A., Vieira, H.L.A., Prevost, M-C., Xie, Z., Matsuyama, S., Reed, J.C., Kroemer, G. Bax and adenine nucleotide translocator cooperate in the mitochondrial control of apoptosis. *Science* (1998) 281, 2027-2031.

Mashima, T., Naito, M., Fujita, N., Noguchi, K., Tsuruo, T. Identification of actin as a substrate of ICE and an ICE-like protease and involvement of an ICE-like protease but not ICE in VP-16-induced U937 apoptosis. *Biochem Biophys Res Comm* (1995) 217, 1185-192.

McCord, J.M. Free radicals and myocardial ischaemia: overview and outlook. *Free Rad Biol Med* (1988) 4, 9-14.

McCord, J.M. Oxygen-derived free radicals in post-ischemic tissue injury. *New Engl J Med* (1985) 312, 159-163.

McDonnell, T.J., Deane, N., Platt, F.M., Nunez, G., Jaeger, U., McKearn, J.P., Korsmeyer, S.J. bcl-2-immunoglobulin transgenic mice demonstrate extended B cell survival and follucular lymphoproliferation. *Cell* (1989) 57, 79-88.

Melrose, D.G., Dreyer, B., Bentall, H.H., Baker, J.B.E. Elective cardiac arrest. *Lancet* (1955) ii, 21-22.

Merrick, W.C. Mechanism and regulation of eukaryotic protein synthesis. *Microbiol Rev* (1992) 56, 291-315.

Merrick, W.C., Dever, T.E., Kinzy, T.G., Conroy, S.C., Cavallius, J., Owens, C.L. Characterization of protein synthesis factors from rabbit reticulocytes. *Biochim Biophys Acta* (1990) 1050, 235-240.

Mestril, R., Chi, S-H., Sayen, M.R., O'Reilly, K., Dillmann, W.H. Expression of inducible stress protein 70 in rat heart myogenic cells confers protection against simulated ischemia-induced injury. *J Clin Invest* (1994) 93, 759-767.

Miller, D.L., Weissbach, H. Studies on the purification and properties of factor Tu from *E. Coli. Arch Biochem Biophys* (1970) 141, 26-37

Mitsos, S.E., Askew, T.E., Fantone, J.C., Kunkel, S.L., Abrams, G.D., Schork, A., Lucchesi, B.R. Protective effects of N-2-mercaptopropionyl glycine against myocardial reperfusion injury after neutrophil depletion in the dog: evidence for the role of intracellular-derived free radicals. *Circulation* (1986) 73, 1077-1086.

Miura, M., Zhu, H., Rotello, R., Hartwieg, E.A., Yuan, J. Induction of apoptosis in fibroblasts by IL-1 beta-converting enyzme, a mammalian homolog of the C. elegans cell death gene, ced-3. *Cell* (1993) 75, 653-660.

Miyashita, T., Krajewski, S., Krajewska, M., Wang, H.G., Lin, H.K., Hoffman, B., Lieberman, D., Reed, J.C. Tumour suppressor p53 is a regulator of bcl-2 and bax gene expression in vitro and in vivo. *Oncogene* (1994) 9, 1799-1805.

Miyashita, T., Reed, J.C. Tumor suppressor p53 is a direct transcriptional activator of the human bax gene. *Cell* (1995) 80, 293-299.

Mizushima, S., Nagata, S. pEF-BOS, a powerful mammalian expression vector *Nucleic Acids Res* (1990) 18, 5322

Moazed, D., Noller, H.F. Transfer RNA shields specific nucleotides in 16s ribosomal RNA from attack by chemical probes. *Cell* (1986) 47, 985-994.

Monaghan, P., Robertson, D., Amos, T.A.S., Dyer, M.J.S., Mason, D.Y., Greaves, M.F. Ultrastructural localization of Bcl-2 protein. *J Histochem Cytochem* (1992) 40, 1819-1825.

Moon, H.M., Redfield, B., Weissbach, H. Interaction of eukaryotic elongation factor EF-1 with guanosine nucleotides and aminoacyl-tRNA. *Proc Natl Acad Sci USA* (1972) 69, 1249-1252.

Mullane, K.M., Read, N., Salmon, J.A., Mancada, S. Role of leucocytes in acute myocardial damage in anaesthetised dogs: relationship to myocardial salvage by anti-inflammatory drugs. *J Pharmacol Exp Ther* (1984) 228, 510-522.

Muzio, M., Chinnaiyan, A.M., Kischkel, F.C., O'Rourke, K., Shevchenko, A., Ni, J., Scaffidi, C., Bretz, J.D., Zhang, M., Gentz, R., Mann, M., Krammer, P.H., Peter, M.E., Dixit, V.M. FLICE, a novel FADD-homologous ICE/CED-3-like protease is recruited to the CD96 (Fas/APO-1) death-inducing signaling complex. *Cell* (1996) 85, 817-827.

Nagata, S., Nagashima, K., Tsunetsugu-Yokota, Y., Fujirama, K., Miyazaki, M., Kaziro, Y. Polypeptide chain elongation factor 1 alpha from yeast, nucleotide sequence of one of the two genes for EF−1α from *Saccharomyces cerevisiae*. *EMBO J* (1984) 3, 1835-1850.

Negrutskii, B.S., Elskaya, A.V. Eukaryotic translation elongation factor 1α: structure, expression, functions, and possible role in aminoacyl-tRNA channeling. *Prog Nucleic Acid Res Mol Biol* (1998) 60, 47-77

Nicholson, D.W., Ali, A., Thornberry, N.A., Vaillancourt, J.P., Ding, C.K., Gallant, M.,

Gareau, Y., Griffin, P.R., Labelle, M., Lazebnik, Y.A. *et al.* **Identification and**

inhibition of the ICE/CED-3 protease necessary for mammalian apoptosis. ***Nature*** **(1995) 376, 37-43.**

Nishigaki, K., Minatoguchi, S., Seishima, M., Asano, K., Noda, T., Yasuda, N., Sano, H., Kumada, H., Takemura, M., Noma, A., Tanaka, T., Watanabe, S., Fujiwara, H. **Plasma Fas ligand, an inducer of apoptosis, and plasma soluble Fas, an inhibitor of apoptosis, in patients with chronic congestive heart failure..*J Am Coll Cardiol* (1997) 29, 1214-1220**

Nishizuka, Y., Lipmann, F. Comparison of the guanosine triphosphate split and polypeptide synthesis with purified *E. Coli* system. *Proc Natl Acad Sci USA* (1966) 55, 212-219.

Nissen, P., Kjeldgaard, M., Thirup, S., Polekhina, G., Reshetnikova, L., Clark, B.F.C., Nyborg, J. Crystal structure of the ternary complex of Phe-tRNA(Phe), EF-Tu and a GTP analogue. *Science* (1995) 270, 1464-1472.

Nohl, H. The biochemical mechanism of the formation of reactive oxygen species in heart mitochondria. In: Caldarera, C.M., Harris, P, eds. "Advances in studies of heart metabolism" Bologna: Cooperativa Libraria Universitaria Editrice (1982) pp 413-421.

Nolan, R.D., Grasmuk, H., Drews, J. The binding of tritiated elongation factors 1 and 2 to ribosome from Krebs II mouse ascites tumor cells. *Eur J Biochem* (1975) 50, 391-402.

Nyborg, J., Liljas, A. Protein biosynthesis: structural studies of the elongation cycle. *FEBS Lett* (1998) 430, 95-99.

Nygard, O., Nilsson, L. Translational dynamics: interactions between the translational factors, tRNA and ribosomes during eukaryotic protein synthesis. *Eur J Biochem* (1990) 191, 1-17

Nygard, O., Westermann, P., Hultin, T. Met-tRNAf is located in the close proximity of the b subunit of eIF2 in the eucaryotic initiation complex. *FEBS Lett* (1980) 113, 125-128.

Oltvai, Z., Milliman, C., Korsmeyer, S.J. Bcl-2 heterodimerizes *in vivo* with a conserved homolog, Bax, that accelerates programmed cell death. *Cell* (1993) 74, 609-619.

Oral, H.B., Arancibia-Caracamo, C.V., Haskard, D.O., George, A.J.T. A method for determining the cytoprotective effect of catalase in transiently transfected cell lines and in corneal tissue. *Anal Biochem* (1999) 267, 196-202.

Orth, K., Chinnaiyan, A.M., Garg, M., Froelich, C.J., Dixit, V.M. The CED-3/ICE-like protease Mch2 is activated during apoptosis and cleaves the death substrate lamin A *J Biol Chem* (1996) 271, 16443-16446.

Owens, C.H., DeRosier, D.J., Condeelis, J. Actin crosslinking protein EF–1α of *Dictyostelium discoideum* has a unique bonding rule that allows sqquare-packed bundles. *J Struct Biol* (1992) 109, 248-254.

Owen-Schaub, L.B., Zhang, W., Cusack, J.C., Angelo, L.S., Santee, S.M., Fujiwara, T., Roth, J.A., Deiseroth, A.B., Zhang, W-W., Kruzel, E., Radinsky, R. Wild-type human p53 and a temperature-sensitive mutant induce Fas/APO-1 expression. *Mol Cell Biol* (1995) 15, 3032-3040.

Pain, V.M. Initiation of protein synthesis in mammalian cells. *Biochem J* (1988) 253, 625-637.

Pain, V.M., Clemens, M.J. Assembly and breakdown of mammailian protein synthesis initiation complexes: regulatio nby guanine nucleotides and by phosphorylation of initiation factor eIF-2. *Biochemistry* (1983) 22, 726-733.

Pellizzoni, L., Cardinali, B., Lin-Marq, N., Mercanti, D., Pierandrei-Amaldi, P. A *Xenopus laevis* homologue of the La autoantigen binds the pyrimidine tract of the 5' UTR of ribosomal protein mRNAs *in vitro*: implication of a protein factor in complex formation. *J Mol Biol* (1996) 259, 904-915.

Petronilli, V., Constantini, P., Scorrano, L., Colonna, R., Passamonti, S., Bernardi, P. The voltage sensor of the mitochondrial permeability transition pore is tuned by the oxidation-reduction state of vicinal thiols. Increase of the gating potential by oxidants and its reversal by reducing agents. *J Biol Chem* (1994) 269, 16638-16642.

Pingoud, A., Gast, F.U., Peters, F. The influence of the concentration of elongation factors on the dynamics and accuracy of protein biosynthesis. *Biochem Biophys Acta* (1990) 1050, 252-258.

Podzuweit, J., Braun, W., Muller, A., Schaper, W. Arrhythmias and infarction in the ischemic pig heart are not mediated by xanthine-derived free oxygen radicals. *Circulation* (1986) 74 (Suppl II), 311-346.

Polyak, K., Xia, Y., Zweier, J., Kinzler, K., Vogelstein, B. A model for p53-induced apoptosis. *Nature* (1997) 389, 300-305.

Proud, C.G. p70 S6 kinase: an enigma with variations. *Trends Biochem Sci* (1996) 21, 181-185.

Przyklenk, K., Kloner, R.A. "Reperfusion injury" by oxygen-derived free radicals: effect of superoxide dismutase plus catalase, given at the time of reperfusion, on myocardial infarct size, contractile function, coronary microvasculature, and regional myocardial blood flow. *Circ Res* (1989) 64, 86-96.

Ray, B.K., Lawson, T.G., Kramer, J.C., Cladaras, M.H., Grifo, J.A., Abramson, R.d., Merrick, W.C., Thach, T.E. ATP-depndent unwinding of messenger RNA structure by eukaryotic initiation factors. *J Biol Chem* (1985) 260, 7651-7658.

Reimer, K.A., Jennings, R.B. Failure of xanthine oxidase inhibitor allopurinol to limit infarct size after ischaemia and reperfusion in dogs. *Circulation* (1985) 71, 1069-1075.

Richard, V.J., Murray, C.E., Jennings, R.B., Reimer, K.A. Therapy to reduce free radicals during early reperfusion does not limit the size of myocardial infarcts caused by 90 minutes of ischemia in dogs. *Circulation* (1988) 78, 473-480.

Riis, B., Rattan, S.I.S., Clark, B.F.C., Merrick, W.C. Eucaryotic protein elongation factors. *Trends Biochem Sci* (1990) 15, 420-424.

Romeo, F., Li, D., Shi, M., Mehta, J.L. Carvedilol prevents epinephrine-induced apoptosis in human coronary artery endothelial cells: modulation of Fas/Fas ligand and caspase-3 pathway. *Cardiovasc Res* (2000) 45, 788-794.

Romson, J.L, Hook, B.G., Kunkel, S.L., Abrams, G.R., Schork, M.A., Lucchesi, B.R. Reduction of the extent of ischemic injury by neutrophil depletion in the dog. *Circulation* (1983) 62, 1016-1023.

Rowlands, A.G., Panniers, R., Henshaw, E.C. The catalytic mechanisms of guanine nucleotide exchange factor and competitive inhibition by phosphorylated eucaryotic initiation factor 2. *J Biol Chem* (1988) 263, 5526-5533

Ryazanov, A.G., Rudkin, B.B., Spirin, A.S. Regulation of protein synthesis at the elongation stage: new insights into the control of gene expression in eucaryotes. *FEBS Lett* (1991) 285, 170-175.

Saikumar, P., Dong, Z., Weinberg, J.M., Venkatachalam, M.A. Mechanisms of cell death in hypoxia/reoxygenation injury. *Oncogene* (1998) 17, 3341-3349.

Salvesen, G.S., Dixit, V.M. Caspases: intracellular signaling by proteolysis. *Cell* (1997) 91, 443-446.

Sambrook, J., Fritsche, E.F., Maniatis, T. *Molecular cloning : a laboratory manual*, 2nd ed. Cold Spring Harbor Laboratory, Cold Spring Harbor, New York, 1989.

Satoh, S., Hijikata, M., Handa, H., Shimotohno, K. Caspase-mediated cleavage of eukaryotic translation initiation factor subunit 2alpha. *Biochem J* (1999) 342, 65-70.

Saugstad, O.D., Aasen, A.O. Plasma hypoxanthine concentrations in pigs a prognostic aid in hypoxia. *Eur Surg Re* (1980) 12, 123-129.

Shi, Y., Sahai, B.M., Greene, D.R. Cyclosporin A inhibits activation-inducd cell death in T-cell hybridomas and thymocytes. *Nature* (1989) 339, 625-628.

Shi, Y., Sahai, B.M., Greene, D.R. Cyclosporin A inhibits activation-induced cell death in T-cell hybridomas and thymocytes. *Nature* (1989) 339, 625-628

Shiina, N., Gotoh, Y., Kubomura, N., Iwamatsu, A., Nishida, E. Microtubule severing by elongation factor 1 alpha. *Science* (1994) 266, 282-285

Shimizu, S., Eguchi, Y., Kamiike, W., Matsuda, H., Tsujimoto, Y. Bcl-2 expression prevents activation of the ICE protease cascade. *Oncogene* (1996) 12, 2251-2257.

Shimizu, S., Narita, M., Tsujimoto, Y. Bcl-2 family proteins regulate the release of apoptogenic cytochrome c by the mitochondrial channer VDAC. *Nature* (1999) 399, 483-487.

Simpson, P.J., Fantone, J.C., Mickeson, J.K., Gallager, K.P., Lucchesi, B.R. Identification of a time window for therapy to reduce experimental canine myocardial injury: suppression of neutrophil activation during 72 hours of reperfusion. *Circ Res* (1988) 63, 1070-1079.

Sonenberg, N., Shatkin, A.J. Reovirus mRNA can be covalently crosslinked *via* the 5' cap to proteins in initiation complexes. *Proc Natl Acad Sci USA* (1977) 74, 4288-4292.

Song, J.M., Picologlou, S., Grant, C.M., Firozan, M., Tuite, G.M., Liebman, S. Elongation factor-1 alpha gene dosage alters translational fidelity *in Saccaromyces cerevisiae*. *Mol Cell Biol* (1989) 9, 4571-4575.

Stridh, H., Kimland, M., Jones, D.P., Orrenius, S., Hampton, M.B. Cytochrome c release and caspase activation in hydrogen peroxide- and tributylin-induced apoptosis. *FEBS Lett* (1998) 429, 351-355.

Suda, T., Takahashi, T., Golstein, P., Nagata, S. Molecular cloning and expression of the Fas ligand, a novel member of the tumor necrosis factor family. *Cell* (1993) 75, 1169-1178.

Sundstrom, P., Deborah, S., Sypherd, P.S. Sequence analysis and expression of two genes for elongation factor-1 alpha from the dimorphic yeast, *Candida albicans*. *J Bacteriol* (1990) 172, 2036-2045.

Tanaka, M., Ito, H., Adachi, S., Akimoto, H., Nishikawa, I., Kasajima, I., Marumo, F., Hiroe, M. Hypoxia induces apoptosis with enhanced expression of Fas antigen messenger RNA in cultured neonatal rat cardiomyocytes. *Circ Res* (1994) 75, 426-433.

Taniguchi, S., Miyamoto, S., Sadano, H., Kobayashi, H. Rat elongation factor 1 alpha: sequence of cDNA from a highly metastatic fos-transferred cell line. *Nucleic Acids Res* (1991) 19, 6949.

Tate, W.P., Caskey, C.T. The mechanisms of peptide chain termination. *Mol Cell Biochem* (1974) 5, 115-126.

Tatsuka, M., Mitsui, H., Wada, M., Nagata, A., Nojima, H., Okayama, H. Elongation factor-1 alpha gene determines susceptibility to transformation. *Nature* (1992) 359, 333-336.

Terada, N., Patel, H.R., Takase, K., Kohno, K., Nairn, A.C., Gelfand, E.W. Rapamycin selectively inhibits translation of mRNAs encoding elongation factors and ribosomal proteins. *Proc Natl Acd Sci USA* (1994) 91, 11477-11481.

Toyozaki, T., Hiroe, M., Tanaka, M., Nagata, S., Ohwada, H., Marumo, F. Levels of soluble Fas ligand in myocarditis. *Am J Cardiol* (1998) 82, 246-248.

Tsan, M-F., White, J.E., Caska, B., Epstein, C.J., Lee, C.Y. Susceptibility of heterozygous MnSOD gene-knockout mice to oxygen toxicity. *Am J Respir Cell Mol Biol* (1998) 19, 114-120.

Tsujimoto, Y., Cossman, J., Jaffe, E., Croce, C.M. Involvement of the bcl-2 gene in human follicular lymphoma. *Science* (1985) 228, 1440-1443.

Turner, J.F., Boveris, A. Generation of superoxide anion by NADH dehydrogenase of bivine heart mitochondria. *Biochem J* (1980) 191, 421-430.

Turner, N.A., Xia, F., Azhar, G., Zhang, X., Liu, L., Wei, J.Y. Oxidative stress induces DNA fragmentation and caspase activation *via* the c-Jun NH2-terminal kinase pathway in H9c2 cardiac muscle cells. *J Mol Cell Cardiol* (1998) 30, 1789-1801

Uetsuki, T.A., Naito,A., Nagata, S., Kaziro, Y. Isolation and characterizaton of the human chromosomal gene for polypeptide chain elongation factor-1 alpha. *J Biol Chem* (1989) 264, 5791-5798.

Uraizee, A., Reimer, K.A., Murray, C.E., Jennings, R.B. Failure of superoxide dismutase to limit size of myocardial infarction after fourty minutes of ischemia and four days of reperfusion in dogs. *Circulation* (1987) 75, 1237-1248.

van Damme, H.T.F., Amons, R., Moller, W. Identification of the sites in the eukaryotic elongation factor 1α involved in the binding of elongation factor 1β and aminoacyl-tRNA. *Eur J Biochem* (1992) 207, 1025-1034.

van Hemert, F.J., van Ormond, H., Moller, W. A bacterial clone carrying sequences encoding for elongation factor-1 alpha from *Artemia*. *FEBS Lett* (1983) 157, 289-293.

van Noort, J.M., Kraal, B., Bosch, L., La Cour, T.F.M., Nyborg, J., Clark, B.F.C. Cross-linking of tRNA at two different sites of the elongation factor Tu. *Proc Natl Acad Sci USA* (1984) 81, 3969-3972.

Villa, P., Kaufmann, S.H., Earnshaw, W.C. Caspases and caspase inhibitors. *Trends Biochem* (1997) 22, 388-393.

von Harsdorft, R., Li, P-F., Dietz, R. Signaling pathways in reactive oxygen species-induced cardiomyocyte apoptosis. *Circulation* (1999) 99, 2934-2941.

Walldorf, U., Hovermann, D., Bautz, E.K. F1 and F2: two similar genes regulated differentially during development of *Drosophila melanogaster*. *Proc Natl Acad Sci USA* (1985) 82, 5795-5799.

Wang, Z.Q., Auer, B., Singl, L., Berghammer, H., Haidacher, D., Schweiger, M., Wagner, E.F. Mice lacking ADPRT and poly(ADP-ribosyl)ation develop normally but are susceptible to skin disease. *Genes Dev* (1995) 9, 509-520.

Weissbach, H., Miller, D.L., Hachmann, J. Studies on the role of factor Ts in polypeptide synthesis. *Arch Biochem Biophys* (1970) 137, 262-269.

Weissbach, H.B., Redfield, B., Moon, H.M. Further studies on the interactions of elongation factor 1 from animal tissues. *Arch Biochem Biophys* (1973) 156, 267-275.

Werns, S.W., Shea, M.J., Driscoll, E.M., Cohen, C., Abrams, G.D., Pitt, B., Lucchesi, B.R. The independent effects of oxygen radical scavengers on canine infarct size: reduction by superoxide dismutase but not catalase. *Circ Res* (1985) 56, 895-898.

Werns, S.W., Shea, M.J., Mitsos, S.E., Dysko, R.C., Fantone, J.C., Schork, M.A., Abrams, G.D., Pitt, B., Lucchesi, B.R. Reduction of the size of infarction by allopurinol in the ischemic-reperfused canine heart. *Circulation* (1986) 73, 518-524.

Wexler, B.C., McMurty, J.P. Allopurinol amelioration of the pathophysiology of acute myocardial infarction in rats. *Arthersclerosis* (1981) 39, 71-87.

Whitacre, C.M., Hashimoto, H., Tsai, M.L., Chatterjee, S., Berger, S.J., Berger, N.A. Involvement of NAD-poly(ADP-ribose) metabolism in p53 regulation and its consequences. *Cancer Res* (1995) 55, 3697-3701.

Williams, M.D., van Remmen, H., Conrad, C.C., Huang, T-T., Epstein, C.J., Richardson, A. Increased oxidative damage is correlated to altered mitochondrial function in heterozygous manganese superoxide dismutase knockout mice. *J Biol Chem* (1998) 273, 28510-28515.

Wyllie, A. Clues in the p53 murder mystery. *Nature* (1997) 389, 237-238.

Wyllie, A.H. Glucocorticoid-induced thymocyte apoptosis is associated with endogenous endonuclease activation. *Nature* (1980) 284, 555-556.

Wyllie, A.H., Morris, G., Smith, A.L., Dunlop, D. Chromatin cleavage in apoptosis : association with condensed chromatin morphology and dependence on macromolecular synthesis. *J Pathol* (1984) 142, 67-70.

Wyllie, A.H., Morris, R.G., Smith, A.L., Dunlop. D. Chromatin cleavage in apoptosis: association with condensed chromatin morphology and dependence on macromolecular synthesis. *J Pathol.* (1984) 142, 67-70

Yaffe, D. Retention of differentiation potentialities during prolonged cultivation of myogenic cells. *Proc Natl Acad Sci USA* (1968) 61, 477.

Yang, F., Demma, M., Warren, V., Dharmawardhane, S., Condeelis, J. Identification of an actin-binding protein from *Dictyostelium* as elongation factor 1α. *Nature* (1990) 347, 494-496.

Yang, J., Liu, X., Bhalla, K., Kim, C.N., Ibrado, A.M., Cai, J., Peng, T-I., Jones, D.P., Wang, X. Prevention of apoptosis by Bcl-2: release of cytochrome c from the mitochondria blocked. *Science* (1997) 275, 1129-1132.

Yang, W., Burkhart, W., Cavallius, J., Merrick, W.C., Boss, W.F. Purification and characterization of a phosphatidylinositol-4-kinase activator in carrot cells. *J Biol Chem* (1993) 268, 393-398.

Yeh, E.T. Life and death in the cardiovascular system. *Circulation* (1997) 95, 782-786.

Yeh, W.C., Pompa, J.L., McCurraah, M.E., Shu, H.B., Elia, A.J., Shahinian, A., Ng, M., Wekeham, A., Khoo, W., Mitchell, K., El-Deiry, W.S., Lowe, S.W., Goeddel, D.V., Mak, T.W. FADD: essential for embryo development and signaling from some, but not all, inducers of apoptosis. *Science* (1998) 279, 1954-1958.

Yonish-Rouach, E. The p53 tumour suppressor gene: a mediator of a G1 growth arrest and of apoptosis. *Experientia* (1996) 52, 1001-1007

Ytrehus, K., Gunnes, S., Myklebust, R, Mjos, O.D. Protetion by superoxide dismutase and catalase in the isolated rat heart reperfused after prolonged cardioplegia: A combined study of metabolic, functional, and morphometric ultrastructural variables. *Cardiovasc Res* (1987) 21, 492-499.

Yuan, J., Shaham, S., Ledoux, S., Ellis, H.M., Horvitz, H.R. The C. elegans cell death gene *ced-3* encodes a protein similar to mammalian interleukin-1 beta-converting enzyme. *Cell* (1993) 75, 653-660.

Zamzami, N., Brenner, C., Marzo, I., Susin, S.A., Kroemer, G. Subcellular and submitochondrial mode of action of Bcl-2-like oncoproteins. *Oncogene* (1998) 16, 2265-2282.

Zoratti, M., Szabò, I. The mitochondrial permeability transition. *Biochim Biophys Acta* (1995) 1241, 139-176.

Zweier, J.L, Rayburn, B.K., Flaherty, J.T., Weisfeldt, M.L. Recombinant superoxide dismutase reduces oxygen free radical concentrations in reperfused myocardium. *J Clin Invest* (1987) 80, 1728-1734.

Zweier, J.L. Measurement of superoxide-derived free radicals in the reperfused heart: Evidence for a free radical mechanism of reperfusion injury. *J Biol Chem* (1988) 263, 1353-1357.

Zweier, J.L., Flaherty, J.T., Weisfeldt, M.L. Direct measurement of free radical generation following reperfusion of ishcemic myocardium. *Proc Natl Acad Sci USA* (1987a) 84, 1404-1407.